To the Graduate Council:

I am submitting herewith a thesis written by Nehemiah Joel Williams entitled "A Performance Analysis of a Rocket Based Combined Cycle (RBCC) Propulsion System for Single-Stage-To-Orbit Vehicle Applications." I have examined the final electronic copy of this thesis for form and content and recommend that it be accepted in partial fulfillment of the requirements for the degree of Master of Science, with a major in Aerospace Engineering.

Gary A. Flandro, Major Professor

We have read this thesis
and recommend its acceptance:

Trevor M. Moeller

Gregory A. Sedrick

Acceptance for the Council

Carolyn R. Hodges

Vice Provost and Dean of the Graduate School

# A PERFORMANCE ANALYSIS OF A ROCKET BASED COMBINED CYCLE (RBCC) PROPULSION SYSTEM FOR SINGLE-STAGE-TO-ORBIT VEHICLE APPLICATIONS

A Thesis
Presented for the
Master of Science
Degree
The University of Tennessee, Knoxville

Nehemiah Joel Williams
December 2010

# Dedication

To my family; my parents Mr. Dallas Williams, Jr, and Mrs. Deborah Williams, and my siblings Jeremiah Joshua Williams, and Leah Elizabeth Mainguy. Thank you all for encouraging me, strengthening my faith, and helping me to continue to believe that " I can do all things through Christ which strengtheneth me" (Phillipians 4:13).

# Acknowledgments

The author would like to express his appreciation to all of those who either through their expertise, inspiration, friendship or support assisted him in the successful completion of this study. In particular, the author would like to specify gratitude to Dr. Gary A. Flandro, his Major Advisor and Committee Chair for unsparingly providing his invaluable insight and advice in the thesis process, particularly in the understanding and modeling of high speed propulsion systems. The author would also like to show appreciation to committee members Dr. Trevor M. Moeller, and Dr. Gregory A. Sedrick, for supplying their valuable knowledge, especially in the constructive critiquing of this thesis, thus making it an even better work of art. Much thanks goes to Ms. Brenda Brooks in UTSI's library for her valuable assistance in the acquisition of many of the research articles and text books which made this thesis study possible. The author would like to express his sincerest gratitude to friend and fellow student Richard Joel Thompson especially for his valuable insight in the writing of the computer codes used in this thesis, and also in the use of the LATEX document writing tool. Finally, the author would like to specifically mention several others who have been extremely encouraging when the 'going got tough'; Ms. Patricia Burks from UTSI's Human Resources Department, long time friend Brittany Amber Gorecki, and of course both of his parents, Mr. and Mrs. Williams.

# Abstract

Rocket-Based Combined Cycle (RBCC) engines combine the best performance characteristics of air-breathing systems such as ramjets and scramjets with rockets with the goal of increasing payload/structure and propellant performance and thus making low earth orbit (LEO) more readily accessible. The idea of using RBCC engines for Single-Stage-To-Orbit (SSTO) trans-atmospheric acceleration is not new, but has been known for decades. Unfortunately, the availability of detailed models of RBCC engines is scarce. This thesis addresses the issue through the construction of an analytical performance model of an ejector rocket in a dual combustion propulsion system (ERIDANUS) RBCC engine. This performance model along with an atmospheric model, created using MATLAB was designed to be a preliminary 'proof-of-concept' which provides details on the performance and behavior of an RBCC engine in the context of use during trans-atmospheric acceleration, and also to investigate the possibility of improving propellant performance above that of conventional rocket powered systems. ERIDANUS behaves as a thrust augmented rocket in low speed flight, as a ramjet in supersonic flight, a scramjet in hypersonic flight, and as a pure rocket near orbital speeds and altitudes.

A simulation of the ERIDANUS RBCC engine's flight through the atmosphere in the presence of changing atmospheric conditions was performed. The performance code solves one-dimensional compressible flow equations while using the stream thrust control volume method at each station component (e.g. diffuser, burner, and nozzle) in all modes of operation to analyze the performance of the ERIDANUS RBCC engine. Plots of the performance metrics of interest including specific impulse, specific thrust, thrust specific fuel consumption, and overall efficiency were produced. These plots are used as a gage to measure the behavior of the ERIDANUS propulsion system as it accelerates towards LEO. A mission averaged specific impulse of 1080 seconds was calculated from the ERIDANUS code, reducing the required propellant mass to 65% of the gross lift off weight (GLOW), thus increasing the mass available for the payload and structure to 35% of the GLOW.

Validation of the ERIDANUS RBCC concept was performed by comparing it with other known RBCC propulsion models. Good correlation exists between the ERIDANUS model and the other models. This indicates that the ERIDANUS RBCC is a viable candidate

propulsion system for a one-stage trans-atmospheric accelerator.

# Contents

# List of Tables

# List of Figures

# Nomenclature

**Symbols Used**

| | |
|---|---|
| $I_{sp}$ | Specific impulse |
| $I_{eff}$ | Effective specific impulse |
| $I^*$ | Equivalent effective specific impulse |
| $I_{spAVG}$ | Mission averaged specific impulse |
| $\eta_0$ | Air-breathing overall efficiency |
| $\eta_{th}$ | Thermodynamic efficiency |
| $\eta_p$ | Propulsive efficiency |
| $\eta_c$ | Compression (Diffuser) efficiency |
| $\eta_b$ | Combustion (Burner) efficiency |
| $\eta_e$ | Expansion (Nozzle) efficiency |
| $TSFC$ | Thrust specific fuel consumption |
| $F/\dot{m}_0$ | Specific thrust |
| $F$ | Thrust |
| $M$ | Mach number |
| $c$ | Speed of sound |

| | |
|---|---|
| $A$ | Engine (or component) cross sectional area |
| $T$ | Temperature |
| $T_t$ | Stagnation temperature |
| $P$ | Pressure |
| $P_t$ | Stagnation temperature |
| $h$ | Specific enthalpy |
| $s$ | Specific entropy |
| $t$ | Time |
| $g_0$ | Acceleration due to gravity, taken at sea level |
| $m$ | Mass |
| $\dot{m}$ | Mass flow rate |
| $\dot{m}_{air}$ | Mass flow rate of air |
| $\dot{m}_{fuel}$ | Mass flow rate of fuel |
| $ER$ | Equivalence ratio |
| $f$ | Fuel to air ratio |
| $f_{st}$ | Fuel to air ratio (stoichiometric) |
| $\Delta t$ | Total thrust time |
| $\Delta V$ | Velocity increment achieved by thrust |
| $V_e$ | Exhaust velocity of propellant ejected during thrust |
| $\mathbf{p}$ | Linear momentum |
| $\mathbf{v}$ | Velocity |
| $C_t$ | Thrust coefficient |

| | |
|---|---|
| $a_0$ | Local acceleration |
| $\Im$ | Stream thrust |
| $Sa$ | Stream thrust function |
| $\beta$ | Bypass ratio |
| $q_0$ | Dynamic pressure |
| $\gamma$ | Specific heat ratio |
| $c_p$ | Constant pressure specific heat |
| $c_v$ | Constant volume specific heat |
| $R$ | Specific (ideal) gas constant |
| $\mathcal{R}$ | Thrust ratio |
| $\Re$ | Universal gas constant |
| $\theta$ | Flight path angle |
| $WF$ | Mode specific weight factor |
| $W$ | Weight |
| $\dot{Q}$ | Heat transfer rate |
| $\dot{W}$ | Work rate |
| $E$ | Total energy of the system |
| $\mathcal{M}$ | Molecular weight |
| $\rho$ | Density |
| $MFP$ | Mass flow parameter |
| $h_{PR}$ | Heat of reaction |
| $\mu$ | Gravitational parameter |

$\psi$ Compression temperature ratio

$I$ Impulse function

$T^o$ Reference temperature for combustion (222 K)

$h_f$ Absolute sensible enthalpy of fuel entering burner

**Ratios**

$C_f \frac{A_w}{A_3}$ Burner effective drag coefficient

$\frac{A_0}{A_i}$ Capture area ratio

$\frac{P}{P_t}$ Local to stagnation pressure ratio

$\frac{T}{T_t}$ Local to stagnation temperature ratio

$\frac{V_{fx}}{V_3}$ Ratio of fuel injection axial velocity to $V_3$

$\frac{V_f}{V_3}$ Ratio of fuel injection total velocity to $V_3$

**Subscripts**

0 Free Stream Condition (inlet entrance)

1 Reference station one (cowl lip location)

2 Reference station two (isolator entrance)

3 Reference station three (trans-section entrance)

4 Reference station four (burner entrance)

10 Reference station ten (nozzle location)

$ij$ Ejector rocket exit area station

$*$ Thermal throat position

$3'$ Trans-section/burner transition location (ramjet mode only)

$i$ Control volume entrance condition

| | |
|---|---|
| $e$ | Control volume exit condition |
| $c$ | Compression |
| $b$ | Combustion |
| $e$ | Expansion (as used for specific heat of expanded gas leaving a nozzle $\gamma_e$) |

# Chapter 1

# Introduction

*Often a science in its infancy, because it is unable to distinguish between a path and barrier, falsely judges many things to be possible and others to be impossible; and an individual, setting out on his career, is often prone to consider that he knows what is open to him and what is closed. But, just as in the sciences we have learned that we are too ignorant safely to pronounce anything impossible, so for the individual . . . we can hardly say with certainty that anything is necessarily within or beyond his grasp. Each must remember that no one can predict to what heights of wealth, fame, or usefulness he may rise until he has honestly endeavored, and he should derive courage from the fact that all sciences have been, at some time, in the same condition as he, and that it has often proved true that the dream of yesterday is the hope of today and the reality of tomorrow* [1] .

— Robert H. Goddard, Graduation Oration, Worchester, Massachusetts, June 24, 1904

## 1.1 Overview and Purpose of this Thesis

For over fifty years staged rockets have dominated the earth-to-orbit spaceflight domain. Virtually all of the launch vehicles both manned and unmanned used in transfer of payload to low earth orbit (LEO) have been at least in part disposable. The use of expendable launch vehicles has produced drastic economical strains on space transportation. For decades engineers in the aerospace industry have dreamed of an alternative launch

vehicle system which could potentially reduce the costs of payload delivery to LEO. One of the most common yet controversial ideas is the concept of a fully reusable vehicle which can reach LEO in one stage: a Single-Stage-To-Orbit launch vehicle (SSTO). All-rocket powered SSTO flight is virtually impractical as physical limitations of chemical rockets require the propellant mass fraction to be roughly 90% of the vehicles gross lift off weight (GLOW), leaving only 10% of the GLOW for payload and inert (structural) mass.

It is believed by many in the aerospace propulsion community [2–4], that increasing the net specific impulse of a trans-atmospheric propulsion system can reduce the required propellant mass and as a result, increase the amount mass available for structure and payload; this could allow the realistic possibility of flight to LEO in one stage. Successful flights of hypersonic vehicles (scramjets) such as the X-43 and the more recent X-51 have allowed for demonstrations of the practicality of high speed air-breathing propulsion in relation to trans-atmospheric flight [5]. Air-breathing engines such as ramjets and scramjets generally have higher performances than rockets, but unlike rockets, they are incapable of producing static thrust, and are also incapable of operation in a vacuum, two necessary requirements for trans-atmospheric propulsion.

The Rocket Based Combined Cycle (RBCC) has the potential to bridge the performance gap between rockets and air-breathing engines by behaving as an augmented (air-breathing) rocket in the static to trans-sonic flight regime, as a ramjet/scramjet in mid to high speed flight, and as a pure rocket near orbital speeds, all sharing roughly the same system hardware. Though the potential of the RBCC engine for use as a trans-atmospheric accelerator has been well known for over 40 years, detailed design of RBCC engines including analytical models and performance analyses in open literature is sparse [6].

This thesis aims to alleviate this problem via the creation of an analytical model of an ejector rocket in a dual combustion propulsion system (ERIDANUS) RBCC engine which does the following:

1. Simulates trans-atmospheric flight in the presence of changing atmospheric conditions from the view point of an RBCC engine

2. Demonstrates the advantages of the integration of the ejector rocket, ramjet, and scramjet on the overall performance of an SSTO against a pure rocket SSTO accel-

erator

3. Verifies the validity of the model by comparing specific performance metrics including net specific impulse, thrust specific fuel consumption, overall efficiency, specific thrust, air mass capture ratio, and total inlet pressure recovery with other theoretical analytical models found in literature

The analytical model presented in this thesis uses two MATLAB codes, an atmospheric code (StandardAtmosphereKM) which interpolates U.S. 1976 Standard Atmospheric Data to create the effects of a changing atmosphere with altitude, and the ERIDANUS code which solves basic one-dimensional compressible flow equations as they relate to an integrated ejector rocket with a dual mode scramjet. This is accomplished by control volume analysis of each engine component (inlet, burner, and nozzle) where flow properties are calculated entering and exiting each component using the appropriate relations.

The ERIDANUS code was closely influenced by the combined works of Billig, Heiser & Pratt, and Shapiro, each for separate sub-systems of the RBCC engine [3, 6, 7]. Performance metrics (e.g. specific impulse, specific thrust) are the outputs from the ERIDANUS code; the outputs are plotted and used in the validation of ERIDANUS via comparison of performance data with other works. The ERIDANUS code is meant to be a preliminary proof-of-concept for an RBCC trans-atmospheric accelerator, but does not include vehicle external drag, boundary layer effects, or vehicle sizing; extensive properties related to the model are calculated on a 'per unit mass' basis to allow direct comparison with other models without concern for vehicle volume or weight. The ERIDANUS model is meant lay a foundation for which future analysis can be applied. Most importantly, this model is meant to use the performance metrics mentioned above to demonstrate the feasibility of the ERIDANUS RBCC concept for trans-atmospheric flight to LEO in one stage.

## 1.2 History and Current State of Space Transportation to Low Earth Orbit

At the dawn of the last century, Konstantin Eduardovich Tsiolkovskiy used the principles of mathematics and Newtonian mechanics to derive relations which describe in detail

the use of the rocket for travel into space. Both the mathematical foundations which Tsiolkovskiy laid and the theoretical principles developed in the application of rocketry to space travel would eventually bring to reality mankinds age old dream of "rising above the Earth to the top of the atmosphere and beyond [to] fully understand the world in which he lives" as was spoken by the classical Greek philosopher Socrates [8].

Over a century has passed since Tsiolkovskiy derived those foundational principles and although space exploration with rockets has changed the lives of countless millions and has reshaped both the way humans interact, communicate, and view their universe, space is not as accessible nor is space travel as routine as many thought it would have been by now. After the dawn of the space age there were many comparisons between the space age and the airplane age; it was suggested by experts in the aerospace industry that in the same way that the Wright brothers first powered flight in 1903 revolutionized transportation through the skies, eventually paving the way for more rapid access to distant places around the globe through the commercialization of air travel, that events of the 1960's and the space race would allow for rapid access to space. Furthermore, the 1970's push for a reusable space transportation system, and the resulting space shuttle program was believed to make space more accessible, more routine, and therefore cheaper. Grand dreams of space stations in earth orbit and hotels for the average space enthusiast resulted from these inspired visionaries [5].

A previous Scientific American article reported that in 1996 a milestone was crossed in the exploration of space: for the first time in history "worldwide commercial revenues in space for the first time surpassed governments' spending on space, totaling some $77 billion" [9]. In this report, it was noted that there was a 300% increase in the total number of commercial payloads from 1996 to 1997 alone. The number has increased even more significantly in the decade which had followed. Just the launching of commercial satellites themselves is a $2.7 billion a year industry [10]. In the last decade, space tourism has also been introduced including the self-funding of space flight participants such as Greg Olsen, Charles Simonyi, and Anousheh Ansari to name a few.

In spite of the significant progress of the exploration of space and the commercialization thereof, the cost of spaceflight has not been significantly reduced. It was thought that the advent of the space shuttle program would gradually reduce the cost of space transporta-

Table 1.1: Heavy Lift Launch Vehicle Systems (FY02) [12]

| |  |  | 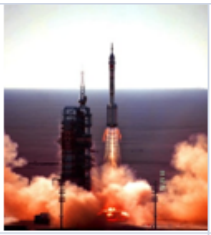 |  |
|---|---|---|---|---|
| Vehicle | Space Shuttle | Proton | Long March | Ariane 5G |
| Country/Region of Origin | USA | Russian Federation | China (PRC) | European Union |
| LEO Capability in pounds (kg) | 63,443 (28,803) | 43,524 (19,760) | 29,956 (13,600) | 39,648 (18,000) |
| LEO Reference Altitude in miles(km) | 127 (204) | 124 (200) | 124 (200) | 342 (550) |
| LEO payload cost per pound (kg) | $4,729 ($10,416) | $1,953 ($4,302) | $2,003 ($4,412) | $4,162 ($9,167) |

tion, but this is was not the case. Though it is often difficult to compare prices per pound for launch vehicles, studies show that Western medium to heavy launch vehicle systems cost in the $4-5000/lb range, and Russian/Chinese medium to heavy launch vehicles cost are lower, in the $2000/lb range [11]. Table 1.1 presents a comprarison of prices per pound and payload placement altitudes for various heavy lift launch vehicles:

The fact is that the launch vehicle systems using current technology have not been able to significantly reduce the cost of spaceflight, to the point where access to space is routine. Space exploration enthusiasts still dream for the day when the common person can hop into the passenger bay of a space bound vehicle and take the journey through the earths atmosphere headed into the expanse of the heavens to experience micro-gravity, a trip to an exotic earth orbiting hotel, or perhaps a further destination such as the moon for those brave enough to venture into the virtually unknown. This day has yet to come.

## 1.3 The Case for the Single-Stage-To-Orbit Launch Vehicle

Proponents of the creation of a routine space access system have pushed for the design of fully reusable launch systems. They believe that a fully reusable launch system would reduce the cost per pound of payload and therefore make access to space an easier task. Indeed engineers have no shortage of alternatives to current space launch systems. Perhaps the most grandiose yet controversial ideas for an alternative, reusable launch system which

could revolutionize and make easier the access to low earth orbit is the Single-Stage-To-Orbit (SSTO) launch vehicle system. The SSTO has been considered the 'Holy Grail' of launch vehicle design because it offers the promise of a space transportation vehicle which operates in airline-like fashion, routinely ferrying crews and cargo to low earth orbit and thus reducing cost of per-pound of payload to space.

Most SSTO concepts are designed to be fully reusable, with the hopes of designing a smaller support crew (including launch and maintenance) so that cost of space travel are lowered drastically when compared to the partially and fully expendable launch vehicle systems. SSTO concepts have been in no shortage in the aerospace engineering community and in fact have been so much under scrutiny that there are those who believe it is simply too impractical. SSTO concepts are not novel in the sense that they have been in the minds and on the drawing boards of the engineering community since the start of the space age. SSTO concepts range from those of Douglas Space and Missile Company's Phil Bono such as the Reusable One Stage Orbital Space Truck (ROOST), and ROMBUS in the 1960's to the National Aerospace Plane (NASP) of the 1980's , to the more recent SSTO concepts including the DC-X, and Lockheed Martins X-33 Venture Star [5, 13]. All of these SSTO concepts with the exception of the National Aerospace Plane were exclusively rocket powered SSTO concepts. The design of an SSTO could be argued as one of the most complex technical challenges known to launch vehicle design. Some of the technical challenges in designing SSTO launch systems simply are a result of the earths gravitational field, but are exacerbated by the fundamental limitations on the performance of rockets.

## 1.4 Fundamental Limitations of the All-Rocket Single-Stage-To-Orbit Vehicle

The fundamental limit to the performance of a rocket is governed by figures of merit such as specific impulse ($I_{sp}$). Electrical Propulsion (EP) rockets have high specific impulses but have such low thrust that the use of any current EP propulsion system for a launch vehicle is stupendously impractical. The best chemical rockets have sea level specific impulses below 400 seconds [14]. Using Tsiolkovskiy's rocket equation and comparing specific impulses of conventional chemical rocket engines such as those used by the Space Shuttle and the first

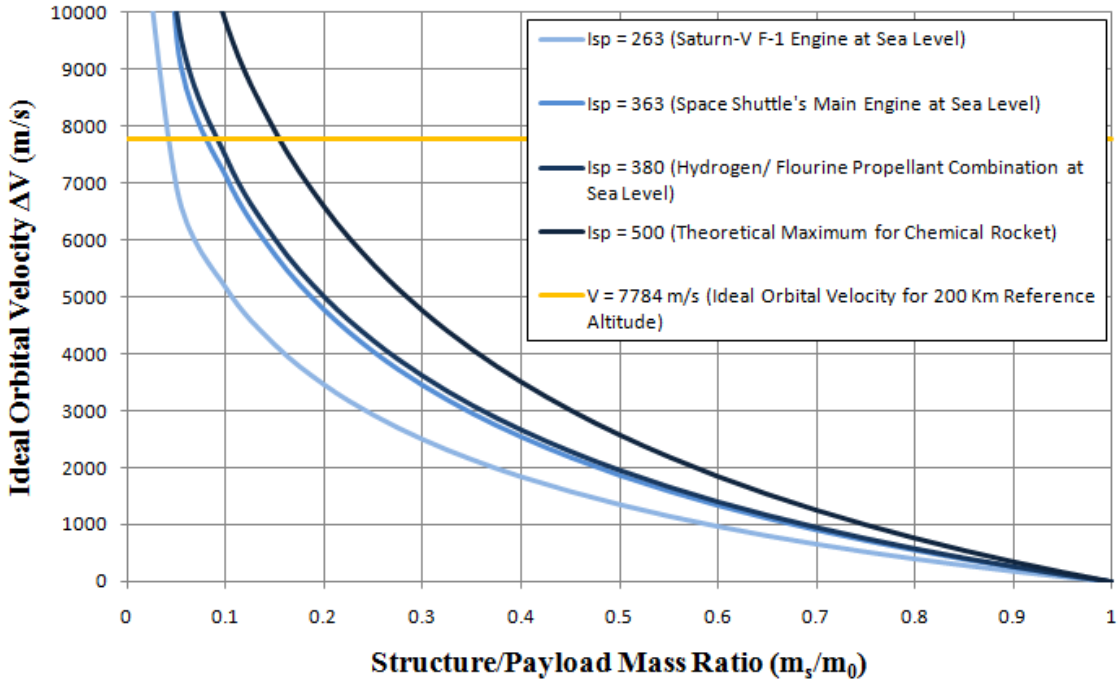


Figure 1.1: Conventional Rocket Propulsion Systems Performance Comparisons

stage of the Saturn-V moon rocket to the resulting structural/payload mass ratio's and $\Delta V$'s one can see that in Figure 1.1, to attain an orbital $\Delta V$ of approximately 8 km/s, the structural/payload ratio is limited to 10% of the vehicle's total weight.

This imposes a requirement that the entire structure - avionics, propellant tanks, engines, payload, and other subsystems be no more than a tenth of the entire weight of the vehicle. By inference, it can be determined that the gross-lift-off-weight (GLOW) of such a launch vehicle must 90% propellant. Fully reusable all-rocket single-stage-to-orbit launch vehicles must therefore carry about nine times their total weight in propellant, and withstand the forces involved with launch, access to orbit, reentry, and landing several times for a total lifetime in service [15]. Engineers working on such projects as X -33 have tried to increase performance to meet these demands by using lighter, stronger materials and increasing the performace of the propulsion system by employing the use of the aerospike nozzle design [5]. The most glaring difficulty involved in the all-rocket SSTO is the requirement to carry onboard the entire amount of necessary propellant. Rockets require that all of the oxidizer and fuel be carried onboard. This is necessary for travel into space but

perhaps could be avoided, and the resulting gross liftoff weight reduced if an air-breathing system were used for at least part of the flight through the atmosphere.

## 1.5 The Combined Cycle Alternative for Single-Stage Launch Vehicles

Air-breathing systems use oxygen from the atmosphere to burn with the fuel being carried on board and thus the GLOW is reduced. Air-breathing devices such as turbojets, turbofans, ramjets, and scramjets or combinations of them have been considered as remedies to compensate for the deficiencies of all-rocket flight. An all air breathing launch vehicle is impractical for spaceflight because air breathing engines will not operate in the vacuum of space; they require oxygen from the atmosphere to burn with fuel to produce thrust. Therefore with current technology, rockets must be used in conjunction with air-breathing engines to launch a payload into space. The advantages of air breathing engines in spaceflight must not be taken lightly though. Air breathers have the potential of reducing

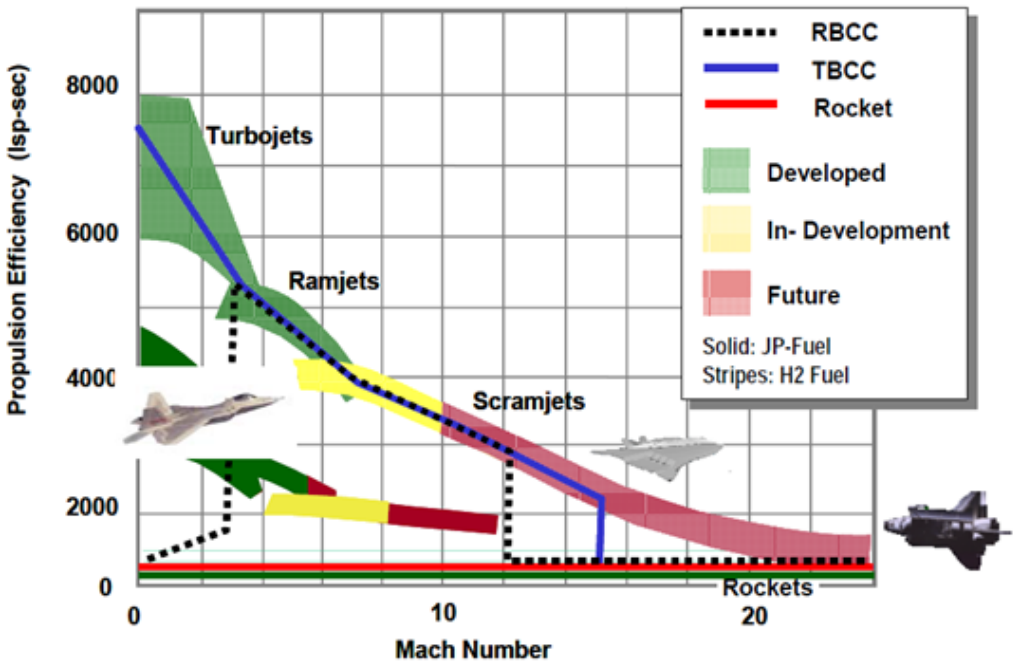


Figure 1.2: Performance Comparisons for Various Air-breathing and Rocket Propulsion Systems [16]

the GLOW of a flight system (and increasing the allowable mass from 10% to 30%), while also increasing the overall specific impulse by a factor of 10. Figure 1.2 shows a comparison of a pure rocket with the air breathing engines (turbojets, ramjets, and scramjets).

The challenge at hand is that no one propulsion system is capable of reaching orbit in one stage. Turbojets are the heaviest of all and require carrying the entire weight of their components (compressor, shaft, turbine) along the entire flight even though they are in use less than 25% of the flight duration. The ejection of a turbine after use defeats the purpose of single-stage-to-orbit flight as this would be considered an 'expendable stage'. The higher specific impulse advantage of the turbine cannot therefore be justified as it also increases the GLOW of the system. This leads to the use of rockets, ramjets, and scramjets used synergistically, and the concept of a rocket based combined cycle (RBCC) engine.

## 1.6 Sectional Summary

The first section in Chapter 1 of this thesis presented the major objectives of this thesis, which was to fill in the void of detailed analytical models of Rocket Based Combined Cycle Engines by creating an model which simulates an ejector rocket in a dual combustion propulsion system (ERIDANUS) accelerating through the atmosphere and into space. The next section of this chapter presented a brief overview of the state of current access to space including mentions of the cost of payload delivery to LEO of several international launch vehicles. The need for higher performing propulsion systems, including SSTO's followed, and eventually the argument and rational for the introduction of alternative propulsion concepts for launch vehicle design was discussed.

Chapter 2 begins first by presenting a loose definition of the combined cycle engine (CCE), followed by a historical survey of combined cycle propulsion, from the first uses of CCE's through the present state of the art. Next CCE's are discussed in the context of the SSTO, including a brief list of requirements for an SSTO worthy CCE. Eventually, the Rocket Based Combined Cycle Engine is shown to be the most viable option for a one-stage trans-atmospheric propulsion system. Chapter 3 is an overview of Rocket Based Combined Cycle Propulsion systems, including a brief discussion of the concept, its history, how it works and both experimental and analytical work on RBCC propulsion.

Chapter 4 presents the theoretical foundations and principles of both rocket and air breathing propulsion, and the one dimensional analytical methods which are necessary for the preliminary design of RBCC's. In Chapter 5, the analytical methods are presented with some detail, including the modeling of the atmospheric property variations with altitude and the control volume method of the RBCC engine. Chapter 6 presents the results of these simulations. The final chapter refines what has been discussed throughout this thesis, and includes allusions to the direction of future work to further analyze the ERIDANUS RBCC concept

# Chapter 2

# Background

*Reach low [earth] orbit and you're halfway to anywhere in the Solar System* [2].

— Robert A. Heinlein, Science Fiction Author

## 2.1 Overview of Combined Cycle Engines

In Chapter 1, the argument was presented for the use of a combined cycle propulsion system for a one stage trans-atmospheric accelerator. The central idea in this argument is that combined cycle propulsion has the potential to alleviate the weight requirements of all rocket SSTO vehicles, by saving propellant mass through the use of oxygen from the air to burn with propellant for thrust production. Though combined cycle concepts can be traced back for half of a century [3], there is a lack of agreement on the definition of the combined cycle. This chapter starts with a formal definition of what will be considered a combined cycle in this thesis. Afterwards, classes of combined cycles will be introduced, followed by discussion on which systems are the most appropriate for an SSTO vehicle.

### 2.1.1 Combined Cycle Engines Defined

The definition of a combined cycle engine is ambiguous as the criteria for what is considered a combined cycle can vary from study to study. Some studies are specific, and demand that all components be in use during any single part of the flight. These

studies make a distinction between combined cycles and 'multiple-cycle installations' or 'combination propulsion systems' (CPS's) which involve distinct engines which share a common inlet or nozzle but retain their separate identity [2]. By this definition, the turbo-ramjet would not be classified as a combined cycle engine, because it consists of a turbojet upstream, and a long afterburner, which is used as a ramjet during high speed flight. While in high speed flight, the turbojet remains as a dead weight when not in use. Other studies are more lenient on what is considered a combined cycle. A recent study done by the Japanese Exploration Agency (JAXA) differentiates between the combination propulsion system (CPS) and the combined cycle propulsion system (CCP) in the following manner:

> When several engines are mounted on a vehicle, it is termed a combination propulsion system. When an engine operates in several modes, it is termed a combined-cycle engine [17].

In "Studies of an Extensively Axis-symmetric Rocket Based Combined Cycle (RBCC) Engine Powered SSTO Vehicle" Richard W. Foster and William J.D. Escher defined the combined cycle propulsion system as follows:

> Combined Cycle Engines functionally and physically integrate more than one propulsion engine cycle into a single engine assembly. They should not be confused with 'combined cycle vehicles', 'combination propulsion systems', 'multi-cycle' propulsion, or 'Multi-Mode Vehicles' having more than one physically separate propulsion cycle in a single engine [18].

A third definition as was described by E.T. Curran in "The Potential and Practicality of High Speed Combined Cycle Engnies" is presented here:

> . . . the term combined-cycle is used, without further justification, to indicate an air-breathing engine system whose main element is the ramjet engine (with subsonic and/or supersonic combustion) that is boosted to ramjet takeover speed by means of a tuboengine (turboaccelerator) or rocket - based system, and that uses ramjet propulsion at the higher speeds.' [19].

This definition would of course exclude systems such air-breather rocket systems as the liquid air cycle engine ( LACE) or the synergic airbreathing engine (SABRE) because

neither at their basic form employ subsonic or supersonic ramjet propulsion systems [20].

In this thesis, a combined cycle propulsion system will be defined as a propulsion system which while using the same station elements or components (e.g. compressor, combustor, and nozzle) can produce thrust in distinctly different operating cycles (modes). The goal of a combined cycle propulsion system is the integration of elements from multiple propulsion systems into one (e.g. turbojets, ramjets, scramjets rockets) using the same elements to avoid dead weight with the purpose of optimizing the flight performance of a launch vehicle or cruise vehicle over a wide range of speeds. The combined cycle engine closely couples elements of various cycles which include turbo-machinery (from turbojets), combustors (from turbojets, ramjets, and scramjets), gas generators (also called ejector rocket engines), heat exchangers, and air-breathing compression/inlet systems. Nozzles also are shared in combined cycle engines [2]. These elements are subsystems of the overall power plant, and when used together in their respective modes constitute a combined-cycle engine.

The two most common modes of operation for combined cycle engine flight are air breathing and rocket. Air breathing modes include flight powered by critical air-breathing subsystems including turbo-accelerators, ramjets, and scramjets. The point is to use the benefits from each propulsion system in the flight regime where it has the best performance, while eliminating undesirable characteristics (including added weight due to using multiple separate propulsion systems). In general the flight regime through which combined-cycle engines operate include low speed flight (Mach 0 - Mach 3), low-supersonic flight (Mach 3 - Mach 6), hypersonic flight (Mach 6 - Mach 10), and rocket-powered flight (Mach 10 - Orbital speeds).

### 2.1.2 Classes of Combined Cycle Engines

#### Turbine Based Combined Cycle Engines (TBCC)

Two major classes of Combined Cycle engines exist: Turbine Based Combined Cycle (TBCC) and Rocket Based Combined Cycle (RBCC). The turbine based combined cycle's primary thrust producing element is the turbo-accelerator. The turbo accelerator produces thrust from static to trans-sonic conditions, but makes use of another cycle to produce thrust in the low to high flight regimes. The typical TBCC employs a turbo-accelerator in

a duct, with two flows, a primary airflow going into the turbo accelerator, and a secondary air flow bypassing the core turbo-accelerator [21].

At subsonic and transonic speeds the turbo accelerator produces thrust, and the secondary airflow is heated downstream of the turbo-accelerator in an afterburner. At supersonic speeds the afterburner operation transitions into a ramjet cycle, with the inlet shock cone and turbo-compressor acting to diffuse the flow entering into the ramjets burner. An example of a TBCC is the Pratt & Whitney J-58 turbo-ramjet engine which was used on the SR-71 Blackbird reconnaissance/research vehicle. Because of the high performance of TBCC's in the subsonic, transonic, and low supersonic flight regimes, TBCC would be very practical for Two Stage to Orbit (TSTO) vehicles such as the German Saenger/Hermes system which was proposed in the 1980s [3].

#### Rocket Based Combined Cycle Engines (RBCC)

Rocket Based Combined Cycle Engines in this study will be defined as combined cycle engines whose primary propulsion element is the chemical rocket. These include ejector rockets (because they behave both as a rocket for producing static thrust, and also as a jet because inlet air is compressed and burned with fuel to produce thrust), and the class of RBCC's commonly referred to as 'Air-breathing Rocket Engines', including Liquid Air Cycle Engines (LACE), and certain derivatives of the LACE engine such as Reaction Engines Ltd.'s Synergetic Air-breathing Rocket Engine (SABRE) [20]. Like Turbine Based Combined Cycle Engines, RBCC's can be used either to enhance the performance of a conventional rocket (as is the case with the air-breathing rockets) or to produce thrust from static conditions through the sub-sonic flight regimes in preparation for take-over in the ramjet and scramjet modes. More detail on the history, theory, and analysis of rocket based combined cycle engines will follow in the succeeding chapters.

## 2.2 A Brief History of Combined Cycle Engines

Combined Cycle Engines in aerospace applications are not new ideas, but have been around since the jet age itself. In fact, one cannot fully appreciate the history of ramjet type engines without observing its relation with the combined cycle engine. According to

one source [3], the first person to theorize the use of ram air pressure and heat addition for producing thrust was Rene Lorin of France, in 1913. Lorin, and his predecessors including Albert Fono of Hungary (who first issued a patent for a ramjet design in 1928), realized that ramjets were impractical using contemporary technology (at that time) because: they are incapable of producing static thrust (because they make use of dynamic pressure for propulsion, and therefore make an initial velocity a pre-requisite), and also because they were ineffective at low (i.e. subsonic speeds). This was still a time when the sonic barrier had not been broken, and some believed it impossible to do so.

In 1949, the Leduce 010, named after its designer Rene Leduc (also of France) was successfully flown after being released from the Languedoc transport aircraft. This was a milestone in ramjet propulsion, because the Leduc 010 was able to reach a tops speed of Mach 0.84, almost reaching the sonic barrier. Nord Aviation realized the usefulness of saving weight and fuel by combining a turbojet and ramjet into the same vehicle in the design of the Nord-Aviation Griffon II Turbo-ramjet aircraft, which became the worlds first combined cycle engine [3]. The SNEMCA Atar 101 E3 turbojet was contained inside of a ramjet, which shared the inlet and nozzle; this combination made use of the higher performance of turbojets in the subsonic flight regime, and the higher performance of ramjets in the supersonic flight regime. The Nord-Aviation Griffon II Turbo-ramjet could achieve as high a speed as Mach 2.

In 1970's the SR-71 Blackbird reconnaissance/research aircraft set altitude and speed world records for manned air-breathing flight. The SR-71 Blackbird was powered by two Pratt & Whitney J-58 supersonic turbojet engines, which were designed for flight through the trans-sonic flight regime. The Pratt & Whitney J-58 engines were designed for turbojet operation in the sub and trans-sonic flight regimes, but as it reached higher Mach numbers, its behavior was synonymic with that of ramjets. It used a diffuser cone which translated rearwards, maintaining shock on lip conditions, as is expected in ramjets, and also decelerated the incoming flow for sub-sonic combustion, using the same chamber as was used in 'turbojet mode'. By the combined cycle definition used in this thesis, the J-58 can be considered a turob-ramjet engine. The SR-71 successfully demonstrated the practicality of 'variable geometry' for compression, which is an important technology in the design of ramjets and combined cycle engines [5].

In the 1950's and 1960's improvements further improvements were made on the design of ramjets. Tests of ramjet powered missiles such as the Bomarc, Talos, Navaho, and X - 7 showed that there were thermal limitations to ramjets, as they approached Mach 5. With increasing Mach number, ramjet performance decayed, and also it became more difficult to cool the airframes of the missiles as they reached higher and higher stagnation temperatures [3, 5]. It became clear that a new solution was needed to compensate for the difficulties involved with near hypersonic propulsion.

The 1950's are generally accepted as the decade in which the Supersonic Combustion Ramjet (Scramjet) was invented, primarily to relieve the high heating and compression technical issues of near-hypersonic subsonic ramjet combustion. At NACA's Lewis Flight Propulsion Laboratory, aerodynamicists Richard Weber and John McKay first published open literature analytical results of a theoretical scramjet in 1958. A year earlier, the Russian E.S. Shchetinkov produced scramjet performance data up to a Mach number of 20, and proved the superiority of scramjet performance over the ramjet [22]. Others who are attributed with developing the scramjet include R. Dunlap, R.L. Brehm, and Antonnio Ferri, all in 1958 [5, 23].

Since scramjets generally have low performance in the low flight Mach number regime, it was the goal of aerodynamicists to consider the possibility of a device which could produce both subsonic and supersonic propulsion with the same system components. In the 1960's Curran and Stull proposed and patented the dual mode combustion system, a true combined cycle engine, which could produce subsonic combustion in ramjet mode, and supersonic combustion in scramjet mode. In 1966, Frederick S. Billig reported the first open-literature test of a dual mode combustion system, operating in ramjet mode [24].

Much progress has been made in the development of dual mode combined cycle propulsion, though none to date have produced thrust to power a flight vehicle. In the broad span of years from the 1970's and mid 1990's research and testing of dual mode combined cycle propulsion was conducted by Russia's Central Institute of Aviation Motors (CIAM). Through the work done by CIAM, supersonic combustion problems including flame holding, cryogenic cooling, and the influence of shocks on supersonic combustion were explored. The culmination of one CIAM project dubbed "Kholod", was a joint NASA-CIAM flight demonstration of a dual mode combined cycle test fixture boosted by a conventional rocket

which could operate between Mach 3.5 and 6.4 in 1998 [22]. Valuable data was collected for subsonic and supersonic combustion in this flight regime.

Though dual mode combined cycle engines could use the same system hardware to operate in low supersonic and hypersonic flight regimes, they are unable to alleviate the impracticality of ramjets and scramjets of producing static thrust. This fact led to the development in the 1950's and 1960's of the ejector ramjet concept. Technically, the ejector concept predates the ramjet by about four decades  it can be traced back to experiments with pressurized streams of airflow in ducts relating to the attempts to design wind tunnels by Horatio Phillips, the late 19th century aeronautics experimentalist [5]. In the 20th century, they were used as a primary propulsive device for producing the ram air pressure necessary for ramjets to produce thrust.

In 1947 a Curtiss-Wright engineer Jack Charshafian filed a patent for an ejector ramjet [5]. The most enticing attribute of the ejector rocket in a ramjet duct was the ability to combine it with a dual mode ramjet/scramjet in a unified engine, which could boost a vehicle from a runway to orbital altitudes in a single stage [5]. Other rocket based combined cycle concepts were introduced in the 1960's by the Marquardt Corporation studies included the Liquid Air Cycle Engine (LACE) and its derivatives with hypersonic engines, including the so called ScramLACE engine though Randolph Rae is given credit for the invention of the LACE engine, dated in 1954 at the Garret Corporation [5].

## 2.3 Combined Cycle Propulsion Sub-Systems

The motivation for the employment of a combined cycle engine for single stage to orbit applications is that no known propulsion system operates efficiently across broad earth-to-orbit flight regime. Combined cycle engines will comprise of a combination of at least two of the sub-systems (or modified versions of the sub-systems) which will be mentioned. A good start for the development of a more detailed understanding of CCPs is the brief technical overview of the inner workings of the sub-systems employed in a combined cycle engine.

### 2.3.1 Turbo-Accelerators

From Figure 1.2 it can be seen that turbo-accelerators (turbojets/turbofans) produce high performance measures (i.e. high specific impulses) from static conditions through the trans-sonic flight regime. Because of the high compression ratios and the corresponding high static and stagnation temperatures required to decelerate flows down to subsonic conditions for stable combustion, turbo-accelerators are have limited performance in the low supersonic flight regime. Furthermore, turbo-accelerators have material limitations, as the blades of the compressor and turbines cannot withstand the high temperatures associated with the required compression ratios in the upper regions of low supersonic flight. Thus, turbo-accelerators must be coupled or combined with another propulsion system for sustained flight in the higher speed flight regimes.

### 2.3.2 Ramjets

Ramjets have the best performance in the low supersonic flight regime, outperforming turbo-accelerators, rockets, and scramjets in specific impulse. Ramjets use ram air pressure from their motion through the atmosphere to produce thrust and therefore do not require any moving parts as turbo-accelerators do. Ramjets cannot however produce thrust from static conditions (they must be already in motion to produce thrust) and are limited in the static to subsonic flight regime. Ramjets are also limited to high supersonic flight and cannot operate in the hypersonic flight regime without exceeding material limits due to high static and stagnation temperatures associated with the required compression ratios for stable subsonic combustion.

### 2.3.3 Scramjets

The introduction of the supersonic combustion ramjet (scramjet) was to alleviate the problems associated with the necessary compression and temperature rises during subsonic combustion. Since combustion in the scramjet is allowed to be supersonic, compression ratios and stagnation/static temperature ratios are allowed to be lower. Scramjets are the 'kings of the air' in the hypersonic flight regime, outperforming all other propulsion systems in specific impulse. Scramjets are also limited by temperature considerations and

flight conditions. Free stream dynamic pressure approach structural material limits at higher hypersonic Mach numbers, and corresponding external heating due to resulting high external temperatures limit the flight regime of the scramjet.

### 2.3.4 Rockets

The venerable rocket is the only propulsion system which can operate in the entire flight regime, though not nearly as efficiently as any of the other previously mentioned systems. It has been the workhorse accelerator which has opened the door of spaceflight, and is a necessity when considering an earth-to-orbit propulsion system.

## 2.4 Combined Cycle Propulsion Considerations

### 2.4.1 Fuel Considerations

Both Figure 1.2 (see Chapter 1) and Table 2.1 (see below) make a strong case for the use of hydrogen ($H_2$) as the fuel of choice in a combined cycle propulsion system. In Figure 1.2 it is clear that the performance of the air-breathing engines using hydrogen as the main source of fuel increases over those which use hydro-carbons by a factor of about 2. This alone is ample reason for the use of hydrogen in an air-breathing engine. Furthermore, the argument for the use of hydrogen is heightened by is heat of reaction values ($h_{PR}$) when compared to the hydro-carbons. Heat of reaction is a measure of the amount of energy

Table 2.1: Heat of Reaction Values for Typical Aerospace Fuels [3]

| Fuel | kJ/kg Fuel | BTU/lbm Fuel |
|---|---|---|
| **Hydrogen ($H_2$)** | 119,954 | 51,571 |
| **Methane ($CH_4$)** | 50,010 | 21,502 |
| **Ethane ($C_2H_6$)** | 47,484 | 20,416 |
| **Hexane ($C_6H_{14}$)** | 45,100 | 19,391 |
| **Octane ($C_8H_{18}$)** | 44,786 | 19,256 |

made available (to produce thrust in accelerator systems) by chemical reactions. This value is used to measure how well chemical energy is converted into mechanical energy available to accelerate the vehicle via thrust production [3]. From Table 2.1 it is made apparent that chemical reactions produced by hydrogen with an oxidizer will have more energy available and thus higher air-breathing overall efficiencies than those produced by hydro-carbons. This is a result of the inherent higher $h_{PR}$ values of hydrogen. Hydrogen has twice as high heat of reaction values per unit mass of fuel than other commonly used chemicals.

The final case for the use of hydrogen as a fuel is the availability of the use of hydrogen for other subsystems within the engine such as use for heat-exchanger coolant. The use of liquid hydrogen requires cryogenic storage which can be used to cool internal flows (as is proposed in the Liquid Air Cycle Engine (LACE) propulsion system), and also to cool external flow surfaces. Cryogenic hydrogen can be used to cool the engine working fluid (air in this case) and thus impact the thermodynamic cycle performance of the engine [25].

### 2.4.2 Weight Considerations

The employment of air-breathers and air-breathing rocket engines makes use of oxygen from the air to reduce the GLOW of the launch vehicle system. The reduction of GLOW enhances the performance of the propulsion system by increasing the thrust-to-weight ratio. The work required by the propulsion system is reduced since instead of carrying all or most of the required oxidizer as in all-rocket systems, the power plant burns oxygen from the air in air-breathing mode and must only carry oxidizer for the final accent in rocket only mode to orbit.

### 2.4.3 Propulsion System/Airframe Integration

The broad range of Mach numbers which an SSTO must traverse in its voyage to orbit through the atmosphere places requirements on the interaction between the propulsion system and the airframe of the vehicle. For instance, ramjets and scramjets using the vehicle fore-body to diffuse the flow to an appropriate speed for stable combustion must be designed to maintain the 'shock on lip' condition for efficient flight [26]. The oblique shock waves formed upstream of the engine cowl decreases the Mach angle with increasing Mach

number. To maintain this condition, the cowl will be required to translate, thus imposing a variable geometry condition on the vehicle. Furthermore the required changes in capture area to inlet area ratio especially in supersonic flight further forces variable geometry conditions on the vehicle. The vehicle must be designed to both allow the proper flow compression via oblique shock waves, as well as minimize external drag, and maintain the proper airflow required for stable combustion. A common approach for hypersonic propulsion system/airframe integration is to consider the entire undersurface of the vehicle as a part of the engine, which is the mechanism which allows the proper fore-body compression and capture area sizes necessary for producing hypersonic thrust [27].

### 2.4.4 Engine Performance

Kors states that at hypersonic speeds the propulsive efficiency must be high [27]. Furthermore the overall engine performance sensitivity to slight changes in component efficiencies (inlet, burner, nozzle) are extremely high. A tabulated list of efficiencies and sensitivities of the three components, their efficiencies and their effect on the overall efficiency is below, and is based both on a NASA Langley scramjet code (SCRAM), and on Kors' article "Design Considerations for Combined Air Breathing-Rocket Propulsion Systems" [27].

Table 2.2 lists the efficiency relation for each component, compares the actual value (nominal) both to the ideal (highest theoretical value) and the value which affects the engine performance to the point of adverse effects (underachieved). From Table 2.2 it can

Table 2.2: Scramjet Component Performance Measures

| COMPONENT EFFICIENCY | EFFICIENCY RELATION | RELATIVE EFFICIENCY (IDEAL = 1) | | |
|---|---|---|---|---|
| | | Ideal | Nominal | Underachieved |
| Inlet, $\acute{\eta}_{KE}$ | Kinetic Efficiency | 1 | 0.975 | 0.95 |
| Burner, $\acute{\eta}_b$ | Ratio of Actual to Ideal Energy Released | 1 | 0.90 | 0.80 |
| Nozzle, $\acute{\eta}_c$ | Ratio of Actual to Ideal Stream Thrust | 1 | 0.975 | 0.95 |

be inferred that both the inlet and nozzle are extremely important components, which must have efficiencies above 0.95. Therefore it is important to have these components operate at optimal performance in order to maximize engine thrust and specific impulse. Combustion efficiency is not nearly as important an efficiency parameter as burner or nozzle values are, but certainly it is still desirable to maintain efficient combustion over the required flight regime.

### 2.4.5 Operation and Stability in Necessary Flight Regimes

Arguable the quintessential goal of the combined-cycle engine is the provision of maintained acceleration over all speeds required for the mission. In fact, it is this very point which became the rational for the theory of combined-cycle flight systems. According to Curran, a major U.S. effort to build a supersonic transport vehicle, led to the recognition that for such a vehicle to exist, it must accommodate both low-speed and high-speed flight requirements [19]. This realization generated research which led to the development of new engine concepts including variable cycle engines. From these developments and others such as the studies done by the Marquardt Corporation in the 1960's came the idea of combining the benefits of low speed air-breathing engines, high-speed air-breathing engines, and rockets. From such studies as those done by Marquardt, it was confirmed that operation over the broad range of flight conditions from subsonic to orbital combined-cycle engines are virtually mandatory for efficient use of all of the specified subsystems. Therefore, a combined-cycle engine designed for Single-Stage-To-Orbit must be able to optimize all operation modes of its accent into orbit [27].

Stability is of significant important in high speed combined-cycle engine design, due to the range of dynamic processes associated with supersonic and hypersonic flight through the atmosphere. Stability is of special concern to ramjet/scramjet combined-cycle systems which require that the inlet flow remains in stable, 'started' conditions. Started refers to the inlet condition which allows supersonic flows to be located at the inlet throat location, a condition which is also referred to as 'supercritical'. Stable flight refers to flight in which the inlet condition contains no fluctuations in the position of the supersonic flows relative to the inlet throat location (i.e. the supersonic flow does not cross the inlet throat

position but remains upstream or directly on the inlet throat) [28]. This is of particular importance to operation in ramjet mode, as the requirement for subsonic combustion is that the choking occur downstream of the inlet and upstream of the combustion chamber as the flow transitions from supersonic to subsonic conditions across the normal shockwave [3].

Rapid flow occlusions, pressure rises, and transient heat addition in the burner can cause a burner back pressure increase, forcing the normal shock upstream of the inlet and causing flow spillage outside of the entrance of the cowl. This can cause the condition referred to as 'unstart' which can have adverse effects on the engine performance. For instance, the abrupt change in the normal shock position can cause such large mechanical loads that inlet structural limitations are exceeded [27]. A constant area duct called an isolator can be introduced to prevent burner back pressures from 'unstarting' the inlet flow. An isolator is well named in that its function is to isolate the inlet flow from the burner flow. Isolators are a crucial element for the combination of subsonic and supersonic combustion within the same propulsion system and will be discussed at length later in this thesis.

### 2.4.6 Mandatory Integration of the Rocket with other Propulsion Modes

Rockets (or non-air-breathing thrust producing engines/modes) are virtually a mandatory ingredient in the design of a combined-cycle engine associated with Single-Stage-To-Orbit capable launch vehicles. The concept of an all-air-breathing single-stage vehicle seems elegant but is virtually impractical due to technical issues including the lack of significant air/oxygen beyond the sensible atmosphere, and also aero-thermal loads produced by atmospheric flight in the high hypersonic flight regime [11]. Figure 2.1 shows the flight regime of an SSTO where the altitude is plotted against Mach number with lines of constant dynamic pressure.

Studies have shown that hypersonic flight beyond Mach 12 introduces aerodynamic heating of the air frame, particularly near the leading edge of the vehicle. These problems can be avoided if a rocket mode is introduced in the combined cycle system. As a result, the vehicle spends the remainder of its trajectory away from the sensible atmosphere and can avoid the previously mentioned aerodynamic heating and thermal issues. The integration

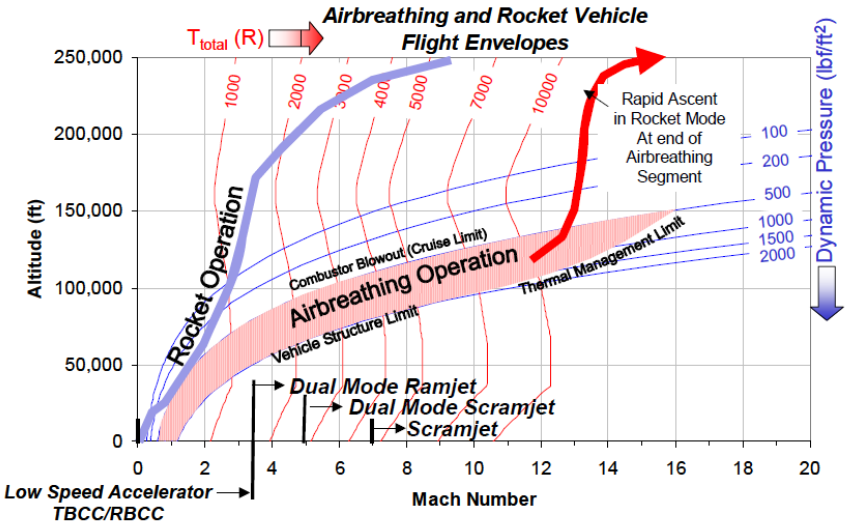


Figure 2.1: Total Temperature Rise with Increasing Mach Number in Trans-atmospheric Flight [16]

of a rocket with the air-breather must be designed with care so that the final configuration minimizes drag and/or weight penalties [27]. A particularly useful design integrates the rocket with the ramjet/scramjet duct as is typical of ejector or ducted rockets (see Figure 2.5a ). This particular configuration allows for flight in rocket mode, but also does not produce any drag on the internal flow, and also minimizes the weight of the system. If sufficient airflow is produced, the flow downstream of the rocket can be heated and therefore enhance the performance of the rocket. More discussion will follow on this particular configuration.

### 2.4.7 Technology Readiness, Cost of Development, Complexity

A paraphrasing of the meta-physical principle of the 14th Century logician/theologian William of Ockham are appropriate in the selection of a SSTO worthy propulsion system:

> "entities must not be multiplied beyond necessity . . .[and] the simplest solution is usually the correct one" [29].

This statement certainly applies in the formulation of a logic which is the basis for which a propulsion system is chosen for an SSTO launch vehicle. Results of this decision should

be based on the most feasible technologies available (e.g. making use of currently existing technologies as opposed to development of new technology to accomplish the same design objective). It is also imperative that the technology selected for employment in the propulsion system be cost effective. Ockham's Razor (as the statement coined by William of Ockham is called) also applies to the associated complexity of the technology in the propulsion system design. It is better for instance to avoid complicated variable geometries for ramjet/scramjet propulsion by using thermal choking in the expansion system of a dual-mode ram/scramjet than to employ a variable angle throat which can physically choke subsonic combustion flows, as the latter concept causes serious design challenges. Other design considerations include thermal management, and lightweight material considerations, but these are beyond the scope of this thesis, and further analysis of these considerations is superfluous.

## 2.5 Combined Cycle Propulsion Candidates for Single-Stage-To-Orbit Vehicles

### 2.5.1 Low Speed Flight Candidates

In the low speed flight regime it is desirable to increase the $I_{sp}$ and thrust/weight ratio of the engine while reducing the payload fraction, GLOW, and vehicle thrust loading. A major problem is that the rockets tend to be less complex, lighter engines which require higher initial accelerations due to lower $I_{sp}$ while air-breathers such as turbojets tend to be more complicated, thus heavier, while exhibiting higher $I_{sp}$ values and thus requiring lower initial accelerations. The low speed propulsion system designer's goal is to find a balance or trade-off between the high $I_{sp}$'s and higher GLOW of turbo-accelerators and the lower $I_{sp}$, higher thrust/weight ratio of rockets.

A particular developmental objective in the design of turbine based combined cycle engines is to offset GLOW deficiencies with increased performance. This can be accomplished by increasing the allowable turbine inlet temperature and also by increasing the efficiencies of the internal flow processes [19]. A means of accomplishing this goal is the combination of turbine and ramjet cycles, and derivatives of the basic turbo-accelerator/ramjet combined

cycle. The performance of rockets used for low speed acceleration can also be enhanced. Increasing the specific impulse of a rocket for low speeds can be accomplished by placing a rocket in an open ended duct, which allows airflow to bypass the actual rocket. This airflow is then mixed with the rockets exhaust products. After sufficient flow mixing, fuel is injected into the flow downstream of the rockets exit area. This system is called an ejector rocket, and the process is called thrust augmentation. Thrust augmentation increases the performance of a conventional rocket. The remainder of this section does not represent the full array of combinations of cycles for low speed flight; it is limited to the most promising concepts associated with combined cycle SSTO flight [26, 27].

**Air Turbo Ramjet/Rocket (ATR)**

The Air-Turbo-Ramjet is an upgrade on the simplest form of the Turbine-Based-Combined-Cycle Engine, the turbo-ramjet. The turbo-ramjet uses the best performance features of the two systems in a hybrid configuration. In Figure 2.2a it can be seen that the variable geometry (translating center body in this case) inlet of a turbo-ramjet bifurcates the inlet mass flow allowing some of the flow to go into the turbojet, and the rest into the ramjet. The turbojet is located upstream of the ramjet (or more precisely, the turbojet is contained inside of the ramjet). At low speeds the center body is extends further upstream of the turbine, allowing more airflow to go into the turbojet than into the ramjet. At higher supersonic speeds the center body is retracted, eventually closing off the turbojet inlet and allowing all of the flow to go into the ramjet, bypassing the entire turbojet [26]. The Air-Turbo-Ramjet (Figure 2.2b) provides enhanced performance over the turbo-ramjet by avoiding the high temperatures and pressures associated with conventional turbo-compression. The ATR powers the turbine in the system by the use of high temperature, fuel rich gas generator. As a result the temperature remains unchanged since it is independent of inlet Mach number and the resulting aerodynamic heating associated with it [26, 27]. The Air-Turbo-Rocket/Ramjet is a modification which has been made to integrate rockets in the ATR configuration. The ATR-ramjet uses rockets as the main source of gas generation. This configuration is promising for SSTO propulsion if it were able to further decrease the GLOW of the system. Other configurations of the

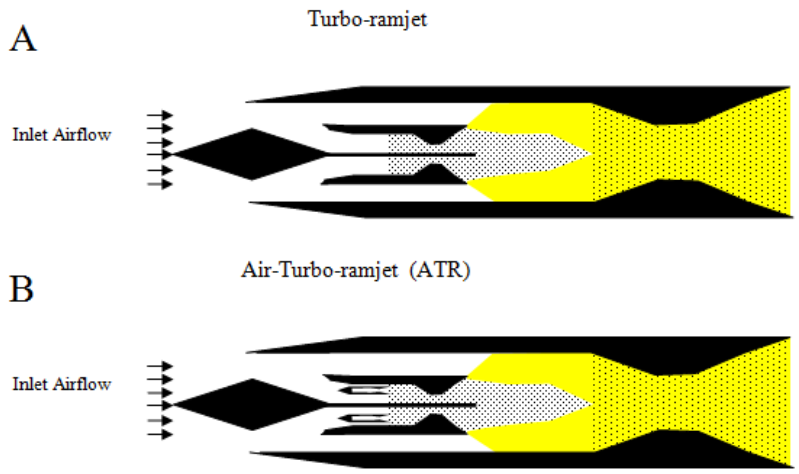


Figure 2.2: Turbo-ramjet (a) and Air Turbo Ramjet (b) Combined Cycle Engines

Turbine-Based-Combined Cycle include the Air-Turbo-Ramjet Hydrogen Expander Cycle (ATREX) cryo-cooled compression cycle.

**Liquid Air Cycle Engine (LACE) and Supersonic Combustion Liquid Air Cycle Engine (ScramLACE)**

Another candidate for low-speed combined-cycle propulsion are engines generally classified as cryo-cooled compression cycle engines. Technically these engines are the so called 'air-breather' rockets. In the mid-1950's research at the Marquardt Company resulted in the concept of the Liquid Air Cycle Engine (LACE) (see Figure 2.3a) which makes use of cryogenic hydrogen as a heat exchanger fluid [30].

The LACE engine has an advantage over the turbo-accelerator based combined cycle engines in that it does not require the use of the entire turbo-accelerator system, although they may employ a turbo compressor. The heat exchanger reduces the temperature (and pressure) of the incoming airflow to burner entry conditions and resulting stable combustion [2]. Thus it avoids the heavy machinery which is required to cool and compress flows in turbo-accelerators. The most attractive feature of these devices is that they attempt to enhance the performance (reducing GLOW, increasing specific impulse) by making use of

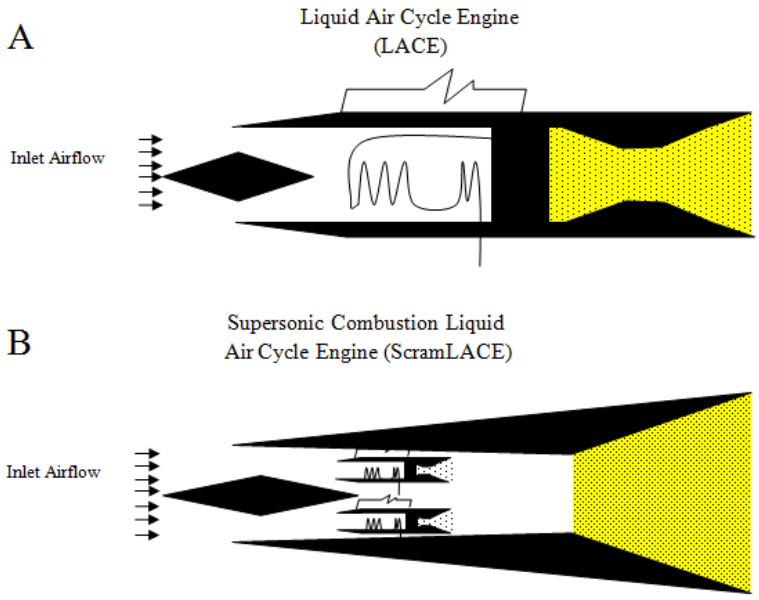


Figure 2.3: LACE (a) and ScramLACE (b) Combined Cycle Engines

oxygen from the surrounding air during flight through the atmosphere, and thus reducing the required weight of the entire vehicle. From Figure 2.3a it can be seen that in the LACE cycle first liquefies the free-stream air in a precooler, and then pumps the liquefied air in a turbopump, preparing it for the high required pressures for heat addition in the combustion chamber [20]. LACE engines also have physical limitations which make them not the best candidates for SSTO propulsion in their purest form. LACE engines require extremely high fuel consumption relative to other airbreathing engines, with specific impulse limitations in the 800 to 1000 second range [20, 30]. Modifications of the LACE to enhance its performance include combining the LACE cycle with the scramjet cycle (ScramLACE engine) Figure 2.3b, or more modern forms of the LACE engine including HOTOL's R545, or SKYLON's Synergetic Air-breathing Rocket Engine [20]. Each of these requires complex cooling systems, and although are promising ideas, are extremely dependant on complicated heat exchanger research, design, and development [20].

#### Ejector Rocket (ER)

Another method of enhancing the performance of a rocket in the low speed regime is thrust augmentation of the ejector rocket (see Figure 2.5a). The ejector operates by producing static thrust in a duct open to the inlet air, and as a result, creates flow into and over the ejector. This results in a pressure rise inside of the duct which can slow down the flow for stable combustion. Downstream of the ejector, the rocket exhaust and the air stream is mixed. Further down from the mixing location, fuel is added to the mixed flow, and the flow is heated, creating more thrust and thus enhancing the overall performance. The flow must be choked, and thermal choking can be employed to avoid the necessity of variable geometry in the nozzle and the complex problems associated with it [2]. The ejector rocket is a promising candidate for integration in an SSTO combined-cycle engine because it can be easily integrated say in a scramjet in such configurations as the ejector-scramjet (SERJ) [30].

### 2.5.2 High Speed Flight Candidates

#### Dual Combustor Ramjet (DCR)

Attempts have been made to design a ramjet which can combine cycles for subsonic combustion and supersonic combustion within the same system. One of these ideas is the Dual-Combustion Ramjet (DCR) which is shown in Figure 2.4a. In this depiction, a duct contains a fore-body compression surface which divides the incoming flow into several regions. For low speed operation, flow is forced into the subsonic combustor, immediately downstream of the diffuser by a subsonic combustor air inlet. This region can provide stable combustion for the appropriate Mach numbers, and can also operate supercritically, keeping the normal shock in its proper place downstream of the inlet. For high speed flights, a second duct (supersonic combustor inlet) allows flow to enter the supersonic combustor (separate and downstream of the subsonic combustor). The dual-combustor ramjet essentially has two combustion chambers, one for subsonic combustion, and one for supersonic combustion. This is a clever means of providing operation over a wider range of Mach numbers, but the requirement for two combustion chambers is superfluous and can be avoided with the design of a Dual-Mode Ramjet/Scramjet (DMRS) Figure 2.4b.

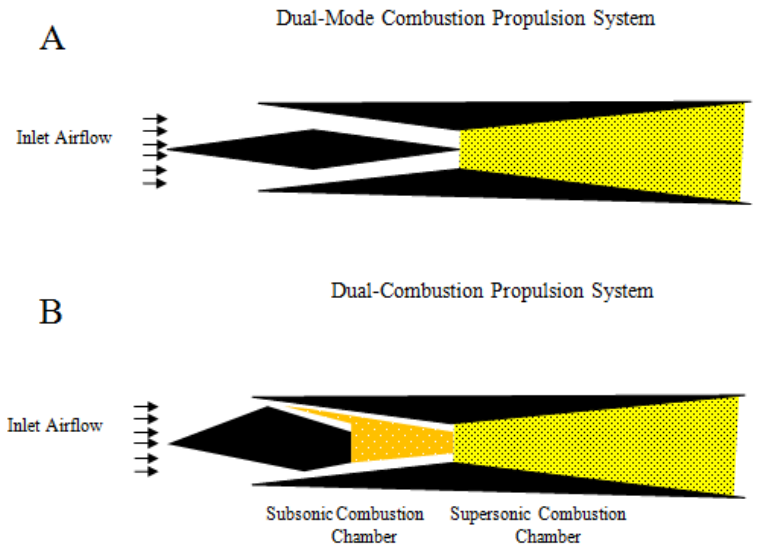


Figure 2.4: Dual-Mode Scramjet (a) and Dual-Combustion Ramjet (b) Combined Cycle Engines

### Dual Mode Ramjet/Scramjet (DMRS)

The advantage of the Dual-Mode Ramjet/Scramjet is the use of a single combustion chamber for subsonic and supersonic combustion [3]. With a Dual-Mode Ramjet/Scramjet, a flight vehicle could be accelerated by one or several of the previously mentioned low speed candidates. At low supersonic speeds, the device behaves as a ramjet, using the forebody (or centerbody) to force oblique shocks into an internal duct called an isolator. The isolator separates the burner from the compression system and keeps the normal shock wave formed by super to subsonic flow transitions from entering the burner and producing adverse effects. At hypersonic speeds, the same duct is used for supersonic combustion. The forebody uses oblique shocks to diffuse the freestream air for stable supersonic combustion. The DMRS does not need a physical throat for ramjet mode, (a thermally choked throat is used). DMRS still needs another form of propulsion to produce the ram-air pressure necessary for thrust production.

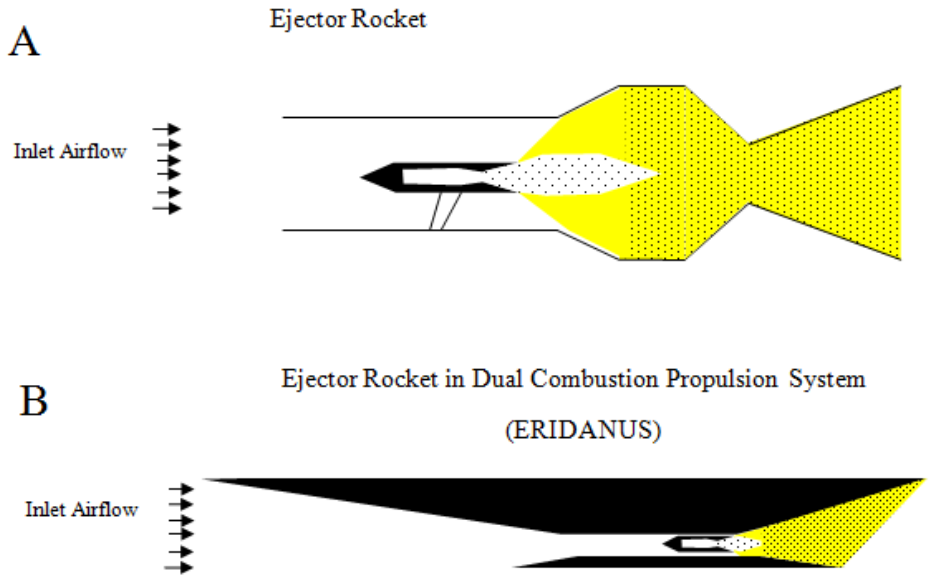


Figure 2.5: Ejector Rocket (a) and ERIDANUS (b) Combined Cycle Engines

**Ejector Rocket in Dual-Mode Combustion Propulsion System Propulsion System (ERIDANUS)**

The Dual-Mode Combustion (Ramjet/Scramjet) Propulsion System can be modified by placing an ejector rocket in the ducted area upstream of the burner (see Figure 2.5b). This ejector rocket acts as the gas generator which is necessary for producing ram-air pressure in ramjet and scramjet modes. This configuration is the main topic of this thesis and will be discussed at length in succeeding sections. The simplicity, yet practicality of the Ejector Rocket in Dual-Mode Combustion Propulsion System (ERIDANUS) makes it a prime candidate for a Single Stage to Orbit propulsion system.

## 2.6 Summary

To obtain a deep understanding of a system being studied a good place to start is the development of a strong definition. Chapter 2 of this thesis began with a definition of the combined cycle engine concept which is specific enough to include many of the traditional concepts including the turbo-ramjet, but also extend the definition beyond those limited to ramjet/scramjet integration. This definition includes the LACE and SABRE

engines as combined cycles. Though major goals of combined cycle propulsion for SSTO include the alleviation of weight requirements imposed on all-rocket engines by fundamental physics, other factors become important to consider, including the effects of fuel choice on performance, weight considerations, engine component performance, operation over the required flight regime, and the mandatory integration of rocket with other modes of propulsion for trans-atmospheric flight. Furthermore, the ideal combined cycle for a SSTO is the one which best meets the requirements mentioned above, while still remaining simple. After all, as William of Ockham stated a long time ago, "the simplest solution is usually the best one."

After briefly observing the characteristics of various combined cycle systems, the ejector rocket in dual-combustion propulsion system (ERIDANUS) RBCC seems to be the most promising. It does not require complex mechanical components (e.g. turbofan blades) like the TBCC concepts, and also does not require a complicated heat exchanger for air liquifications as the LACE and LACE derived RBCC systems do. Chapter 3 will give a review of the research performed on RBCC engines, followed by a technical overview of the ejector rocket RBCC concept.

# Chapter 3

# An Overview of the Rocket Based Combined Cycle

*"[A reusable vehicle is within the limits of todays technology] . . . However, if the signal to go ahead . . . was deferred a few years, then we would undoubtedly be able to come up with a superior, more advanced engine concept such as the ScramLACE [a variation of a Rocket Based Combined Cycle Propulsion System] . . . With such a propulsion engine, it seems feasible to fly with a single-stage vehicle directly into low orbit."*

– Werner Von Braun during a testimony to the staff of the House Space Committee taken from Space Daily, March 31, 1967 [18].

## 3.1 Overview

The Rocket Based Combined Cycle (RBCC) is neither a new concept, nor should it be thought of as a recently introduced technology. In fact, the elements of what are considered applicable to RBCC propulsion (ejector rockets/ramjets, ducted rockets, and air-augmented rockets) have been around since the middle of the 20th century. To avoid confusion from the various terminologies associated with air-augmented rockets, a brief description will be presented on the basic sub-systems associated with RBCC propulsion systems. The history of RBCC's will be presented, including a review of analytical and

experimental work in RBCC propulsion which has been published throughout the years. The final section of this section will be a brief technical overview, explaining the interactive synergism between RBCC sub-system components, and technical challenges with the design of RBCC propulsion. The goal of this section is to present a view of the RBCC not as a new concept, but as one which has both demonstrated experimental and analytical validity, and also one which has promising potential in the future of space transportation.

## 3.2 Rocket Based Combined Cycle Engines Defined

An extensive investigation of 'advanced' rocket concepts (those which include rockets and other subsystems operating in hybrid configurations) will reveal that there is much ambiguity in the description, labeling, and classifications of rocket augmentations. For instance, the term 'ejector rocket' in one publication is called an 'ejector ramjet' in another textbook, though they describe essentially the same device [3, 4]. Also, because few publications and text books define exactly what consists of a Rocket Based Combined Cycle Engine, some publications describe such a device as an RBCC when others might use the term 'air-augmented rocket', though an air-augmented rocket is not necessarily an RBCC engine. For clarification purposes, this thesis will (as much as possible) create definitions for these devices and follow these definitions with consistency.

The term 'air-augmented rocket' often used as a synonymy with the 'ram-rocket' will refer to a rocket which has an end open to the free stream, (like a ramjet or scramjet), but has a nozzle and burner, where its own propellant is used to burn and create thrust. In this context, the rocket behaves as an air-breather, and will be described also as thus. Therefore the 'air-augmented rocket' and 'air-breather rocket' are synonymous. If an air-augmented rocket has a diffuser or some free stream compression device upstream of the burner, it behaves similar to a ramjet, and the term 'ram-rocket' properly applies. All air-breathing rockets can be classified as 'air-augmented rockets', but all 'air-augmented rockets' are not necessarily 'ram-rockets'. The term 'ducted rocket' often is used to refer to air-augmented rockets, but can also refer to a device which encloses an entire rocket sub-system inside of a duct or a channel. The terms 'ejector ramjet', 'ejector scramjet' or 'ejector rocket' have been associated with this type of engine.

In this thesis, the term ejector rocket will be used to define a propulsion system where an entire rocket subsystem is placed in a channel or duct, with an open area to the free stream upstream of the rockets location, and with the flow mixing, burner, and nozzle immediately downstream of the 'rocket-in-a-duct'. Whether the internal rocket is synergistically integrated with the upstream flow path of a ramjet, or scramjet will not redefine the type of propulsion system; therefore the terms 'ejector rocket', 'ejector ramjet', and 'ejector scramjet' are virtually synonymous.

If the system operates in several modes, e.g., as an ejector rocket and as a ramjet and/or scramjet, it becomes by definition a Rocket Based Combined Cycle engine. It can be inferred from several sources that at least two variants of the Rocket Based Combined Cycle engine exist, namely the 'ejector rocket' class (including the ejector ramjet (ERJ), ejector scramjet (ESR), and their 'supercharged' cousins) and the Liquid Air Cycle Engine (LACE) class (including the ramLACE and scramLACE engines). The differentiation is simply the type of rocket which is used as the primary accelerator for the ramjet/scramjet modes of operation [18, 30].

## 3.3 Literature Review of Rocket Based Combined Cycle Research

Several experimental studies were performed with topics related to RBCC engines and air-augmented rockets. In 1962 a USAF funded Martin Marietta experiment with a simple ejector rocket in a constant area duct demonstrated specific impulse augmentation of about 10% when compared to a non-augmented rocket of the same class [18]. Improvements were made in the form of the Rocket Engine Nozzle Ejector (RENE) project, which mixed free-stream air with the ejector exhaust, and added heat to the fluid mixture in a divergent area duct. These modifications allowed for specific impulse augmentation up to about 55%, and also reduced the required bypass ratio (of air to fuel) from 20 to 3 (Figure 3.1 [18]).

A few years later the Marquardt Corporation in conjunction with Rocketdyne and Lockheed participated in a detailed NASA funded project which performed detailed analysis of over 36 types of combined cycle propulsion systems associated with TSTO launch vehicles. In "A Study of Composite Propulsion Systems for Advanced Launch Vehicle

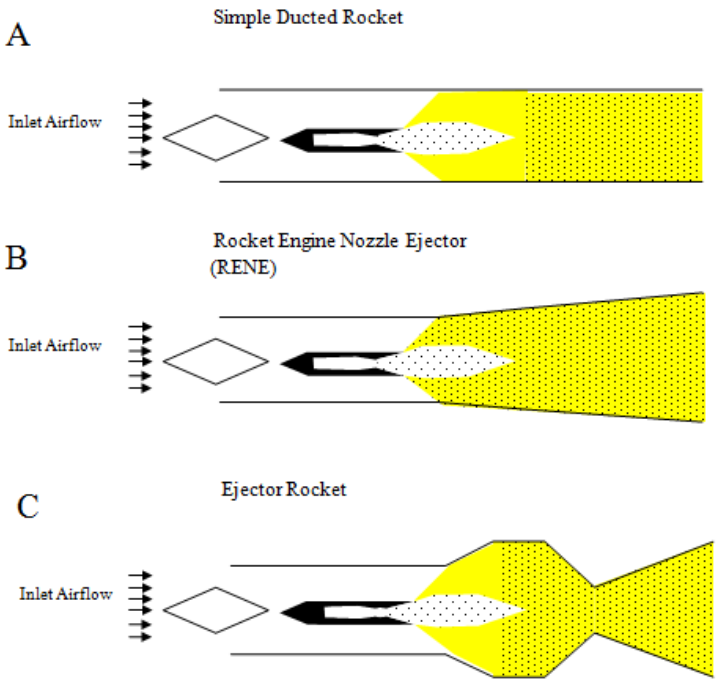


Figure 3.1: Progression of the Air Augmented Rocket

Applications", Marquardt and its collaborators identified 12 of these systems which were promising propulsion systems for TSTO applications. This document focused on the two major classes of RBCC engines mentioned, namely the ejector and supercharged ejector ramjet (SERJ) (Engines # 10 and # 11), and the scramLACE (Engine # 22). From this study, the mission averaged specific impulses produced by these engines were in the 630 - 780 second range, as opposed to all rockets which generally have sea level specific impulses below 400 seconds [4, 18, 30].

In the 1980s USAF Astronautics Laboratory awarded a contract to Martin Marietta labeled "Air-Augmented Rocket Concepts" with the intent of further studying the 12 promising concepts produced in the Marquardt study in detail. This study narrowed the 12 propulsion concepts to 5 specific configurations of both ESJ (ejector scramjet) and scramLACE engines. A summary of this report presents the ejector scramjet (defined as an ejector rocket in this thesis) as a prime candidate for an SSTO propulsion system because it is the simplest and lightest engine configuration studied and has the highest thrust-to-

weight ratio of the five engines. [18]. Another advantage derived from the study indicated that the ejector rocket has the least new technology demands, making it arguably an easier and perhaps cheaper system to implement as opposed to scramLACE type engines. Daines reports that in the 1990's an ejector rocket engine was tested [4]. This study was done using four strut/rocket nozzles in the same flow path in a continuously diverging duct. Liquid Hydrogen was the fuel of choice, burned with oxygen from the air. The struts had a dual purpose, serving both as compression surfaces (for diffusing the incoming air flow), and as an isolator (which separated the compression system from the burner and prevented the dreaded un-start condition). Tests indicated that the mission averaged specific impulse was about 580 seconds, with burner efficiencies being about 95% in ramjet and scramjet modes. A collection of attempts at analytical models of Rocket Based Combined Cycle engines exists in open literature.

Dr. John Olds, a former Georgia Tech professor, and current CEO of SpaceWorks Engineering published a series of AIAA articles including the following titles: "SCCREAM (Simulated Combined Cycle Rocket Engine Analysis Module): A Conceptual RBCC engine design tool", "Results of a Rocket-Based Combined Cycle SSTO Design Using Parametric MDO Methods", and "Multi-disciplinary Design of a Rocket Based Combined Cycle SSTO Launch Vehicle Using Taguchi Methods" [31–33]. Olds' work makes use of a computational tool which applies CFD principles to analyze the flow paths of RBCC concepts. Olds' later work includes analysis of entire RBCC SSTO vehicles. In the late 1990's and early 2000's NASA's Glenn Research Center published several NASA technical manuals describing the performance of a conceptual RBCC powered vehicle called the GTX Reference Vehicle. These technical manuals used CFD modeling to determine whether or not an air-breathing type rocket engine could power a reusable SSTO vehicle [15, 34].

## 3.4 Technical Overview of the Rocket Based Combined Cycle Engine

A promising variation of the RBCC, the Ejector Rocket in Dual-Combustion Propulsion System (ERIDANUS) is shown in Figure 3.2. In this diagram, a rocket is synergistically integrated within the flow path of a super/hypersonic vehicle. The rocket actually forms

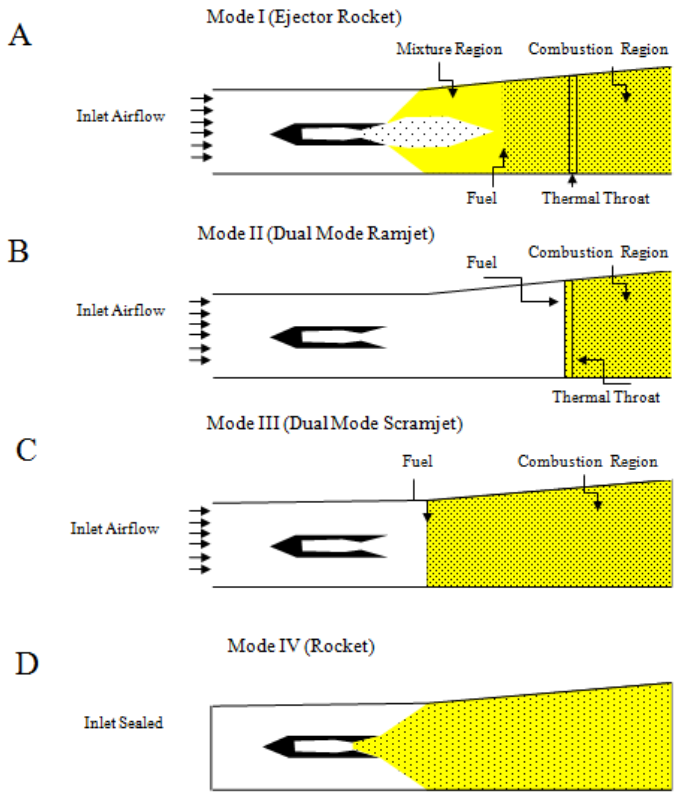


Figure 3.2: The Operational Modes of the Ejector Rocket in Dual-Mode Combustion Propulsion System (ERIDANUS)

the subsystem, which is placed in a fixed location upstream of the mixture region, burner, and expansion surface. The ejector rocket shown in Figure 3.2a operates as a gas generator (power providing device) for the entire system. The fuel/air mixture from the ejector exhaust becomes the primary mass flow for the system. The high velocity/ low pressure exhaust produces momentum thrust which accelerates the engine from static conditions to some Mach number greater than zero. This resulting motion produces a ram-air effect from the collision between the engines frontal area and the free stream, and therefore forces pressurized air (the secondary stream) from the free stream into the engine inlet. The relatively higher pressure of the secondary stream to the lower pressure primary stream creates a Venturi effect and creates suction of the secondary air from an upstream position to a region downstream of the ejector nozzle exit area.

The ratio of the secondary airflow to the primary ejector exhaust is called a bypass

ratio, and its behavior is similar to the bypass airflow in a turbofan. The bypassed flow is allowed to mix in a mixture region between the ejector exit area and the burner. Once the flow is fully mixed, heat is added to it via fuel injection. Fuel injectors are located at various positions to control the amount of airflow going into the burner. The flow is then expanded in a nozzle and net thrust is produced. A thermal throat is used instead of a physical nozzle to eliminate the necessity of variable geometry (since the same duct will be used for a scramjet mode later in the flight). The ejector effectively provides the burner with pressurized mass flow which would be equivalent to the ram-air pressure it would experience if the air were traveling at higher speeds [3]. This is the propulsion which is produced in the first mode of a Rocket Based Combined Cycle Engine. This is the primary mode of propulsion from static to low supersonic speeds (Mach 0 to Mach 3).

The engine behavior becomes more ramjet-like as the Mach number approaches Mach 3 (Figure 3.2b). At Mach 3, the engine transitions to ramjet mode. Mach 3 is generally chosen as a transition point to ramjet mode because ramjets generally attain maximum performance in the Mach 2 - 4 flight range [28]. The air is compressed with the fore body by a series of oblique shock waves forced on the lip of the engine. A translatable cowl lip is necessary to maximize compression efficiency. An isolator receives a series of resulting normal shocks and prevents the compression surface and burner from interacting to produce un-start. The compression produces subsonic burner entry Mach numbers for stable combustion. The thermal throat is still used though its axial location is different than in ejector mode. The expansion surface (nozzle) tries to match the pressure to ambient conditions and thrust is produced.

Limitations on ramjet performance occur near hypersonic speeds, Mach 5-6, which becomes a good transition point for scramjet mode Figure 3.2c. The compression need not produce subsonic combustion now, but supersonic speeds slow enough to match those of the fuel injector flows. The scramjet has optimal performance in this flight regime, but its performance decays as it approaches Mach 10 [16]. After Mach 10 the scramjet no longer functions, limited by increasing stagnation temperatures, and gas dissociations related to high burner and surface temperatures on the vehicles surfaces. The inlet is closed off, and the ejector rocket is 'turned on'. It is the only source of propulsion until the vehicle reaches orbital velocities (Mach 25). The rocket is in 'all-rocket mode' now Figure 3.2d.

## 3.5 Summary

In summary, the RBCC concept is an idea which has been introduced decades ago, yet it has limited though sufficient experimental and analytical validation. It is the intention of this thesis to revisit this old and largely under-rated yet promising idea. The goal of re-introducing the RBCC concept in the context of SSTO flight is to derive a preliminary analysis of the concept, prove its validity against known data, and re-generate a new wave of interest the synergism between rocket and air-breathing propulsion concepts. The following sections will explain the theoretical foundations used in this analysis, followed by descriptions of the methods of analysis used here. Finally a review of the engine performance code will be described and validated by comparing the analytical results here with known data.

# Chapter 4

# Theoretical Principles

## 4.1 Theoretical Principles of Thermodynamics and Fluid Mechanics

*"Consider a cask filled with a highly compressed gas. If we open one of its taps the gas will escape through it in a continuous flow, the elasticity of the gas pushing its particles into space will continuously push the cask itself. The result will a continuous change in the motion of the cask. Given a sufficient number of taps (say, six), we would be able to regulate the outflow of the gas as we liked and the cask (or sphere) would describe any curved line in accordance with any law of velocities."*

– Konstantin E. Tsiokovsky, explaining how a rocket works in space, 1883 [35].

### 4.1.1 Introduction

A proper treatment of the study of propulsion systems is incomplete and cannot be fully understood without the pre-requisites of foundational principles associated with the basic thermodynamic relations and the fundamental conservation equations associated with the mechanics of fluid motion. In this section, fundamental concepts including the control volume, thermodynamic system, and the continuum will be introduced with the purpose of providing background in the relationship between thermodynamics and fluid mechanics. Next, the general integral equations for the thermodynamics of fluid motion will be

introduced, including conservation of mass, momentum, and energy. The second law of thermodynamics will also be introduced, and discussion of the ideal gas laws will follow. These relations will allow the introduction of the key assumptions which are necessary for the development of one-dimensional gas dynamics analysis; the one-dimensional gas relations are crucial for the preliminary analysis of both air-breathing and rocket propulsion systems. Finally compressible flow relations will be formulated, including the compressible flow in ducts and the normal and oblique shock relations. This section closely follows the writings of Hill & Peterson, Anderson, Heiser & Pratt, and Oates [3, 28, 36, 37]. For more detailed derivations of the conservation laws any of these sources will be of considerable assistance. Without further ado, the concepts of control volume, the thermodynamic state, and the continuum will be introduced, followed by the conservation laws.

### 4.1.2 Definitions

#### Thermodynamic System

A system can be defined as a fixed collection of matter which maintains its identity (properties) as it undergoes changes of state. The state of a system is described as the conditions of a system as is specified by its properties (characteristics). A system can be thought of as the subject that is under study or analysis.

#### Control Volume

The boundary of a system is that which separates the system from its surroundings. The boundary of a system is known as a control volume. Boundaries of systems are allowed to change position, shape, or size. One definition of work is based on the ability of a force to change the shape (position) of a systems boundary [37]. The control volume describes the finite region through which a fluid propagates. Control Volume Analysis is a method of fluid mechanics analysis which selects a fixed region of a flow and performs calculations of the flow properties at the entrance and exit of the control volume of interest. A control volume is allowed to become fixed (not moving relative to the fluid) or can be free flowing (moving with the fluid). In general it is desired to know how a collection of mass behaves as it passes through the control volume. The control volume analysis method is crucial in studies of

systems which allow flows through their boundaries. Calculation of fluid properties at the entrance and exit of a control volume describes the influence of the control volume on the fluid.

### Continuum

The concept of a continuum is based on the simplifying assumption that fluid atomic structures will be ignored, and that the fluid is divided into infinitesimal identical structural components. Of course in reality fluids do not behave this way, and are not uniform in content but will vary as they are affected by external forces. This assumption just simplifies the equations which analyses flows, and is necessary for one-dimensional flow analysis [28].

### The Conservation Laws

The analysis of fluids is based on four governing relations, namely:

1. Conservation of Mass (Continuity)
2. Newtons Second Law of Motion (Momentum conservation)
3. The First Law of Thermodynamics (Energy conservation)
4. The Second Law of Thermodynamics (Irreversibility of processes)

These relations are fundamental in the study of fluids. The continuity law requires that the total mass of the system remain constant irrespective of size, shape, or quantity of fluid particularly for "non-relativistic" velocities of the fluid particles. Flows studied in this thesis will not approach 10% of the speed of light and hence all flows discussed here will be "non-relativistic" [28]. The effects of the continuity equation are best expressed in terms of relationships between fluid properties at various stations (locations in the control volume). For instance, for consecutive control volumes in a flow, properties can show that the flow is being heated if the temperature at'station 2' is larger than it is at 'station 1'. The statement of the conservation of mass is as follows: for mass given in a control volume, the total rate of change of mass in the control volume is equal to the difference between the mass flow rates entering and exiting the control volume. The mass flow rate out of the

control volume can be represented with the concept of flux, that is scalar product of the mass flow crossing the control surface $dA$ and the unit vector $\mathbf{n}$ which is perpendicular to the area $dA$. The general integral form of the continuity equation is expressed by the following relations:

$$\frac{D}{Dt}\iiint_{cv} \dot{m}\, dV = \frac{\partial}{\partial t}\iiint_{cv} \rho\, dV + \iint_{cs} (\rho \mathbf{v} \cdot \mathbf{n})\, dA \tag{4.1}$$

If there is no mass flow added to the system, the total rate of mass flow is fixed and the mass flow in the control volume is equal to the flux exiting the system. This expression is given by equation 4.2:

$$\frac{\partial}{\partial t}\iiint_{cv} \rho\, dV + \iint_{cs} (\rho \mathbf{v} \cdot \mathbf{n})\, dA = 0 \tag{4.2}$$

Newtons Second Law states that for a mass $m$ which is in motion with some velocity $\mathbf{v}$, the force $\mathbf{F}$ acting on the mass is equal to the rate of change of the total momentum $\mathbf{P}$ of the mass. This relation is given by the following expression:

$$\frac{d}{dt}\mathbf{P} = \frac{d}{dt}(m\mathbf{v}) = \frac{dm}{dt}\mathbf{v} + m\frac{d}{dt}\mathbf{v} = \mathbf{F} \tag{4.3}$$

Generally, there are two types of forces exerted on a control volume: body forces and surface forces. Body forces include gravitational and electromagnetic effects exerted on the fluid inside of the control volume from some distance from the system. Surface forces include shear and pressure effects which act along the surface of the control volume. The total force acting on the control volume can be expressed as the difference between integrals of the body forces per unit area $B$, and pressure/shear effects represented by $P$. Combining equation 4.3 for a control volume with the integral of all forces acting on the control volume gives the momentum equation as:

$$\begin{aligned} \mathbf{F_{cv}} &= \frac{D}{Dt}\iiint_{cv} \rho\mathbf{v}\, dV = \iiint_{cv} \rho\mathbf{B}\, dV - \iint_{cs} \rho\mathbf{P}\, dA \\ &= \frac{\partial}{\partial t}\iiint_{cv} \rho\mathbf{v}\, dV + \iint_{cs} (\rho(\mathbf{v})^2 \cdot \mathbf{n})\, dA \end{aligned} \tag{4.4}$$

The First Law of Thermodynamics relates the work and heat interactions between a system an its surroundings with the net effect of changing the state of the system through some thermodynamic process. Heat (or more precisely heat transfer) is a thermal interaction between surfaces with different temperatures. Heat transfer is a process and not a property, and thus cannot be stored but only transient action. The Zeroth Law of Thermodynamics governs the direction of heat transfer processes, only allowing them to go from a surface of a higher temperature to one of a lower temperature but never the converse. Work also is a process and not a property; work is the act of displacing the boundary of a system from one location to another under the action of a force. In 1840, the English physicist James Prescott Joule (1818 — 1889) conducted an expirement to explore the interaction between heat and work [37]. The result of the experiment can be expressed in the following relation of integral form relating the change of internal energy from an initial state $E_0$ to a final state $E$ to the difference between heat and work interactions on the system:

$$\Delta E = E - E_0 = \int_0 dQ - \int_0 dW \tag{4.5}$$

In general, the energy equation relates the total rate of energy change of the system to the work and heat rates through the system and can be described by the following relation:

$$\begin{aligned} \frac{D}{Dt}\iiint_{cv} e\rho\mathbf{v}\ dV &= \frac{\partial}{\partial t}\iiint_{cv} e\rho\mathbf{v}\ dV + \iint_{cs} e(\rho(\mathbf{v})^2\cdot\mathbf{n})\,dA \\ &= \iint_{cs}\dot{Q}\,dA - \iint_{cs}\dot{W}\,dA + \iiint_{cv}\rho\mathbf{B}\cdot\mathbf{v}\ dV \\ &+ \iint_{cs}(\rho(\mathbf{v})^2\cdot\mathbf{n})\,dA \end{aligned} \tag{4.6}$$

If there is no energy being added to the control volume, equation 4.6 becomes:

$$\begin{aligned} -\frac{\partial}{\partial t}\iiint_{cv} e\rho\mathbf{v}\ dV &= \iint_{cs} e(\rho(\mathbf{v})^2\cdot\mathbf{n})\,dA + \iint_{cs}\dot{Q}\,dA - \iint_{cs}\dot{W}\,dA \\ &+ \iiint_{cv}\rho\mathbf{B}\cdot\mathbf{v}\ dV + \iint_{cs}(\rho(\mathbf{v})^2\cdot\mathbf{n})\,dA \end{aligned} \tag{4.7}$$

The final general forms of the conservation equations are presented by the following:

Mass:

$$\frac{\partial}{\partial t}\iiint_{cv}\rho\,dV+\iint_{cs}(\rho\mathbf{v}\cdot\mathbf{n})\,dA=0 \tag{4.8}$$

Momentum:

$$\begin{aligned}\mathbf{F_{cv}}&=\frac{D}{Dt}\iiint_{cv}\rho\mathbf{v}\;dV=\iiint_{cv}\rho\mathbf{B}\;dV-\iint_{cs}\rho\mathbf{P}\;dA\\&=\frac{\partial}{\partial t}\iiint_{cv}\rho\mathbf{v}\,dV+\iint_{cs}(\rho(\mathbf{v})^2\cdot\mathbf{n})\,dA\end{aligned} \tag{4.9}$$

Energy:

$$\begin{aligned}-\frac{\partial}{\partial t}\iiint_{cv}e\rho\mathbf{v}\;dV=\iint_{cs}e(\rho(\mathbf{v})^2\cdot\mathbf{n})\,dA=\iint_{cs}\dot{Q}\,dA-\iint_{cs}\dot{W}\,dA\\+\iiint_{cv}\rho\mathbf{B}\cdot\mathbf{v}\;dV+\iint_{cs}(\rho(\mathbf{v})^2\cdot\mathbf{n})\,dA\end{aligned} \tag{4.10}$$

**The Second Law of Thermodynamics**

In the previous section, the first law of thermodynamics was described as a statement which asserts the fact that energy can only be transfered and that the total amount of energy remains the same through the process of transfer. From the Joule experiment, it was shown that energy transfer always seem to go in one direction: in heat and work interactions, when work is done on the system the internal energy increases. The reverse never occured: work done by the system decreasing the internal energy [37]. It is unrealistic to expect that a region surrounding a system could be an 'internal energy' container, where all of the energy from the surroundings could be converted to work interactions, but with no losses. The second law of thermodynamics implies the following statement: in a cyclical process, internal energy or heat cannot be drawn from the surroundings and converted into work [37]. A restatement of this law, when applied to the first law and zero'th law of thermodynamics can be expressed in the following relationship, which necessitatse the introduction of a quantity measuring the irreversability of thermodynamic processes: entropy $s$:

$$\Delta s=s_i-s_e=\int\frac{dq}{T} \tag{4.11}$$

Entropy, like heat and work is not a quantity which can be defined at a single state, but is a measure which is applied to the difference between states. The previous equation relates entropy to heat transfer and temperature. Entropy keeps a thermodynamic process from returning exactly to its previous state. If such an assumption is made which ignores this limitation the process is an isentropic process. Isentropic processes imply 'the most idealized' case possible (which is when there are no losses in the energy transfer). Real life cases are never truly isentropic, but isentropic analysis can tell what the 'best possibility' is.

## 4.2 The Thermodynamics of Quasi - One Dimensional Compressible Flows

The continuity, momentum, and energy equations from section 4.1 are in their integral forms are generalized for three special coordinates. The selection of governing equations to accurately model aerothermodynamic flows with simple relations (e.g. those which do not necessitate the use of CFD for preliminary analysis) is no easy task. Fortunately generations of aerodynamicists have used with confidence the quasi- one dimensional flow assumption to simplify solutions to aerothermodynamic fluid flows, while still having approximately accurate results [3]. The one-dimensional flow assumption in principle states that flow properties vary significantly only in the stream wise (axial) direction, but are uniform in directions perpendicular to the free stream. A more mathematical description of the one-dimensional assumption is that the flow properties depend only on one special coordinate (in the axial direction) [38]. This assumption effectively simplifies the conservation laws, making them solvable with simple algebraic relations. Advantages of the quasi  one dimensional assumption include the ability to use the stream thrust average method (assumes fluid properties are perfect at axial stations). This allows for the ability to analyze aerospace propulsion systems with control volume analysis methods by tracking fluid properties at the inlet and outlets between system components [3]. The modified continuity, momentum, and energy equations for quasi - one dimensional assumptions are:
Mass:

$$\rho_i \mathbf{v}_i A_i = \rho_e \mathbf{v}_e A_e \tag{4.12}$$

Momentum:

$$\rho_i \mathbf{v}_i^2 A_i + F_{by} = \rho_e \mathbf{v}_e^2 A_e \tag{4.13}$$

Energy:

$$\dot{m}_i \left( h_i + \frac{\mathbf{v}_i^2}{2} \right) = \dot{m}_e \left( h_e + \frac{\mathbf{v}_e^2}{2} \right) + \dot{Q} + \dot{W} \tag{4.14}$$

where the term $F_{by}$ in the momentum equation (equation 4.13) represents the momentum flow of fuel addition to the free stream air during combustion.

It is realized that the one-dimensional assumption ignores fluid phenomena including viscosity, boundary layer effects, and therefore is more appropriate for a preliminary study. With this truth in mind, the results produced in this thesis will not exactly match reality (because of the limits of the one dimensional assumption) and should be thought of as idealized or approximated results (since real aerospace flows are never truly one-dimensional). With this assumption in mind, flows through the control volumes of interest will be taken as steady (not time dependant) [28].

The only forces acting on the flow will be those related to changes at each station; no gravitational or electro-magnetic effects will be considered. Several important concepts related to the quasi-one dimensional compressible assumption are important. Those which will be considered in the remainder of this section include the perfect gas assumption, compressible flow relations, the isentropic compressible relations, the adiabatic and heat addition in duct relations, and finally the normal shock relations. The sum total of these concepts will be the foundations of the creation of the RBCC propulsion model mentioned in the next few chapters.

### 4.2.1 The Perfect Gas Relations

A perfect (ideal) gas can be described as one which behaves as if no molecular forces are acting within it [39]. The governing aerothermodynamic relations of one-dimensional compressible flow are simplified with the assumption that the gas behaves perfectly. Two relations (the perfect gas relation and the adiabatic/isentropic relation) are used to describe flows which have perfect behavior:

$$P = \rho RT = \frac{RT}{v} \tag{4.15}$$

and

$$\left(\frac{P}{\rho}\right)^{\gamma} = constant \tag{4.16}$$

A gas which obeys these laws (for which these relations are true) are called perfect gases. These relation simply represent the ideal observed behavior of gases [38]. A third relation describes a gases departure from perfect gas behavior, and is given by:

$$\frac{P}{\rho RT} = Z \tag{4.17}$$

Z is the compressibility factor, a number which in the ideal assumption is one, and in reality is always less than unity. R in the ideal gas and adiabatic/isentropic relation is the ideal gas constant, which is related by the equation:

$$R = \frac{\Re}{\mathcal{M}} \tag{4.18}$$

Where $\Re = 8.314\ kJ\ kg^{-1}K^{-1}$ and $\mathcal{M}$ is the molecular weight of the fluid of interest. In the analysis of supersonic and hypersonic vehicle propulsion these relations allow demonstrate the dependence of control volume property changes on the intrinsic properties of gases, namely mass, density (specific volume), temperature, and pressure. Four independent variables are necessary to specify the state of the flow - mass flow ( $\dot{m}$ ), velocity $\mathbf{v}$, or any pair of the variables $P$, $\rho$, or $T$ [38].

Perfect gases can be either calorically perfect, thermally perfect or both. To describe these concepts, specific enthalpy $h$, and specific internal energy $e$ will be introduced. Specific internal energy $e$ is associated with the random molecular motions summed over the entire gas [39]. Specific enthalpy $h$ can be thought of as the sum of the flow work and the internal energy of the gas. Both $e$ and $h$ have temperature dependence, though $h$ is sensitive to pressure, and specific volume $v$. Specific enthalpy and specific internal energy are described by the following relations:

$$h = e + PV \tag{4.19}$$

$$h = h(T, P) \tag{4.20}$$

$$e = e(T, v) \tag{4.21}$$

The temperature dependant rate of change of enthalpy at constant pressure describes the constant pressure specific heat $C_P$, while the temperature dependant rate of change of internal energy with specific volume fixed describes the constant volume specific heat $C_V$. These relations are as follows:

$$C_P = \left| \frac{\partial h}{\partial T} \right|_P \tag{4.22}$$

$$C_V = \left| \frac{\partial e}{\partial T} \right|_V \tag{4.23}$$

Specific heat is by definition the amount of heat transfer is necessary to raise the temperature of a given substance. A thermally perfect gas implies the specific heats are constant along constant temperature lines and shows the direct dependence of enthalpy and internal energy on temperature alone.

As long as the gas remains within the temperature range which will not allow temperature dissociation, the gas can be considered thermally and calorically perfect. At temperatures below about 2000 K air behaves as an equilibrium gas (that is there are no chemical reactions occurring within it). At temperatures 2000 K, $O_2$ begins to dissociate [3, 28]. At temperatures above 4000 K, $N_2$ also begins to dissociate. For the thermally and calorically perfect cases, the constant pressure and constant volume specific heats can be combined the following form:

$$\gamma = \frac{C_P}{C_V} \tag{4.24}$$

which can then be related to the ideal gas constant by:

$$C_P - C_V = R \tag{4.25}$$

In a calorically perfect gas, it is assumed that :

$$\frac{\partial C_P}{\partial T} = \frac{\partial C_V}{\partial T} = 0 \tag{4.26}$$

This statement is true as long as air has equilibrium behavior, and complete molecular dissociation does not occur, nor do chemical composition changes.

### 4.2.2 Mach Number

Until this point, no mention of the compressibility of flows has been mentioned. Compressibility can be thought of as the ability of the flow to change its density under compression. The measure of compressibility of a flow is essential in the study of high speed propulsion systems. Perhaps the most important parameter in compressible flow is the Mach number M [40]. When a disturbance occurs in a fluid, its ability to propagate through the fluid is dictated by the relation:

$$a^2 = \frac{\partial P}{\partial \rho} = \frac{\gamma P}{\rho} = \gamma RT \tag{4.27}$$

These relations describe the speed of sound, or the speed at which planar disturbances are allowed to propagate through a medium. The speed of sound can also be thought of as the measure of the compressibility of a fluid. For a fluid in motion the Mach number is a measure of the velocity of the fluid relative to the speed of sound and is defined by the following relations:

$$M = \frac{\mathbf{v}}{a} = \frac{\mathbf{v}}{\sqrt{\gamma RT}} \tag{4.28}$$

The Mach number is such an important measure of compressible flow properties that it is useful to relate other flow relations are often expressed in terms of the Mach number. The flow regimes which will be studied in this thesis are described based on their Mach numbers:

When $M < 1$ , the flow is in the subsonic flow regime,
When $M \approx 1$ , the flow is in the transonic flow regime,
When $M > 1$ , the flow is in the supersonic flow regime,
When $M > 6$ , the flow is in the hypersonic flow regime

Hypersonic flows are not rigidly defined, and their exact starting point will vary from one study to another. It is generally accepted by aerodynamicists that hypersonic flows are those which kinetic energy effects of the flow dominate over the energy related to molecular motions of the flow [3, 38].

### 4.2.3 Isentropic Compressible Flows and Normal Shock Relations

The one dimensional analysis method is useful in analyzing many flow conditions where the calorically and thermally perfect assumptions are valid. Such cases include simple flows in ducts where no heat is added (adiabatic flows), flows in ducts with stagnation temperature change (heat addition), and calculations across normal shocks. Each of the types of flow conditions which will be briefly examined will be directly applied in the analysis of the RBCC propulsion system in the next few chapters.

#### Adiabatic Flow in channel (Case 1)

The adiabatic flow condition is perhaps the simplest form of an isentropic compressible flow problem. In an adiabatic flow (no heat is added) the stagnation temperature at the entrance and exit of the control volume is the same $T_{te} = T_{ti}$. If an adiabatic one dimensional flow has no energy interactions with its surroundings the energy equation across any two stations is reduced to:

$$h_e + \frac{\mathbf{v_e}^2}{2} = h_i + \frac{\mathbf{v_i}^2}{2} = h_t \tag{4.29}$$

Where $h_t$ represents the total enthalpy of the flow. Total conditions (also called stagnation conditions) describe the total energy of a fluid element would contain if it were isentropically brought to rest [39, 40]. In other words, stagnation conditions explain how much of the energy of the flow is due to energy forms which are not kinetic. This form of the conservation of energy can be re-arranged to represent flow conditions in terms of total (stagnation) temperature as follows:

$$C_P T_e + \frac{\mathbf{v_e}^2}{2} = C_P T_i + \frac{\mathbf{v_i}^2}{2} = C_P T_t \tag{4.30}$$

Introducing the Mach number, and expressing the energy equation for total temperature in terms of Mach number and local temperature, the energy equation becomes:

$$\frac{T_t}{T} = 1 + \frac{\gamma - 1}{2} M^2 \tag{4.31}$$

This relation can be thought of as a ratio of kinetic energy effects of the flow to other energy forms. Pressure can also be expressed using the Mach number dependant isentropic compressible flow relations:

$$\frac{P_t}{P} = \left(\frac{T_t}{T}\right)^{\frac{\gamma-1}{\gamma}} = \left(1 + \frac{\gamma-1}{2}M^2\right)^{\frac{\gamma-1}{\gamma}} \tag{4.32}$$

These relations are useful in relating local and total flow properties of any perfect gas across any pair of locations in a flow field. It is now useful to introduce relations which govern mass flow per unit area for a given adiabatic one dimensional flow in a channel. The velocity of a flow leaving a control volume can be expressed using the isentropic pressure relations, yielding:

$$\mathbf{v_e} = \sqrt{2C_P T_{ti}\left\{1 - \left(\frac{P_e}{P_{ti}}\right)^{\frac{\gamma-1}{\gamma}}\right\}} \tag{4.33}$$

From this equation, after re-arrangements are performed, the mass flow per unit area leaving the control volume can be expressed by the following relations:

$$\frac{\dot{m}_e}{A_e} = \rho_e \mathbf{v_e} = \frac{P_e \mathbf{v_e}}{RT_e} = M_e\left(\frac{P_e}{P_{ti}}\right)\sqrt{\frac{T_{ti}}{T_e}}P_{ti}\sqrt{\frac{\gamma}{RT_{ti}}} \tag{4.34}$$

Additional rearrangements as described by Heiser & Pratt [3] form the equation known as the mass flow parameter:

$$MFP_e = \frac{\dot{m}_e\sqrt{T_{ti}}}{P_{ti}A_e} = \sqrt{\frac{\gamma}{R}}M_e\left(1 + \frac{\gamma-1}{2}M_e^2\right)^{\frac{-\gamma+1}{2(\gamma-1)}} \tag{4.35}$$

The mass flow parameter $MFP_e$ is a Mach number dependant relation which relates the mass flow leaving a control volume to gas properties. From Figure 4.1 it can be seen that for any Mach number and pressure ratio $(P/P_t)$ the mass flow parameter cannot increase indefinitely. The mass flow parameter $MFP_e$ is fixed by the Mach number, and approaches a maximum value as the Mach number approaches unity. When the Mach number approaches unity, the flow velocity is equal to the speed of sound and the flow is said to be choked. Choked flow conditions are those which exist when M = 1. These conditions areconventionally marked with an asterisk $(*)$. When M = 1 the maximum area

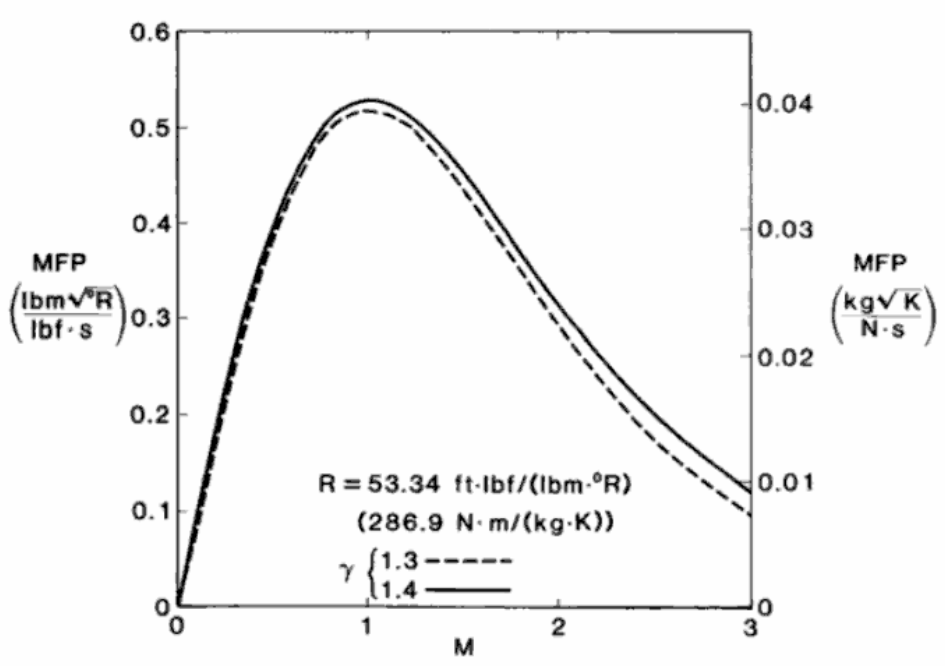


Figure 4.1: Mass Flow Parameter as a Function of Stream Mach Number [3]

contraction is represented by:

$$\frac{A}{A^*} = \frac{1}{M}\left[\frac{2}{\gamma+1}\left(1+\frac{\gamma-1}{2}M^2\right)\right]^{\frac{\gamma+1}{2(\gamma-1)}} \tag{4.36}$$

Other flow properties can be expressed at the choked condition:

$$\frac{T}{T^*} = \frac{\gamma+1}{2\left(1+\frac{\gamma-1}{2}M^2\right)} \tag{4.37}$$

$$\frac{P}{P^*} = \left[\frac{\gamma+1}{2\left(1+\frac{\gamma-1}{2}M^2\right)}\right]^{\frac{\gamma}{\gamma-1}} \tag{4.38}$$

$$\mathbf{v}^* = a^* = \sqrt{\frac{2\gamma}{\gamma-1}RT_t} \tag{4.39}$$

The choked flow property variations with control volume entrance Mach number for $\gamma = 1.2$ and 1.3 can be seen in the plot from Figure 4.2. The previous relations, and those ratios plotted in Figure 4.2 can be used to determine the necessary through flow

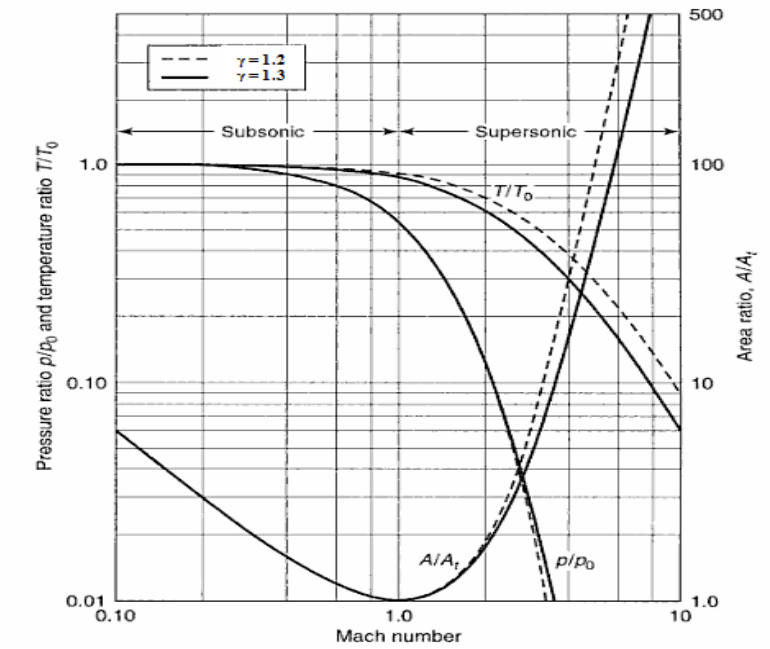


Figure 4.2: Choked Flow Conditions for $T/T_t$, $P/P_t$, $A/A^*$ [41]

area required for a given Mach number, or to determine the Mach number with the other conditions given. This type of analysis is used in the design of rocket engine nozzle which uses the choked throat to expand flows after combustion [28, 38, 41].

**Constant Area Heat Addition With Stagnation Temperature Change (Case 2)**

A second special case for which the one-dimensional equations can be used to analyze is frictionless flow in a constant area duct, with a change in stagnation temperature. In such an analysis, heat addition can be replaced with a change in stagnation temperature at the inlet and exit conditions of the duct represented by a control volume. This case is a classical example of a special type of flow called Rayleigh flow [3, 7, 28]. The continuity equations for constant area heat addition are of the following forms:

$$\frac{d\rho}{\rho} + \frac{d\mathbf{v}}{\mathbf{v}} = 0 \tag{4.40}$$

$$\frac{dP}{d\mathbf{v}} = -\rho\mathbf{v} \tag{4.41}$$

$$dh_t = dh + \mathbf{v}d\mathbf{v} = dq - w \tag{4.42}$$

By using the Mach number, a relation for the pressure across the control volume can be expressed as:

$$\frac{P_e}{P_i} = \frac{1+\gamma M_i^2}{1+\gamma M_e^2} \tag{4.43}$$

Using the perfect gas law, pressure and temperature can be related with the equations:

$$\frac{M_e}{M_i} = \frac{\mathbf{v_e}a_i}{\mathbf{v_i}a_e} = \frac{\mathbf{v_e}}{\mathbf{v_i}}\sqrt{\frac{T_i}{T_e}} \tag{4.44}$$

$$\frac{T_e}{T_i} = \frac{M_e^2\left(1+\gamma M_i^2\right)^2}{M_i^2\left(1+\gamma M_e^2\right)^2} \tag{4.45}$$

The isentropic total pressure relation can be given using the local pressure ratio and the local temperature ratio in terms of Mach number:

$$\frac{P_{te}}{P_{ti}} = \frac{1+\gamma M_i^2}{1+\gamma M_e^2}\left(\frac{\left(1+\frac{\gamma-1}{2}M_e^2\right)}{\left(1+\frac{\gamma-1}{2}M_e^2\right)}\right)^{\frac{\gamma}{\gamma-1}} \tag{4.46}$$

The energy equation expressed by total temperatures is expressed using the relation:

$$\frac{T_{te}}{T_{ti}} = \frac{M_e^2\left(1+\gamma M_i^2\right)^2}{M_i^2\left(1+\gamma M_e^2\right)^2}\frac{\left(1+\frac{\gamma-1}{2}M_e^2\right)}{\left(1+\frac{\gamma-1}{2}M_e^2\right)} \tag{4.47}$$

Heat transfer can be measured directly from stagnation temperature difference by the following:

$$Q = C_P(T_e - T_i) + \frac{\mathbf{v_e^2} - \mathbf{v_i^2}}{2} = C_P(T_{te} - T_{ti}) \tag{4.48}$$

Fundamental limitations exist relating how much heat can be added to a subsonic or supersonic flow. These limits can be visualized by in the Rayleigh heating diagram in Figure 4.3. It should be noted that as a subsonic flow is heated (the stagnation temperature is raised) the flow approaches a Mach number of unity. When a supersonic flow has stagnation temperature increase, its Mach number also approaches unity. When a subsonic or supersonic flow is forced to reach unity by heat addition, the flow is said to be choked, meaning no more heat can be added to the flow [7]. Relations for temperature and pressure

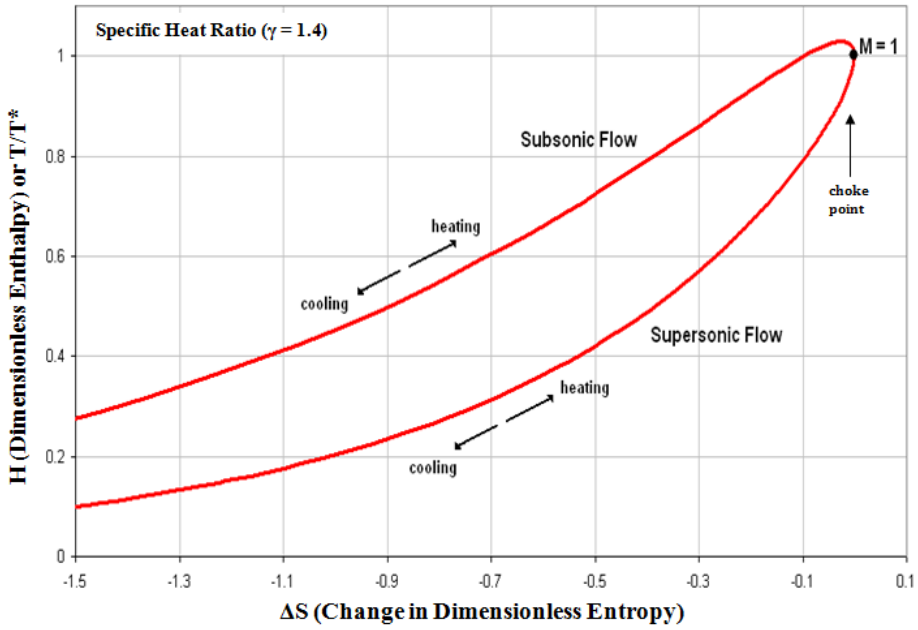


Figure 4.3: Heating and Choking in Rayleigh Flow

for choking conditions are given as they are in Shapiro [7] by the following:

$$\frac{T}{T^*} = \left(\frac{1+\gamma}{1+\gamma M^2}\right)^2 M^2 \tag{4.49}$$

$$\frac{T_t}{T_t^*} = \frac{2(\gamma+1)M^2\left(1+\frac{\gamma-1}{2}M^2\right)}{(1+\gamma M^2)^2} \tag{4.50}$$

$$\frac{P}{P^*} = \frac{1+\gamma}{1+\gamma M^2} \tag{4.51}$$

$$\frac{P_t}{P_t^*} = \left(\frac{2}{\gamma+1}\right)^{\frac{\gamma}{\gamma-1}} \left(\frac{1+\gamma}{1+\gamma M^2}\right)\left(1+\frac{\gamma-1}{2}M^2\right)^{\frac{\gamma}{\gamma-1}} \tag{4.52}$$

Thermal choking is useful in the expansion of subsonic flows to supersonic conditions in non-converging ducts. This eliminates the necessity of a physical throat. With these relations, thermal choking of ramjet and ejector rocket flows leaving the burner can be modeled.

**Normal Shock Relations (Case 3)**

The final consideration which will demonstrate the usefulness of the one-dimensional analytical methods will be in the calculations of non-isentropic gas flow properties across normal shock waves. In the formation of a normal shock is produced by a discontinuous rise in pressure, temperature, and density. A normal shock wave can be modeled as a differentially small control volume, where flow properties depend on the Mach number on both sides of the shock wave [38,39]. In a normal shock, one side of the shock will always be greater than one, and the other side will be less than one. Since a normal shock is adiabatic, the basic one dimensional normal shock relation are derived from the same forms of the continuity equations from Case 1. The Mach number immediately down stream of the normal shock exit is given by the following:

$$M_e^2 = \frac{1 + \left[\frac{(\gamma-1)}{2}\right] M_i^2}{\gamma M_i^2 - \frac{(\gamma-1)}{2}} \tag{4.53}$$

The temperature, pressure, velocity, and density losses across a normal shock wave can be expressed by the following relations:

$$\frac{T_e}{T_i} = \left[1 + \frac{2\gamma}{\gamma+1}\left(M_i^2 - 1\right)\right]\left[\frac{2 + (\gamma-1)\, M_i^2}{(\gamma+1)\, M_i^2}\right] \tag{4.54}$$

$$\frac{P_e}{P_i} = 1 + \frac{2\gamma}{\gamma+1}\left(M_i^2 - 1\right) \tag{4.55}$$

$$\frac{\mathbf{v_e}}{\mathbf{v_i}} = \frac{\rho_e}{\rho_i} = \frac{(\gamma+1)\, M_i^2}{2 + (\gamma-1)\, M_i^2} \tag{4.56}$$

Finally, these relations are important in the design of ramjet compression systems, which make use of normal shock waves to diffuse the incoming flow to speeds low enough for stable combustion. With these relations gas properties across the shock can be found [38].

## 4.3 Performance Metrics

The purpose of a propulsion system is to produce thrust. Several methods of thrust production for various aerospace systems exist, including, chemical reactions, nuclear reac-

tions, electromagnetic field interactions. In this study, the thrust producing methods are limited to chemical reactions both of air-breathing and rocket engines. A RBCC engine behaves as an air-breathing engine in atmospheric flight, making use of fuel carried on board and burning it with oxygen from the air, and as a rocket in the vacuum of space. Several performance relations exist to analyze how efficiently an aerospace system produces thrust. Some relations apply for both air breathing and rocket engines including thrust and specific impulse. Others are unique to air breathing engines (Thrust Specific Fuel Consumption (TSFC), fuel air ratio, and specific thrust). The next two sections will briefly explain the theory and relations which describe the performance of air breathing and rocket engines.

### 4.3.1 Air-Breathing Performance Metrics

The one dimensional analytical method is applicable to the measure of the performance of air-breathing engines. This method uses the engine control volume method to calculate changes in the quantities related to engine performance. In general thrust in an air-breathing engine is generated by inhaling free stream air, heating it, and expanding it through a nozzle [39]. Effectively this process is momentum transfer of mass through the system, and the momentum change leaving the system imparts a force in the opposing direction, according to Newtons third law (as is described by equation 4.3) for a fluid. Momentum transfer is produced either by heat addition or area changes in ducts [3].

#### Stream Thrust Function

A useful performance relation which describes the momentum transfer of a flow is the stream thrust parameter (also called the impulse function). On a cross sectional area the force which is acts on the control volume is given by:

$$\Im = PA + \dot{m}\mathbf{v} = AP(1 + \gamma M^2) \tag{4.57}$$

This equation is a modified version of the momentum equation which is relevant to ideal compressible flows. A modified version of the stream thrust parameter can be introduced, which accounts for the stream thrust parameter per unit mass. This quantity is called the stream thrust function and is given by [3]:

$$S_a = \frac{\Im}{\dot{m}} = \mathbf{v}\left(1 + \frac{RT}{\mathbf{v}^2}\right) \tag{4.58}$$

The stream thrust function allows for a simple means of determining mass flow rate specific thrust, which is useful in performance evaluations without accounting for absolute size.

**Specific Thrust**

The true nature of thrust is the net force produced by pressure and shear stress distributions on the surface of the engine. In one dimensional analysis the axial thrust on the engine is the integrated effects of pressure and shear forces produced both by engine internal pressures and atmospheric pressure effects on the engine given by the equation:

$$F_{total} = \int P_a dA + P_a(A_i - A_e) \tag{4.59}$$

After simplifications (including accounting for fuel and air mass flows), the final form of the air-breathing engine thrust equations is given by:

$$F = (\dot{m}_{air} + \dot{m}_{fuel})\,\mathbf{v_e} + (P_e - P_a)A_e \tag{4.60}$$

Specific thrust is defined as the uninstalled thrust $F$ per unit entry mass flow $\dot{m}_0$. The term 'uninstalled thrust' refers to only to forces internal to the system (as produced by the engine). Uninstalled thrust neglects forces external to the engine including vehicle drag. The term 'installed thrust' refers to difference between the uninstalled thrust and the external drag forces produced by the vehicle in flight through the atmosphere [3]. In this thesis, the baseline propulsion model focuses only on the forces produced by the engine and therefore specific thrust will be derived from the uninstalled thrust. Here thrust and uninstalled thrust will be used synonymously. The emphasis here is on the dependence of uninstalled thrust on the mount of mass flow entering the system. Specific thrust can be derived in terms of ideal gas/ compressible flow characteristics, and also in terms of the stream thrust function:

$$\frac{F}{\dot{m}_0} = (1+f)Sa_e - Sa_i - \frac{R_i T_i}{\mathbf{v}}\left(\frac{A_e}{A_i} - 1\right) \tag{4.61}$$

In this relation $f$ is the fuel to air ratio, and will be described in more detail shortly.

**Thrust Specific Fuel Consumption**

The thrust specific fuel consumption (TSFC) is defined as the ratio of the fuel mass flow rate to the uninstalled thrust:

$$TSFC = \frac{\dot{m}_f}{F} \tag{4.62}$$

This parameter shows the dependence of engine fuel mass flow on the uninstalled thrust. Another way to see TSFC is the amount of thrust is being generated for each unit mass of engine fuel every second [3].

**Specific Impulse**

Specific impulse is one of the most important figures of merit for the overall performance of an aerospace engine. Specific impulse ($I_{sp}$) is generally described in literature as the ratio of the uninstalled thrust to weight flow rate, as is described by the following relation:

$$I_{sp} = \frac{F}{g_0 \dot{m}_f} \tag{4.63}$$

where $g_0$ is the sea level value of the gravitational constant. In this thesis, the term specific impulse (when applied to the air-breathing mode of RBCC operation) will be used synonymously with uninstalled specific impulse. This convention specifies that the specific thrust and the specific impulse calculated from specific thrust includes only forces produced by the engine and not external vehicle drag forces. Specific impulse is a measure of the amount of thrust produced per unit mass of fuel. It can be thought of as the amount of force produced for each amount of fuel. It has the inverse effect of specific fuel consumption, which measures the amount of fuel is burned for every unit of thrust. Both of these quantities are of extreme importance to engine performance, primarily because they allow direct comparison of engine performance regardless of engine or vehicle size. [3].

**Fuel / Air Ratio**

Though not a true performance parameter the fuel to air ratio, has a direct influence on the combustion performance of an aerospace engine. The fuel to air ratio is the ratio of the mass flow of fuel to that of air entering the vehicle inlet:

$$f = \frac{\dot{m}_f}{\dot{m}_0} \tag{4.64}$$

The fuel to air ratio is limited by the chemical composition of the fuel of choice. The stoichiometric fuel to air ratio is a measure of the available molecules of fuel to those of air available for combustion. When the fuel and air elements are completely burned, the combustion is said to be stoichiometric. Fuel rich and fuel lean burns indicate combustion processes in which either fuel is left after combustion, or there was not enough fuel for continued combustion. The expression of the stoichiometric fuel to air ratio is:

$$f_{st} = \frac{36_x + 3_y}{103(4_x + y)} \tag{4.65}$$

The xs and ys represent the amount of carbon and hydrogen atoms in the fuel. In an all-hydrogen fuel this equation leads to the comclusion that x = 0, y = 2, and $f_{st} = 0.0291$. Finally, the equivalence ratio $ER$ tells how close to stoichiometric a fuel mixture is. The equation for $ER$ is:

$$ER = \frac{f}{f_{st}} \tag{4.66}$$

**Airbreathing Engine Efficiency Relations**

In thermodynamics, the concept of efficiency relates the actual energy in a system to the ideal efficiency. In aerospace propulsion systems, efficiency is a measure of the engines ability to convert chemical energy into mechanical energy. A parameter is introduced to describe this process: the air breathing overall efficiency $\eta_o$. Overall efficiency is given by the ratio of the thrust power $FV$ and the chemical energy rate $\dot{m}_f h_{PR}$:

$$\eta_0 = \frac{FV}{\dot{m}_f h_{PR}} \tag{4.67}$$

Two other efficiency parameters can be introduced to further describe the overall efficiency: thermal efficiency $\eta_{th}$ and propulsive efficiency $\eta_p$. Thermal efficiency relates the engines mechanical power to the rate at which chemical energy is transferred:

$$\eta_{th} = \frac{(1+f)\frac{\mathbf{v_e^2}}{2} - \frac{\mathbf{v_0}^2}{2}}{fh_{PR}} \tag{4.68}$$

The propulsive efficiency relates the thrust produced to the engines mechanical power in the relation:

$$\eta_p = \frac{FV}{\dot{m}_0\left((1+f)\frac{\mathbf{v_e^2}}{2} - \frac{\mathbf{v_0^2}}{2}\right)} \tag{4.69}$$

Together, the product of the thermal and propulsive efficiencies gives the airbreathing overall efficiency:

$$\eta_0 = \eta_{th}\eta_p = \frac{(1+f)\frac{\mathbf{v_e^2}}{2} - \frac{\mathbf{v_0^2}}{2}}{fh_{PR}} \frac{FV}{\dot{m}_0\left\{(1+f)\frac{\mathbf{v_e^2}}{2} - \frac{\mathbf{v_0^2}}{2}\right\}} \tag{4.70}$$

The overall, thermal, and propulsive efficiencies introduced in this section are extremely useful in the analysis of airbreathing engines. These efficiencies take values between 0 and 1 because of the Second Law of Thermodynamics. The closer the efficiencies are to one, the better the engine performs [3].

### 4.3.2 Rocket Performance Metrics

Rockets are devices which use Newton's 2nd Law of motion to convert the chemical energy of a propellant (usually by the combustion of a fuel with and oxidizer) to mechanical energy ejected from a nozzle facing in the opposing direction of desired travel. Newton's law states that force applied to move an object is proportional to the rate of change of its linear momentum and is described by equation 4.3. From these relations Tsiolkovskiy was able to find the exhaust velocity and the specific impulse required for a certain amount of acceleration $\Delta V$. The relationship which Tsiolkovskiy derived is the most important relation in rocket propulsion, relating $I_{sp}$ (or the maximum exhust velocity $V_e$) with the maximum attainable $\Delta V$, and the mass fraction $m_f/m_i$ (where $m_i$ represents the initial mass at rocket takeoff and $m_f$ represents the amount of mass after the propellant has been

fully exhausted) [14, 41]. Integrating and re-arranging equaiton 4.3 gives Tsiolkovskiy's famed rocket equation:

$$\int dV = V_e \int \frac{dm}{m} = V_e \ln\left(\frac{M_f}{M_i}\right) = g_0 I_{sp} \ln\left(\frac{M_f}{M_i}\right) = \Delta V \tag{4.71}$$

The exhaust velocity $V_e$ of a rocket is perhaps the most influential parameter which governs the performance of a rocket. Through the relationship:

$$V_e = g_0 I_{sp} \tag{4.72}$$

it governs the maximum amount of specific impulse a rocket can produce assuming the rocket is fully expanded. A higher exhaust velocity produces a higher rocket velocity. Limitations exist on the maximum amount of exhaust velocity a rocket produces, which are based on the chemical reactions of the propellant. For instance, gunpowder can produce $V_e$'s of 2000 $m\ s^{-1}$, while the most advanced liquid-fueled rockets can produce $V_e$'s of 4500 $m\ s^{-1}$, limiting the theoretical maximum $I_{sp}$ to about 500 seconds [14].

A modified version of equation 4.71 can be introduced, which includes the effects of acceleration due to thrust produced by the rocket engine. This modification has the following relation [42]:

$$\Delta V = g_0 I_{sp} \left[\ln\left(\frac{m_f}{m_i}\right) - \frac{1}{\mathcal{R}}\left(1 - \frac{1}{\frac{m_f}{m_i}}\right)\right] \tag{4.73}$$

where the Thrust Ratio $\mathcal{R}$ is defined as the thrust of the rocket divided by its weight at liftoff:

$$\mathcal{R} = \frac{T}{m_0 g_0} = \frac{a_0}{g_0} + 1 \tag{4.74}$$

and $a_0$ is the initial acceleration during the rocket's accent. This equation makes it possible to plot $\Delta V$ vs. $m_f/m_i$ with constant $I_{sp}$'s for calculating the payload/structure or conversely the propellant percentage of the entire GLOW of the vehicle for a given $I_{sp}$ of any rocket engine [42].

Much discussion has been made about the $\Delta V$ or conversly Mach number required for

orbit. The $\Delta V$ for orbital velocity is given by the following equation:

$$\Delta V = \sqrt{\frac{GM}{r}} \tag{4.75}$$

where $GM = \mu$ is the Earth Standard Gravitational Parameter ($\mu = 3.986 \times 10^5\ km\ s^{-1}$). Coupling this relation with equation 4.29 gives the Mach number for orbital insertion, which depends on the orbital altitude of interest ($r$):

$$M = \frac{\Delta V}{a} = \frac{\sqrt{\frac{GM}{r}}}{\sqrt{\gamma RT}} \tag{4.76}$$

Generally, open literature will place the Mach number for orbital insertion to be about M = 25 [26].

Finally, equations which describe the performance of rockets based on the one dimenisional compressible flow relations will be introduced. Many of the relations described in previous sections including the total to local temperature and pressure relations $T/T_t$, and $P/P_t$ are applicable to rocket nozzle thermodynamics and will not be reintroduced (see section 4.2) The exit velocity $V_e$ can be also be described using compressible flow relations which are Mach number dependant. It is expressed in terms of the ideal gas constant $R$, and the total to local pressure ratio $P/P_t$ [41, 43] :

$$V_e = \sqrt{\frac{2\gamma}{\gamma - 1}\left[1 - \left(\frac{P_e}{P_i}\right)^{\frac{\gamma-1}{\gamma}}\right]} \tag{4.77}$$

The thrust of a rocket is given by modified version of the thrust equation for the air-breathing engine equation 4.61:

$$F = \dot{m}V_e + (P_e - P_a)A_e \tag{4.78}$$

Thrust can also be expressed with the compressible thermodynamics relations [41, 43]:

$$F = A^* P_c \sqrt{\frac{2\gamma^2}{\gamma - 1}\frac{2}{\gamma - 1}^{\frac{\gamma+1}{\gamma-1}}\left[1 - \left(\frac{P_e}{P_i}\right)^{\frac{\gamma-1}{\gamma}}\right]} + (P_e - P_a)A_e \tag{4.79}$$

where $A^*$ is the flow at the choke location in the rocket (from equation 4.37 ), and $P_c$ is the combustion chamber pressure. These relations and others mentioned in this section can be used to model the thermodynamics and performance of rocket engines.

### 4.3.3 RBCC System Performance

In Chapter 1, it was stated that one of the objectives of this thesis was the analysis of the performance of the ERIDANUS RBCC concept. Performance is to be measured through the use of metrics commonly used in aerospace propulsion related literature, and those mentined in the previous section including $I_{sp}$, $TSFC$, $F/\dot{m}$, and $\eta_0$. Other metrics which measure individual component performance (e.g. diffuser performance which is measured by the air capture and pressure recovery ratios $A_0/A_i$ and $P_{t3}/P_{t0}$) will be discussed in the following section. Since Rocket Based Combined Cycle Engines demonstrate both air-breathing and rocket behavior, one can expect that any given plot of the overall performance of the system will show visible air-breather and rocket like traits. Unfortunately, some metrics only measure the system's performance in an air-breathing mode (e.g. TSFC), but is not applicable to the RBCC in rocket mode.

There is a necessity to introduce performance metrics which measure the performance of the RBCC system from takeoff to orbital insertion, across the necessary flight regimes. Since specific impulse and specific thrust are applicable to air-breathing and rocket powered systems, these metrics are useful for entire system performance studies. The measure of specific impulse for the entire flight is of primary importance here. Chapter 1 briefly mentions the influence of increased propulsion perfomance on the propellant weight requirement of a trans-atmospheric accelerator.

For all-rocket systems, equations 4.71 and 4.72 give the mass fraction, or inversely the mass ratio which dictates the amount of total launch vehicle weight is available for propellant, structure, and payload, for a given engine specific impulse. Since rocket specific impulses do not change drastically during their accent into orbit, averaged $I_{sp}$'s are used in equations 4.71 and 4.72. For air-breathing accelerator systems, $I_{sp}$ varies dramatically. Several approaches exist to quantitify the amount of propellant required for a trans-atmospheric accelerator employing an air-breathing engine.

In "A User's Primer for Comparative Assessments of All-Rocket and Rocket-Based Combined-Cycle Propulsin Systems for Advanced Earth-to-Orbit Space Transport Applications", William Escher and Eric Hyde developed a method of analyzing the propellant performance of combined cycle engines as based on the rocket equation [30]. In this article, two performance metrics are introduced, effective specific impulse ($I_{eff}$), and equivalent effective specific impulse ($I^*$). Effective specific impulse is a measure of the conventional specific impulse, but is modified to account for system losses associated with the ascent trajectory and vehicle drag. Effective specific impulse is given by the following relation:

$$I_{eff} = I_{sp}\left[1 - \frac{W\sin\theta}{F} - \frac{D}{F}\right] \tag{4.80}$$

where $W/F$ is the weight/thrust ratio, $\theta$ is the vehicle flight path angle, and $D/F$ is the drag/thrust ratio. Effective specific impulse is analogous to the conventional specific impulse, and represents an instantaneous value for engine performance for a given position and time during the vehicle's acceleration through the atmosphere and into LEO. Effective specific impulse is based on the acceleration components of all forces acting on the vehicle added together, with the vehicle aligned with its velocity vector [30].

In its purest for, effective specific impulse is useless in calculating payload, structure or inversely propellant mass requirements, because the rocket equation requires an average value for specific impulse rather than an instantaneous one. Escher introduced the equivalent effective specific impulse to address this problem. The equivalent effective specific impulse is a modification of the conventional specific impulse which takes into account the effects of non-idealities such as drag and gravity effects. Equivalent effective specific impulse generally will be lower than its conventional counterpart [30]. Mathematically, the equivalent effective specific impulse is defined as:

$$I^* = \frac{\Delta V_{flight}}{\int \frac{dV}{I_{eff}}} = \frac{\Delta V_{flight}}{g_0 \ln\left(\frac{M_i}{M_f}\right)} \tag{4.81}$$

In equation 4.81, it is obvious that equivalent effective specific impulse includes an integration of the effective specific impulse over the flight range of interest. This effectively acts as an averaging value of specific impulse, which takes into account gravity and drag losses.

Effective specific impulse, and equivalent effective specific impulse are useful metrics for detailed RBCC models which include trajectory analysis and external vehicle drag effects. In this thesis, the ERIDANUS model is meant to be a basic model which does not include trajectory analysis or external vehicle drag. It is therefore necessary to calculate specific impulse across the flight regime in another way. Since drag or trajectory effects are not included, the propellant performance in this thesis will use two specific impulse metrics: the mission averaged specific impulse or $I_{spAVG}$, and the conventional $I_{sp}$. The mission averaged specific impulse ( $I_{spAVG}$) uses a weighted averaging method to produce a single value which represents the specific impulse of the RBCC system in all modes of operation. Since ejector mode, ramjet mode, scramjet mode, and rocket mode, all produce different specific impulse values and ranges, and operate in different Mach number intervals, the mission average is based off of the sum of $I_{sp}$ averages in each mode. The weighting factor was calculated by the ratio of the Mach number interval for the mode (e.g. scramjet mode is Mach 10 - Mach 6 = 4) to the total range of flight Mach numbers. The equation for the mission averaged specific impulse derived here is as follows:

$$\begin{aligned} I_{spAVG} &= I_{spMODE1} + I_{spMODE2} + I_{spMODE3} + I_{spMODE4} \\ &= WF_1 \frac{I_3 + I_0}{2} + WF_2 \frac{I_6 + I_3}{2} + WF_3 \frac{I_{10} + I_6}{2} + WF_4 \frac{I_{25} + I_{10}}{2} \end{aligned} \tag{4.82}$$

where $WF_i$ in each term represent the relative weights of ejector, ramjet, scramjet, and rocket mode on the entire flight profile. The subscripts for in the $I_{sp}$ terms in equation 4.82 represent the begining and end points (Mach numbers) for each mode of operation. This method is more appropriate in this thesis because it does not include terms for drag or other effects not originally calculated in the code. Fortunately, those items can be included in the code in the form of more detailed analysis.

Finally, this method can produce an average value of an RBCC performance metric which can be easily included in the rocket equation and used to estimate the amount of propellant required for a vehicle powered by an ERIDANUS RBCC engine. Furthermore, the mission averaged specific impulse as derived here can be used to figure out via the rocket equation the percentage of the GLOW is available for structure and propellant.

# Chapter 5

# Analytical Methods and Procedures

*"If a higly respected and well-established authority tells you something is possible, then he is probably right; if he tells you something is impossible, he is probably wrong "*

– Arthur C. Clarke, 'Clarke's Law' [44]

## 5.1 Introduction

The previous section presented the foundations which allow for the preliminary analysis of airbreathing and rocket engine performance using the one dimensional method. This section will accomplish the goal of demonstrating how the theoretical approach to the use of one dimensional analysis will be applied. Several approaches exist in one dimensional analysis, including the closed thermodynamic cycle analysis method, the first law of thermodynamics method, and the stream thrust method. This thesis used the stream thrust method, which will be discussed later in this section. Several limited models exist for the analysis of ejector rockets, ramjets, and scramjets using one dimensional methods; this thesis follows the methods used by F.S. Billig, Heiser Pratt, Shapiro, Sutton, and Hale [3,6,7,41,43]. After a brief detailed description of the analytical methods and computational tool used, the remainder of this section will describe the procedure through which

the RBCC propulsion system model was created. This section is the link between the theory of airbreathing and rocket performance, and the results which the code produced.

## 5.2 Methodology

### 5.2.1 Analytical Methods

#### Thermodynamic Closed Cycle Method

The thermodynamic closed cycle analysis (also called the Brayton Cycle) is often used in association of aerospace or airbreathing performance estimations [3]. The usefulness of the closed cycle method is that the behavior and processes under which flows experience in aerospace engines can be represented by thermodynamic cycle diagrams such as the T-s diagram of classical thermodynamic literature. In such an analysis, the working fluid is said to be a pure substance, where two independent intensive thermodynamic properties fix all the values of other thermodynamic properties [3]. The assumption that air is in equilibrium states ubiquitously allows for this statement to be true for the analysis presented here. The combustion process is assumed to be equivalent to heat addition, where no mass is added to the flow of air, nor do any chemical changes occur in the air. The fluid is assumed to experience equilibrium processes which eventually return it to its original state. The behavior of fluids in aerospace engines can be approximated by four thermodynamic processes, compression, combustion (heat addition), expansion, and heat rejection. The classic thermodynamic processes in the form of the T-s diagram is depicted in Figure 5.1. Each process is assigned a set of points (0 - 3) represents compression, (3 - 4) represents combustion, (4 -10) represents expansion, and (10 - 0) represents heat addition.

Points (0 - 3) is adiabatic in nature since no heat is added to the flow. Compression therefore occurs at constant stagnation temperatures ($T_{t0} = T_{t3}$). In ramjets and scramjets compression can occur with a diffuser (centerbody) or with external compression produced by oblique shocks formed against the forebody of the engine. Entropy rises due to skin friction and shock waves themselves in irreversible processes. If irreversibilities are ignored then the adiabatic compression is ideal or isentropic.

Points (3 - 4) represent isobaric or constant pressure heat addition with the total tem-

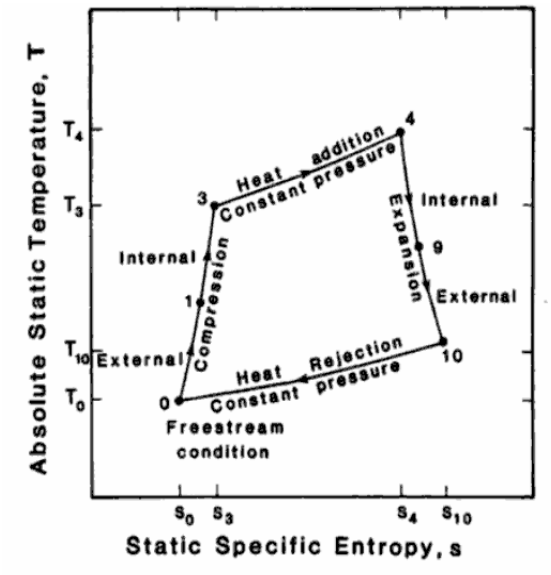


Figure 5.1: Temperature - Entropy Cycle Diagram for Brayton Cycle Engine [3]

perature rising from the burner entry temperature $T_{t3}$ to a higher burner exit temperature $T_{t4}$. One dimensional analysis ignores friction associated with combustion, and it is assumed that mass addition from the fuel is small when compared to the air flow and thus it is also ignored [21]. It was chosen to model heat addition under constant pressure because it avoids boundary layer separation effects, is consistant with similar types of analysis done in traditional gas turbine generators, and also is much simpler than analysis of combustion which constrain Mach number or static temperatures [3].

Points (4 - 10) represent adiabatic expansion (in ramjets and scramjets the nozzle accomplishes this). The local temperature drops from $T_4$ the burner exit temperature to some nozzle exit temperature $T_{10}$ though total temperatures are fixed $T_{t4} = T_{t10}$. The local pressure also drops from its burner entry / exit values ($P_3 = P_4$) to some local pressure $P_{10}$ close to or equal to the free stream local pressure $P_0$. Irreversabilities do occur in adiabatic expansion due to skin friction and shock wave losses. Here once again with irreversabilities ignored the expansion is considered isentropic.

Points (10 - 1) represent a return to the original state of the process. In such a case, heat is rejected, and pressure is returned to the values which they had at the start of the process. Heat rejection can be thought of as the equivalent of the heat added to the burner

which was not able to be converted to cycle work [3].

#### Stream Thrust Method

The stream thrust method can be thought of as a modification of the thermodynamic closed cycle (Brayton cycle) analysis method which accounts for mass, momentum, and kinetic energy transport contributed by the fuel [3]. Also, the stream thrust analysis method accounts for the affects of the engine geometry, such as area increases and decreases for compression and expansion. These effects can be accounted for by using modified versions of equations including the conservation laws with the one dimensional flow assumptions. This method especially relies on the conservation of momentum as it applies to the control volume. Because of the relationship between the conservation laws and control volume laws, the analysis of individual components of the propulsion system can be performed by approximating each component to be an individual control volume. Flows into and out of a component are calculated with stream thrust related conservation equations. A detailed description of this process as it applies to the performance of ramjets and scramjets will be described in the next few sections.

### 5.2.2 Computational Methods

#### MATLAB

For the analysis of an aerospace system, limitations exist on calculations made 'analytically'. In this context the term essentially means 'by hand'. Computational tools are necessary for analysis which requires iterative processes such as those necessary to calculate engine performance over a range of flight Mach numbers, atmospheric temperatures, altitudes, and pressures. The computational tool MATLAB (MATrix LABoratory) was chosen for the analysis of the RBCC propulsion system. MATLAB makes the use of matrices and arrays to store data [45]. For instance, an array was created from a range of Mach numbers, where an iteration was implemented to calculate $I_{sp}$ for all flight Mach numbers in the range of interest. MATLAB also makes use of 'built-in' functions (functions which are pre-programmed) which are optimized vector operations pre-defined by the creators of MATLAB. MATLAB also is able to tabulate data in sets of arrays called a workspace.

The workspace stores the tabulated data in the computers memory, allowing for references when desired. Plots can be created in MATLAB; this is useful for creating visual aids for the comparison of varied ranges of data values. The actual code is written in what is called an 'm' file, named for its '.m' extension in the file name. The 'm file' can be run to solve the equations describing the system of interest.

## 5.3 Analytical Precedures

### 5.3.1 The Atmospheric Model

The analysis of an airbreathing engine is incomplete without a description of the environment which affects the performance of the engine. In fact, a performance analysis of an airbreathing engine which operates in the wide range of Mach numbers or altitudes which will be handled here is not accurate without accounting for the temperature, pressure, and density variations with altitude. Fundamental limits exist on the operating range of airbreathing engines; these limits are imposed on the engine from the atmosphere itself. Fortunately, a wide number of experimental research on atmospheric conditions have been performed throughout the years by high altitude weather balloons and sounding rockets that a relatively accurate atmospheric model can be created.

In this thesis, the atmospheric model was created by incorporating data from the U.S. 1976 Standard Atmospheric Tables into a MATLAB m-file called StandardAtmosphereKM. Units from the International System (SI) were chosen for ease of use. The altitude range chosen for the model was 0 through 120 kilometers. Local temperature, pressure, and density arrays were created in MATLAB based on their values at each altitude sampled. In the U.S. 1976 table, altitude are spaced in non-uniform increments, so a piece-wise linear interpolation was used in the code to calculate temperature, pressure, and density values at 1 kilometer increments throughout the atmospheric range of interest. A new altitude $h_{next}$ was sepcified, and from that the pressure and density variations were calculated using the following equations which are modifications of the buoyancy relations [36]:

$$T_{next} = T + a(h_{next} - h) \tag{5.1}$$

$$\frac{P}{P_{next}} = \frac{T}{T_{next}}^{-g_0/aR} \tag{5.2}$$

$$\frac{\rho}{\rho_{next}} = \frac{T}{T_{next}}^{-g_0/aR+1} \tag{5.3}$$

where $a$ is given by:

$$a = \frac{dT}{dh} \approx \frac{\Delta T}{\Delta h} = \frac{T_{next} - T}{h_{next} - h} \tag{5.4}$$

The constant $a$ represents the slope which accounts for the variation of atmospheric properties, and was originally found from experimental data [36]. The interpolation scheme works can be described in the following manner: An initial altitude (0 kilometers) has a temperature, pressure, and density associated with it; these are the sea level static temperature, pressure, and density values. The interpolation scheme calculates the pressure, and density for the next altitude, 1 kilometer using the buoyancy relations [3]. Since these equations couple temperature with pressure and density, the temperature at 1 kilometer from the surface can then be calculated.

The regions of the atmosphere of interest in this thesis include the troposphere (0 - 11 kilometers), the stratosphere (20 - 47 kilometers), and the mesosphere (50 - 120 kilometers). Atmospheric conditions vary linearly in these regions and can be represented by slopes (negative slopes for decaying conditions and positive slopes for increasing values). The values of the slopes are also provided by experimental data from the U.S. 1976 tables. Transition regions exist between layers (tropopause, and stratopause). Conditions in these regions do not change, and therefore have no slope. A different set of equations must be used in atmospheric transition regions, for temperature, pressure, and density variation. For the transition regions (tropopause, stratopause) the following equations where used:

$$\frac{P}{P_{next}} = e^{-\left[\frac{g_0}{RT}(h-h_{next})\right]} \tag{5.5}$$

$$\frac{\rho}{\rho_{next}} = e^{-\left[\frac{g_0}{RT}(h-h_{next})\right]} \tag{5.6}$$

Plots of the atmospheric conditions can be seen in Figure 5.2, Figure 5.3 and Figure 5.4.

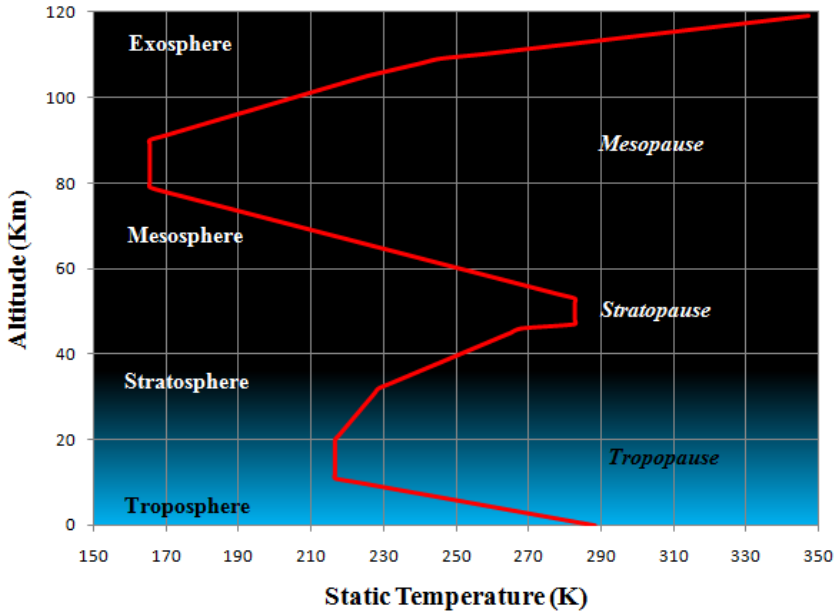


Figure 5.2: Temperature Variations in the Earth's Atmosphere as Calculated by StandardAtmosphereKM

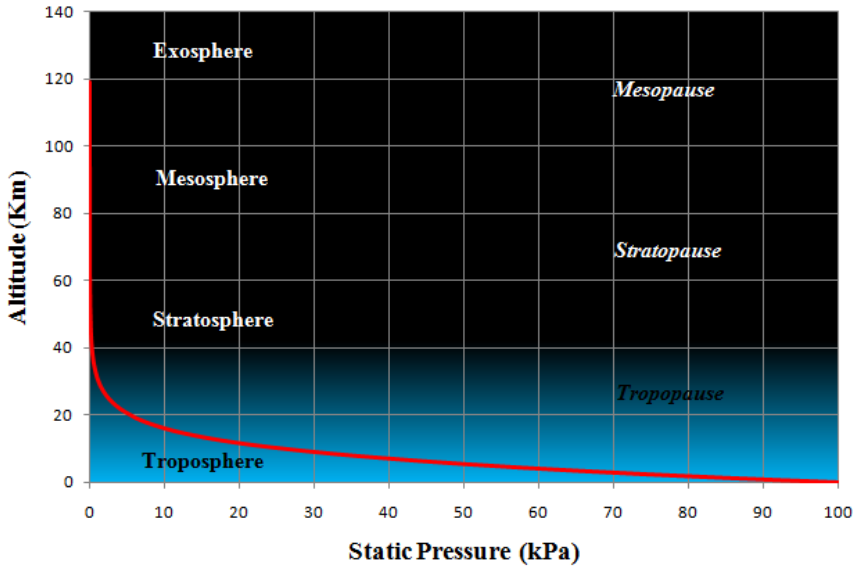


Figure 5.3: Pressure Variations in the Earth's Atmosphere as Calculated by StandardAtmosphereKM

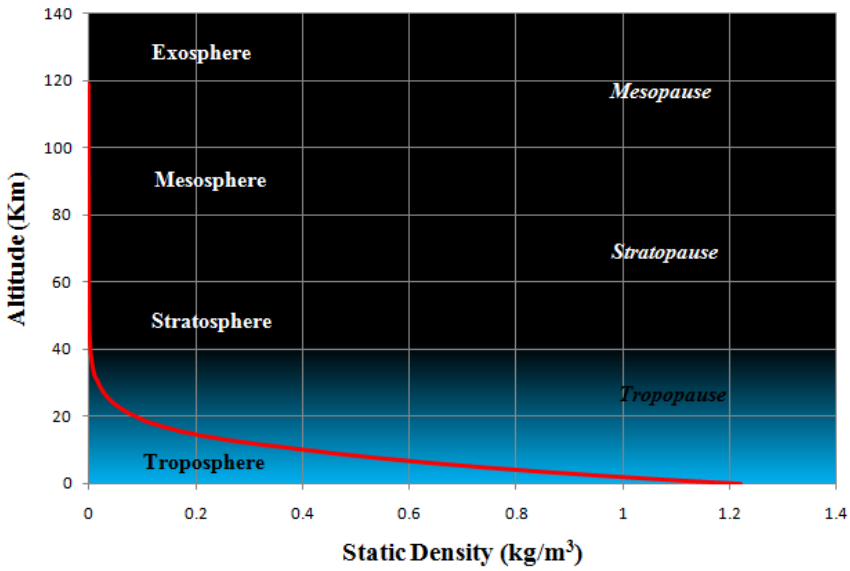


Figure 5.4: Density Variations in the Earth's Atmosphere as Calculated by StandardAtmosphereKM

The creation of the atmospheric model StandardAtmosphereKM allows for calculation of several atmospheric effects related to the propulsion system, including dynamic pressure $q_0$. The dynamic pressure of the atmosphere is produced by the resistance imparted from the air to the vehicle in motion through the atmosphere. From StandardAtmosphereKM the calculations of dynamic pressure and its dependence on altitude and Mach number can be performed using the following relations [3]:

$$q_0 = \frac{\rho_0 a_0^2 M_0^2}{2} = \frac{P_0}{R_0 T_0} \gamma R_0 T_0 \frac{M_0^2}{2} = \frac{\gamma_0 P_0 M_0^2}{2} \tag{5.7}$$

Dynamic pressure is important for both vehicle and engine performance, because it imparts on a vehicle a specific flight envelope of operation. Dynamic pressures which are significantly small require a ridiculously large wing surface area for stable operation of a flight vehicle. On the other hand, if dynamic pressures are too large, structural and airframe limits may be breached, resulting in the destruction of the vehicle. Fortunately there is a prescribed flight envelope of operational dynamic pressures. These have been plotted against free stream Mach number and altitude from StandardAtmoshereKM in Figure 5.5.

The range of dynamic pressures for operation of a flight vehicle are between 23.9 kPa

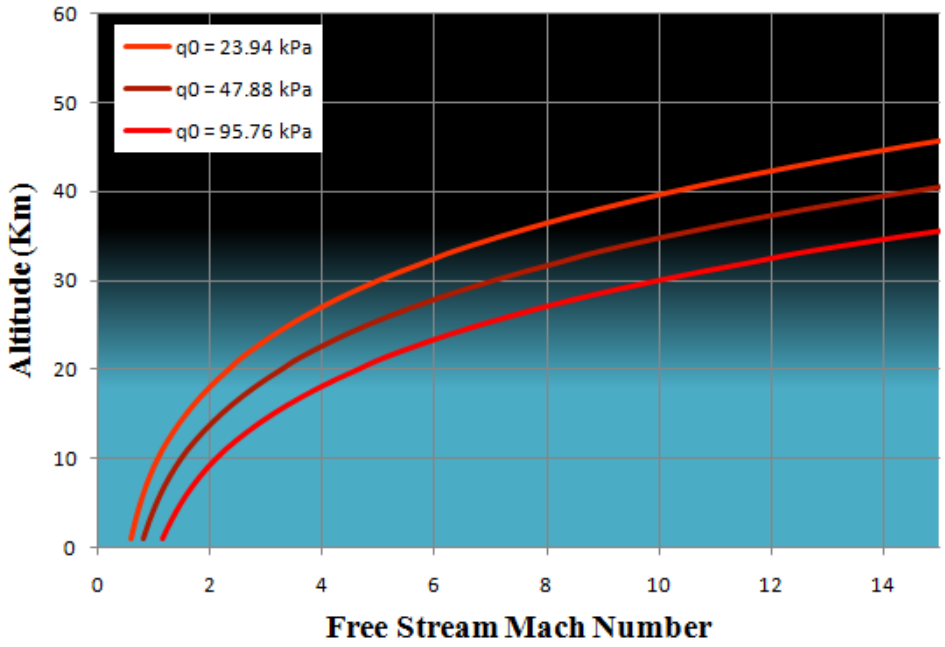


Figure 5.5: Dynamic Pressure Trajectories across SSTO Flight Range

(500 psf) and 95.769 kPa (2000 psf). The completion of the atmospheric model provides a relatively accurate representation of the environment through which the ERIDANUS RBCC propulsion system operates. With a proper treatment of atmospheric conditions accomplished, a decent propulsion model could now be constructed. This will be the topic discussion in the next section.

### 5.3.2 The Rocket Based Combined Cycle Propulsion Model

Finally, the topic for which this thesis was written can now be discussed! The previous discourses related to the theory and other relevant topics have presented the proper background and fundamentals for understanding the challenges associated with the creation of such a model. Before the model is fully discussed, a summary of the key assumptions, and the introduction to new assumptions will be mentioned. Afterwards, the actual model of the RBCC propulsion system will be analyzed. The analysis will be divided into modes and flight regimes: Mode I (Mach 0 - 3: ejector rocket), Mode II (Mach 3 - 6: dual mode ramjet), Mode III (Mach 6 - 10: dual mode scramjet), and Mode IV (Mach 10 - 25: all-rocket).

Without further ado, the key assumptions will be listed in the subsequent section:

### A Review of Key Assumptions

Throughout this thesis, and up until this point, assumptions have been mentioned. In order to allow the reader the entire collection of assumptions necessary to proceed, a review of these previously mentioned assumptions and new assumptions will be mentioned. It is helpful to see the assumptions listed in a bullet form for easy of review. Here are the key assumptions used in this thesis for creating the RBCC model:

- Quasi - One dimensional flow (axially anti-parallel flow properties are uniform)
- Perfect Gas (flow behaves as a calorically and thermally perfect gas)
- Pure Substance (flow is pure in substance that is evenly distributed)
- Isentropic flow (properties at the entrance and exit of control volumes have no entropy changes occur at control volume boundaries)
- Frictionless (forces at the surface from boundary layer effects are neglected in conjunction with the one dimensional assumption)
- Neglected Body Forces (no forces act on the control volume other than those imposed by the engine and atmosphere, e.g. gravitational, electromagnetic forces)
- Combustion is approximated by heat addition (stagnation temperature change across the burner control volume entrance/ exit stations)
- Engine components are approximated as control volumes
- External oblique shock wave compression is approximated by a single oblique shock
- Isolator weak normal shock train in ramjet mode is approximated by one single strong normal shock
- Flow mixing and combustion occur simultaneously in Mode I (ejector rocket mode)
- Scramjet operates with a shock-free isolator (isolator effects in scramjet mode are ignored)

- In ejector rocket and ramjet modes the flow entering the nozzle is thermally choked, meaning there is no physical throat but heat addition forces the sonic condition necessary for flow expansion and thrust production
- Thermal choking occurs in an infinitesimally small constant area duct, which allows the use of the Rayleigh heating and choking equations
- Variable geometries effects are replaced by area ratios

The previously mentioned assumptions are important to this analysis, and without them, the methods applied are useless. Many of them have been explained in previous sections. The assumptions which have not already been justified will be in the sections to which they apply.

### Reference Station Designation

In Figure 5.6 several diagrams of the ERIDANUS RBCC engine are shown, one representing station components (a), and the second including control volume component

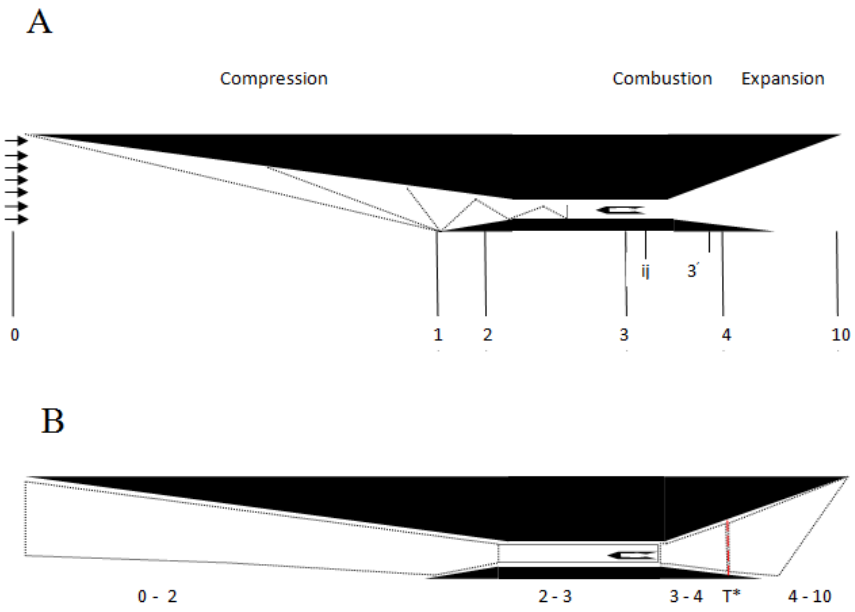


Figure 5.6: (a) Engine Station References for ERIDANUS. (b) Individual Stations Represented as Idealized Control Volumes.

visualizations (b). The analysis of an aerospace system can be simplified if components can be replaced by control volumes for one dimensional assumptions. In this analysis the RBCC engine was divided into sections called reference stations each of which represents a major component of the propulsion system. The reference stations are placed at critical axial locations, and the end of one station becomes the beginning of the next. Flow properties at a given station were represented with a numerical subscript, which will be the same number by which the station is represented. The station designations were based off of the combined works of Heiser & Pratt and Billig [3, 6]. From Figure 5.6a, it can be seen that the station numbers signify separation between engine components of interest:

where:

| | |
|---|---|
| Station 0: | represents the undisturbed or free stream conditions. External compression begins at this point |
| Station 1 : | represents the start of internal compression. Internal compression takes place at the cowl lip entrance point |
| Station 2 : | represents the beginning of the isolator section. The isolator separates the compression and burner from interaction. |
| Station 3 : | represents the burner entry station. |
| Station ij : | represents the rocket ejector exit area. In Mode I, stations 3 and ij mark the beginning of the bypass flow mixture region. |
| Station 3' : | represents the beginning of the infinitesimally small choking region. |
| Station 4 : | represents the burner exit condition. |
| Station 10 : | represents the nozzle exit, and the end of external expansion. |

Table 5.1 shows the control volumes, shown in Figure 5.6 bounded by the station references. Each control volume represents a specific component, as explained in the following table:

| Station | Engine Component | Function |
|---|---|---|
| (0 - 2 ) | Compressor | Diffuses free stream with oblique shocks |
| (2 - 3) | Isolator | Internal diffusion / prevents unstart |
| (3/ij - 4) | Fuel Mixer/ Burner | Mixes flow (ejector only) heats flows |
| (T*) | Thermal Throat (ramjet mode only) | Marks the location of the thermal choking |
| (4 - 10) | Nozzle | Expands flow and produces thrust |

Table 5.1: Station Components and Table

### Operation Mode Analysis

A MATLAB m-file (ERIDANUS.m) was used to create the model of the RBCC engine. The model solves equations related to the one-dimensional isentropic compressible equations at each reference station. In conjunction with the RBCC modes of operation described in section 3.4 the MATLAB based ERIDANUS RBCC code solves the flow equations for each mode. Temperature, pressure, and density values from the atmospheric model code (StandardAtmosphereKM) are fed into the ERIDANUS propulsion model via a data importing algorithim to simulate changing atmospheric effects relative to the engine's performance.

A 'for- loop' was created in ERIDANUS.m to distinguish between modes. When the iteration reaches the right Mach number, the code solves the new set of equations for the appropriate mode of operation. Mach number increments of 0.5 were used ranging from Mach 0.5 to Mach 25 to simulate orbital conditions. As was described in section 3.4, the code starts in Mode I (ejector rocket mode), and performs calculations of all the flow properties of interest through Mode IV (all rocket mode). The tabulated results (e.g. Specific Impulse) are plotted against Mach number, which provides insight into the performance of the engine.

**Mode I Analysis (Ejector Rocket)**

The Ejector Rocket mode was modeled using similar relations to those used by Billig [6]. In this analysis the ejector rocket produces the static thrust necessary to move the vehicle from rest conditions to ramjet mode take over. Initially, compression is produced by ram air pressure produced by the ejector, as is described in section 3.3. The reference stations used in the ejector analysis include inlet 0, burner inlet 3, ejector exit area ij, burner exit 4, and nozzle 10. In this model, bypass flow is mixed and burned instantaneously, and the flow is choked thermally. The inlet conditions (total pressure recovery) was calculated in MATLAB using the following relations taken from Billig's work [6]:

$$\frac{P_{t3}}{P_{t0}} = 0.96 - 0.02586 M_0^2 \tag{5.8}$$

Conditions at the bypass/ burner entry reference station (3/ij) were given by modified conservation of mass and momentum equations to account for total and local pressure, temperature, and stream thrust variation. Area contraction was accounted for by using ratio's of areas. Unknown ejector conditions also were found using similar relations. These were calculated with the following equations from Billig [6]:

$$\frac{P_{t3}}{P_3} = \left(1 + \frac{\gamma_c - 1}{2} M_3^2\right)^{\frac{\gamma - 1}{\gamma}} \tag{5.9}$$

$$M_{ij}^2 = \left(\frac{2}{\gamma_{ij}} - 1\right) \left[\frac{P_{tij}}{P_{ij}}^{\frac{\gamma_{ij} - 1}{\gamma_{ij}}}\right] \tag{5.10}$$

$$\frac{T_{tij}}{T_{ij}} = \left(1 + \frac{\gamma_{ij} - 1}{2} M_{ij}^2\right) \tag{5.11}$$

$$\frac{A_3}{A_{ij}} = \beta \frac{P_{ij}}{P_3} \frac{T_3}{T_{ij}} \frac{M_{ij}}{M_3}^2 \frac{a_{ij}}{a_3} \tag{5.12}$$

Where $\beta$ is the bypass ratio, which varies from about 1.9 at Mach 0.5 to 31 at Mach 2.5 according to the work of Billig [6]. The stream thrust values were calculated at this point using the stream thrust equations. Conditions at the burner exit reference station (4) were calculated using similar equations. For thermal choking, the burner exit Mach

number was fixed to a value of unity. The area, temperature, and pressure ratios for the choked condition were found using the constant area heat addition relations (4.46, 4.48, 4.50, and 4.51). Similar analysis was performed to find the conditions at the nozzle exit areas. Performance calculations for the ejector and total engine were done [6]:

$$I_{spij} = \left[ \frac{(PA(1+\gamma M^2))}{PAM\sqrt{\frac{\gamma g}{RT}}} \right]_{ij} \tag{5.13}$$

$$I_{sp} = \left[ \frac{\Im_{10} - \Im_0 - P_0(A_{10} - A_0)}{\Im_{ij}} \right] I_{spij} \tag{5.14}$$

**Mode II Analysis (Dual Mode Ramjet)**

The dual mode component of the RBCC engine operates as both a ramjet (subsonic combustion) and a scramjet (supersonic combustion). The MATLAB solves equations from Heiser & Pratt, and Shapiro to solve for the flow conditions at each system component. Several crucial assumptions were made to model the dual mode ramjet operation in the ERIDANUS RBCC code. Isentropic external compression is accomplished with the vehicle forebody, forcing the oblique shocks to turn into the internal compression ducts. Studies have shown that optimal external turning of oblique shock waves is between 8 and 11 degrees [26]. Since this analysis is one dimensional in nature, oblique shocks were replaced with one 'simple integrated compression wave' [3]. Since the measure of the compressive ability of the system can be measured by the local temperature ratio between the free stream (station 0) and the cowl lip (station 0), the effective compression produced by the oblique shock train was then calculated in the performance code with the following relations:

$$\psi_1 = \frac{T_1}{T_0} = 1 + \frac{\gamma_c - 1}{2} M_0^2 \left\{ 1 - \left( \frac{\mathbf{v_1}}{\mathbf{v_0}} \right)^2 \right\} \tag{5.15}$$

The maximum allowable compression temperature ($T_3$) is fixed around 1560 K. This is limited by the fact that at this local temperature entering the burner, heat addition limitations related to dissociation occur. Any more heat addition at higher burner entry temperatures will cause gas dissociation [3]. The relationship between total and local temperatures for the burner entry is given by equation (4.31). For a ramjet, the compression temperature

is limited by burner entry Mach number ($M_3$), which must be subsonic. This imposes limitations on the compression temperature ratio $\psi = T_3/T_0$. In this thesis, the compression temperatures were chosen by solving the following equation for subsonic burner entry Mach numbers [3]:

$$M_0 < \sqrt{\frac{2}{\gamma_c - 1}\left\{\left(\frac{\gamma_c + 1}{2}\right)\psi - 1\right\}} \tag{5.16}$$

The resulting temperature ratios were placed into a MATLAB array, for each inlet Mach number across the Mode II flight regime (Mach 3 - 5.5). Thecontrol volume for the isolator (stations 2 - 3) was modeled by replacing the weak normal shock train typically found in isolators with one strong normal shock. The shock relations (equations 4.54 - 4.57) were used to find flow properties downstream of the isolator. A constant area diffuser was used, in accordance with commonly accepted isolator designs [3, 24]. An adiabatic trans-section was placed between the isolator and burner in the ramjet mode to further diffuse the flow entering the burner.

The section exists between stations 3 and 3', where $A_3$ the area at the burner entry/ diffuser exit is greater than $A_3$ the isolator exit region. The continuity and momentum equations were modified for the analysis of this control region. This ramjet mode uses a thermal throat instead the physical throat used in conventional ramjets for two reasons: first, it was desired to avoid the use of variable throat geometry for nozzle flow expansion, and second, the same duct would be used for scramjet mode. Scramjets do not need area restriction for expansion and therefore a thermal throat was implemented in ramjet mode. Thermal choking was modeled in the ERIDANUS RBCC code in the following manner: combustion was assumed to take place in a very small constant area region between the diffuser trans-section, and the expansion surface (see Figure 5.6b). This region was designated 3'.

The Rayleigh heating equations (4.46, 4.48, 4.50, and 4.51) were used to calculate flow properties across this differentially small control region [7]. Area ratios were assigned the region to represent the axial location where choking occurs. The area ratio values were based on previous models of thermal choking in ramjets [34]. Equivalence ratio and fuel to air ratio's were allowed to vary in the same methods used by Trefey [34].

After the flow was choked, it was expanded through the nozzle using the continuity,

mass and momentum relations from Chapter 4. Variation of geometry for the capture and inlet areas was modeled using the following relations [6]:

$$\frac{A_0}{A_i} = 1 - [M_D - M_0](0.155 - 0.0094M_D + 0.00018M_D^2) \tag{5.17}$$

$$\frac{A_0}{A_3} = -3.5 + 2.17M_D - 0.017M_0^2 \tag{5.18}$$

The inlet compression ratio was modeled using the relation [6]:

$$\frac{P_3}{P_0} = -8.4 + 3.5M_0 + 0.63M_0^2 \tag{5.19}$$

The performance measures (specific thrust, specific impulse, thrust specific fuel consumption) were calculated using the equations mentioned in the theory section.

**Mode III Analysis (Dual Mode Scramjet)**

The dual mode scramjet makes use of the stream thrust method described in Chapter 4. The scramjet was divided into 3 main control regions (compressor, burner, nozzle). Each component was modeled using the one dimensional equations and the stream thrust equations mentioned in Chapter 4. The compression, combustion, and expansion systems were assumed to have component efficiencies of 0.9 [3].

The scramjet was assumed to possess a shock free isolator, where the isolator transition between ramjet and scramjet mode was abrupt though in reality the isolator slowly transitions from a subsonic isolator with weak normal shock trains to a supersonic isolator with oblique shocks. With this assumption, the scramjet mode analysis essencially ignores the existence of the isolator, as flow properties are uniform across an adiabatic constant area supersonic duct with no friction losses. The analysis goes from station 0 to 3 for compression. The capture and inlet area ratio relations from Billig [6] were used to calculate the amount of geometry variation occurring in the scramjet compression. Similar burner entry temperature limitations occur for supersonic combustion. The glaring difference, is that the temperature ratio for supersonic combustion is limited by the free stream Mach

number inequality:

$$M_0 > \sqrt{\frac{2}{\gamma_c - 1}\left\{\left(\frac{\gamma_c + 1}{2}\right)\psi - 1\right\}} \tag{5.20}$$

where once again $\psi$ represents the ratio of ambient to burner entry temperatures $T_3/T_0$. This inequality forces the flow entering the burner to be supersonic, or will allow the maximum $T_3$ to be exceeded. The value chosen for the free stream temperature ratio was chosen to be 5 to prevent the supersonic flow in equation 5.20 from attaining subsonic values for low hypersonic inlet flight Mach numbers. Conservation of energy was used to calculate the velocity going into the burner with the following relation:

$$\mathbf{v_3} = \sqrt{\mathbf{v_0}^2 2 C_{pc} T_0 (\psi - 1)} \tag{5.21}$$

The adiabatic compression process was used to calculate the pressure ratio between the compression system and the burner:

$$\frac{P_3}{P_0} = \left\{\frac{\psi}{\psi(1 - \eta_c) + \eta_c}\right\}^{\frac{C_{pc}}{R}} \tag{5.22}$$

Conservation of mass was used for the calculation of the area ratio across the compression/ burner face:

$$\frac{A_3}{A_0} = \psi \frac{P_0}{P_3} \frac{\mathbf{v_0}}{\mathbf{v_3}} \tag{5.23}$$

The combustion process in the scramjet burner was modeled using different equations than were used in the subsonic burner mode. Here the relation was used to simulate effects of drag and flow variation between free stream and perpendicular directions on supersonic flows. The following relations were introduced to describe this process:

| | |
|---|---|
| $\frac{V_{fx}}{V_3}$ | : ratio of fuel injection axial velocity to $V_3$ |
| $\frac{V_f}{V_3}$ | : ratio of fuel injection total velocity to $V_3$ |
| $C_f \frac{A_w}{A_3}$ | : burner effective drag coefficient |
| $T^o$ | : reference temperature for combustion (222 K) |
| $h_f$ | : absolute sensible enthalpy of fuel entering burner |

The burner entry velocity can be represented in terms of the fuel injection ratio $\frac{V_f}{V_3}$ and the combustor drag $C_f \frac{A_w}{A_3}$ in the following manner [3]:

$$\mathbf{v_4} = \mathbf{v_4} \left\{ \frac{1 + f\frac{V_f}{V_3}}{1+f} - \frac{C_f \frac{A_w}{A_3}}{2(1+f)} \right\} \tag{5.24}$$

The conservation of energy and the combustor drag, and fuel injection ratios can be used to represent the temperature after heat is added to the supersonic burner [3]:

$$T_4 = \frac{T_3}{1+f} \left\{ 1 + \frac{1}{C_{pc} T_3} \left[ \eta_b f h_{PR} + f C_{pb} T^o + \left( 1 + f \frac{V_f}{V_3}^2 \right) \frac{\mathbf{v_3^2}}{2} \right] \right\} - \frac{\mathbf{v_4^2}}{2C_{pb}} \tag{5.25}$$

Conservation of mass was used for the area ratio similar to equation 5.23. The combustion process was assumed to take place at constant pressure $P_3 = P_4$ and so the pressure ratio in equation 5.23 is unity for isobaric heat addition at stations (3 - 4). The conservation laws were used to calculate the stream thrust function (equation 4.59), exit velocity, exit temperature and the area ratios for expansion. Finally, the performance relations for specific thrust, specific fuel consumption, and specific impulse were used from equations (4.62, 4.63, 4.64).

### Mode IV (All Rocket Mode)

The analysis of the all rocket mode was very simple. The combustion process in rocket chamber was assumed to be a heat addition in the manner of the other propulsion modes of operation. Properties which are typical of the combustion of liquid hydrogen, $LH2$, and liquid oxygen, $LOX$, were used to calculate the rocket isentropic relations: The burner chamber pressure was set to 2730 kPa and the burner chamber combustion temperature was 2700 K after the combustion temperatures and pressures of $LOX$ / $LH2$ gases [43]. The equations from the rocket theory section in chapter four were used to calculate flow properties exiting the rocket nozzle. The rocket was assumed to be expanded at the altitude of rocket mode takeover (40 kilometers, 4.7246 kPa). Performance plots of the rocket mode were also produced.

## 5.4 Summary

The performance of the RBCC engine as modeled in MATLAB was presented in this section. The results of the analysis and comparisons between the values in this model and other models will be performed in the next section. It is with the motivation to prove whether or not this model is valid with the assumptions made that the next chapter was written.

# Chapter 6

# Results and Validations

*" . . . faith in hypersonics'is akin to belief in the Second Coming: one knows and trusts that it will occur, but one can't be certain when.' Scramjet advocates will continue to echo the defiant words of Eugen Sanger: 'Nevertheless, my silver birds will fly!' "*

– T. H. Heppenheimer, closing statement in "Facing the Heat Barrier: A History of Hypersonics", 2006 [5].

## 6.1 Baseline Performance Results

This section reveals the results (outputs) of the ERIDANUS RBCC code which was designed to simulate engine performance through the atmosphere during trans-atmospheric acceleration to LEO. The engine's performance is measured through specific impulse, specific thrust, thrust specific fuel consumption, and overall efficiency. There are many performance metrics which could be used, and those mentioned here should not be thought of as an exhaustive list. The one's mentioned in this section were chosen because they are most commonly found in literature related to the rocket based combined cycle engine [3, 26, 46].

In its analysis of flight through the atmosphere, the ERIDANUS code outputs variations in the given performance metrics which are directly associated with changing atmospheric conditions as well as the necessary acceleration during the vehicle's (or more appropriately the engine's) climb toward LEO. Also, included in this section are performance metrics

which are specific to certain components. Of particular interest here is the performance of the compression system. As was mentioned in Chapter 2, the ability of the diffuser to produces high compression performance across the necessary flight regime is of prime importance. Finally, a sample cycle analysis for each mode is presented, to give the reader an idea of the capabilities of the ERIDANUS model.

### 6.1.1 System Overall Performance

#### Specific Impulse

The uninstalled specific impulse produced by the ERIDANUS engine code is is plotted against free stream Mach number in Figure 6.1. Included in the plot (Figure 6.1) are vertical lines which denote the cutoff points between modes of operation. $I_{sp}$ starts off with rocket like-values ($I_{sp} \leq 500$ seconds) in the subsonic and transonic flight regimes. At Mach 2 in accordance with increasing bypass ratios, the RBCC behaves more like a ramjet, and the $I_{sp}$ increases from about 1000 seconds at Mach 2.5 to over 4000 seconds at Mach 3.5. In the transition from ramjet to scramjet operation of the dual mode combustion system, the

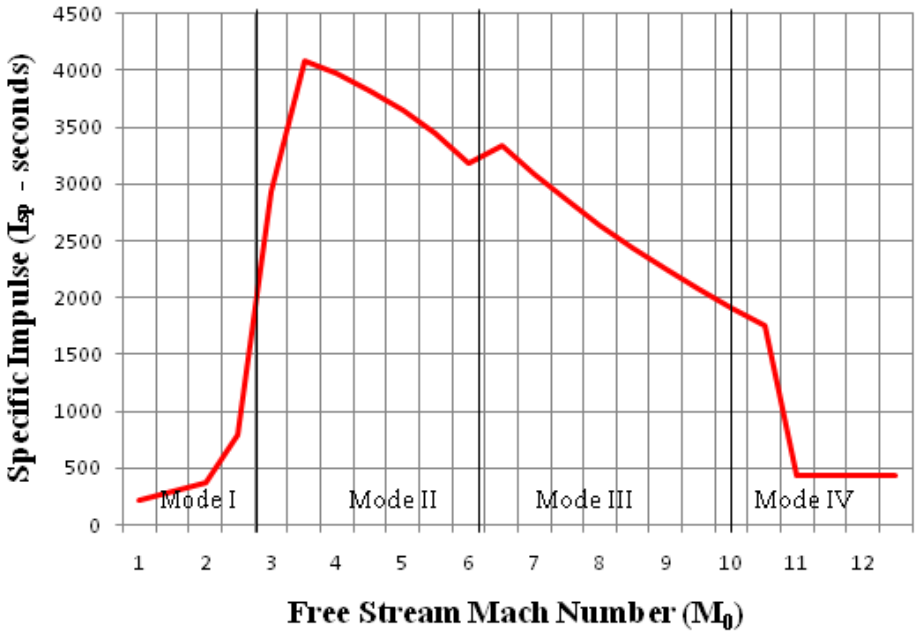


Figure 6.1: Variation of $I_{sp}$ with Flight Mach Number

$I_{sp}$ decays. As the Mach number of the free stream air approaches 10, the performance of the engine approaches pure rocket like behavior. After Mach 10, the RBCC $I_{sp}$ remain virtually constant at about 450 seconds, approximately what is expected of a chemical rocket in near vacuum conditions.

### Specific Thrust and Thrust Specific Fuel Consumption

The specific thrust and thrust specific fuel consumptions are plotted in Figure 6.2 and Figure 6.3 respectively. The specific thrust values correlate strongly with $I_{sp}$ values, as they are linearly related by equation 4.64. The most thrust per unit mass of fuel is produced in ramjet mode (Mach 3 - 6). The thrust specific fuel consumption has interesting behavior. It starts at $5 \times 10^4 g\ [kN \cdot s]^{-1}$ at Mach 0.5 and drops substantially to $0.25 \times 10^2 g\ [kN \cdot s]^{-1}$ at ramjet mode takeover. An explanation for the behavior of the TSFC of the RBCC engine is that in low flight regimes the required fuel is much higher for thrust production, since the amount of air/mass flow is lower than at higher speeds. At higher Mach numbers, mass flow demands are higher, and hence fuel demands decrease in the conservation of mass for thrust production in the engine.

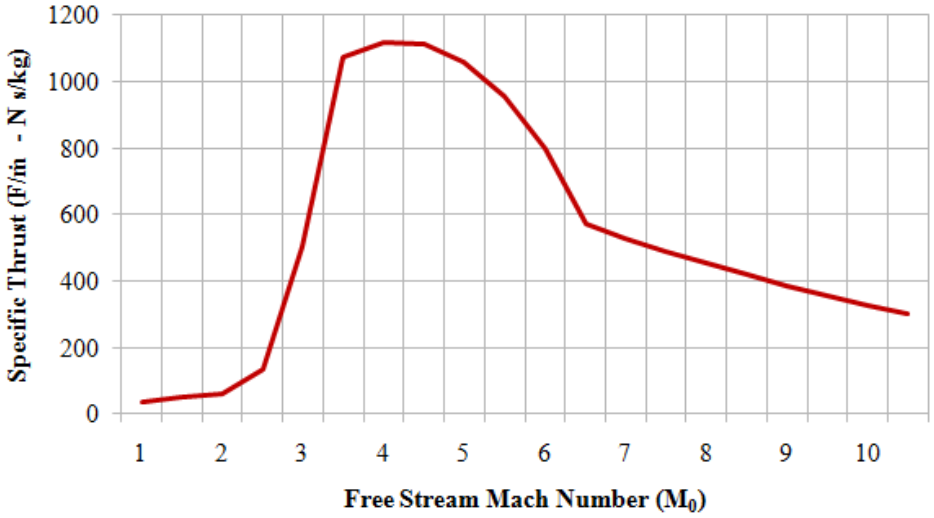


Figure 6.2: Variation of $F/\dot{m}_0$ with Flight Mach Number

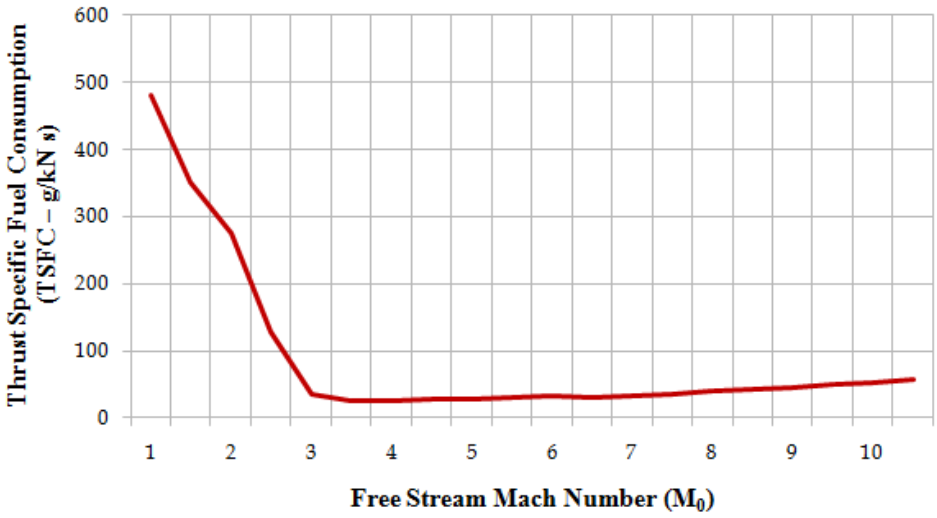


Figure 6.3: Variation of TSFC with Flight Mach Number

### Air Breathing Overall Efficiency

A plot of the system's overall efficiency ($\eta_o$) is shown in Figure 6.4. Of particular interest is the behavior of the overall efficiency in the transition between ramjet and scramjet mode. As was mentioned in Chapter 4, overall efficiency is a measure of an air-breathing engine's ability to convert chemical to mechanical energy. It can also be thought of as an indicator of an engine's ability to make use of fuel stored onboard [3]. From Figure 6.4 it can be seen that $\eta_0$ has lower values in ramjet mode than in scramjet mode. When operating as a ramjet, the equivalence ratio (ER) has higher values than in scramjet mode. As the engine goes torwards scramjet-like operation, the fuel requirements are lower, and the overall efficiency increases. The overall efficiency seems to be sensitive to changes in performance metrics, in particular specific impulse and specific thrust. Notice that there is a jump in overall efficiency from the transition from subsonic to supersonic combustion in figure 6.4. The highest value of overall efficiency ($\eta_0 = 0.48$) occurs at the onset of scramjet mode, but as the $I_{sp}$ and $F/\dot{m}$ decays towards pure rocket like values, the overall efficiency drops as well.

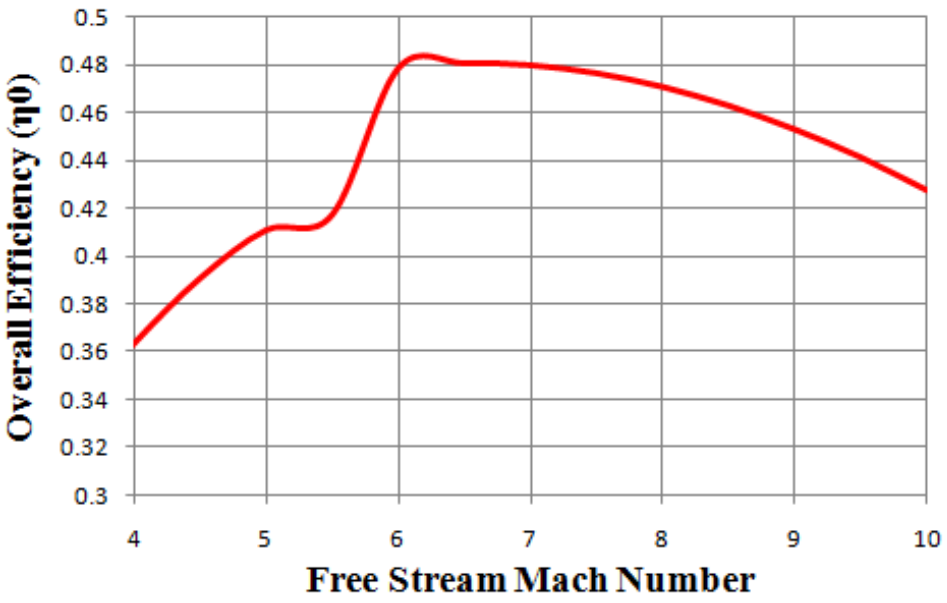


Figure 6.4: Variation of Overall Efficiency with Flight Mach Number

### 6.1.2 Mode Performance and Sample Cycle Analysis Results

From the data produced in MATLAB with the RBCC propulsion model, tabulations were made for each mode of operation. Tables 6.1, 6.2, and 6.3 demonstrate a sample cycle analysis for each mode of operation (e.g. a cycle analysis for the ejector rocket at Mach 1, ramjet at Mach 3, and scramjet at Mach 10). Rocket Mode behavior did does not produce significant or 'interesting' changes since the diffuser and dual mode burner are not in use. Rocket Mode tables were therefore not included here. Each mode has total and stagnation pressure and temperature variations at each station, as well as area ratios, and Mach numbers at each station.

#### Ejector Rocket Mode Performance

The ejector rocket mode sample cycle analysis (Table 6.1) shows the stagnation pressure recovery is very close to one. At this low speed, compression losses are small. Also, area contraction is not as important in ejector mode as it is in the other modes. The area ratio $A/A_0$ varies from 1 to 0.89 in the inlet system. This implies that spillage of the inlet air is occuring. Since the rocket is the primary source of thrust, this concern is not an

Table 6.1: Ejector Mode Station Cycle Analysis ($M_0 = 2$)

| **Station** | **0** | **3** | **4** | **10** |
|---|---|---|---|---|
| **$P/P_0$** | 1 | 1.15 | 2.07 | 1 |
| **$P/P_t$** | 1 | 0.93 | 1.99 | 1 |
| **$T/T_0$** | 1 | 1.06 | 8.94 | 1.4 |
| **$T/T_{t0}$** | 1 | 1 | 8.47 | 8.5 |
| **M** | 2 | 0.8 | 1 | 1 |
| **$A/A_0$** | 1 | 0.9 | 2.98 | 2.98 |

issue. The expansion area is roughly 3 times the inlet area ratio. Stagnation temperatures are unity everywhere except places where heat is transferred. This is consistent with the replacement of combustion with heat addition. The difference in stagnation temperature ratios in ejector mode ($T_{t4}/T_{t0} = 8.5$) than in ramjet and scramjet modes ($T_{t4}/T_{t0} = 4.78$, 1.09) is due to the relatively low stagnation temperatures at low flight speeds. At low speeds more heat is allowed to be added to the free stream than at higher speeds.

### Ramjet Mode Performance

The ramjet mode sample static cycle analysis is shown in Table 6.2. It should be noted that there is a contrast in the pressure ratio $P/P_0$ and the stagnation temperature ratio $T_t/T_{t0}$ values as compared to those in the ejector rocket mode. Compression is of more consequence in ramjet mode, where the ram air pressure allows for high speed flows entering the burner. For subsonic combustion, external and internal compression is required to diffuse the Mach number to appropriate values. At station 4, the flow is choked and the burner exit Mach number is unity. This is the result of a maximum stagnation temperature ratio $T_{t4}/T_{t0}$ of 4.78. Thermal choking occurs when the maximum heat allowable is added to the flow.

### Scramjet Mode Performance

In scramjet mode (Table 6.3), at the design Mach number $M_D = 10$, the area distribution is interesting. The capture to minimum duct area $A_3/A_0$ is 16.5. The area inlet

Table 6.2: Ramjet Mode Station Cycle Analysis ($M_0 = 3$)

| Station | 0 | 2 | 3 | 3´ | 4 | 10 |
|---|---|---|---|---|---|---|
| $P/P_0$ | 1 | 24.52 | 7.77 | 24.64 | 11.18 | 1.4 |
| $P/P_t$ | 1 | 5.01 | 0.25 | 25.55 | 0.55 | 0.16 |
| $T/T_0$ | 1 | 4.12 | 2.93 | 2.78 | 11.23 | 8.36 |
| $T/T_{t0}$ | 1 | 1 | 1 | 1 | 4.78 | 4.82 |
| M | 3 | 2 | 0.57 | 0.23 | 1 | 2.01 |
| $A/A_0$ | 1 | 2.86 | 2.85 | 0.87 | 0.87 | 3.21 |

Table 6.3: Scramjet Mode Station Cycle Analysis ($M_0$ =10)

| Station | 0 | 3 | 4 | 10 |
|---|---|---|---|---|
| $P/P_0$ | 1 | 114.39 | 114.39 | 1.4 |
| $P/P_t$ | 1 | 0.21 | 1.4 | 0.0021 |
| $T/T_0$ | 1 | 5 | 11.37 | 6.03 |
| $T/T_{t0}$ | 1 | 1 | 1.09 | 1.07 |
| M | 10 | 3.94 | 2.59 | 4.49 |
| $A/A_0$ | 1 | 16.5 | 0.16 | 4.17 |

is capturing the most air flow which it is allowed to based on the design. Air capture is more important at Mach 10 than at lower speeds because the engine is operating in low air density, high altitude atmospheric environments. To keep the mass flow balance, more a larger area capture is necessary. The pressure ratio $P/P_0$ is even higher (114) than in ramjet mode. At higher flight speeds, compression becomes of major concern, since compression ratios which are too high can lead to structural failure. Therefore Mach 10 was a good choice for scramjet cutoff, to keep the pressure ratio $P/P_0$ within reasonable values.

### 6.1.3 Compression System Performance Results

The actual capture area to projected inlet area ratio $A_0/A_i$ is shown in Figure 6.5. This ratio expresses the ability of the engine to capture a certain amount of mass flow at a given Mach number and altitude. The plot in Figure 6.5 shows that $A_0/A_i$ decreases

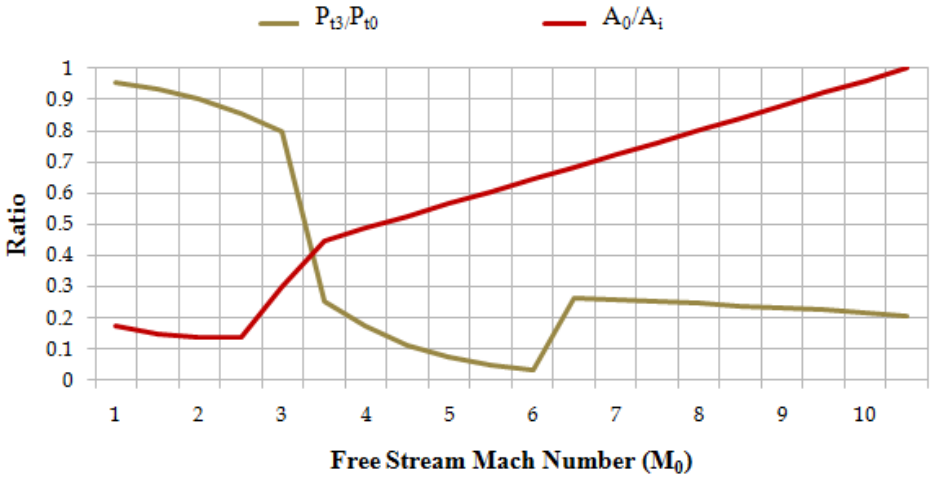


Figure 6.5: Variation of $A_0/A_i$ with Flight Mach Number

from 0.2 to a minimum value of about 0.14 in the subsonic, transonic, and low supersonic flight regimes. This is because in the ejector rocket mode, air capture ability of the engine at low speeds do not have as near an impact on engine performance as does the ejector rocket. At low speeds ram air pressure is low, and the necessity to collect air is not as important as it is at higher speeds. In the higher supersonic and hypersonic flight regimes, $A_0/A_i$ increases from 0.47 at ramjet mode transition to 1 at the $M_D = 10$ at the end of the scramjet mode. At this point, the inlet is able to capture as much air as is it was designed to do. Physically the variation of $A_0/A_i$ represents variable geometry; the cowl lip rotates about a hinge to increase the amount of air flow entering the compression system.

The pressure recovery ratio $P_{t3}/P_{t0}$ is also plotted in Figure 6.5. The pressure recovery ratio is a measure of the compression system's ability to recapture free stream conditions [3, 26]. In other words, the ratio $P_{t3}/P_{t0}$ is a measure of energy losses due to adiabatic compression. The ratio $P_{t3}/P_{t0}$ can never be greater than unity. In the plot, it is apparent that the pressure recovery ratio decays with increasing Mach number. It steeply drops as the RBCC engine transitions from ejector rocket to ramjet conditions. The increase in $P_{t3}/P_{t0}$ (Mach 5 - Mach 10) in scramjet mode is due to an abrupt rise in burner entry Mach numbers ($M_3$) for supersonic combustion.

## 6.2 Comparison of ERIDANUS' Performance with the All-Rocket SSTO

The second major objective of this thesis was the comparison of the performance of the ERIDANUS RBCC concept against that of an all-rocket SSTO. Of particular interest here is the ability of both types of propulsion systems to maximize the payload/structural mass placed into LEO, and therefore reduce the required propellant mass of the system. Though no detailed model or computer code was written for the all-rocket SSTO, it is evident that equations 4.71 and 4.73 are sufficient enough for calculating the propellant efficiency of a one staged launch vehicle [42].

Figure 6.6 reveals that an SSTO using engines which have performance simillar to the Space Shuttle's Main Engines (SSME's) at vacuum conditions ($I_{sp}$ = 450 seconds), and an estimation of the thrust ratio ($\mathcal{R}$ = 2) that the best such a system could do is increase the mass available for payload/structure to a little over 12%, leaving about 88% of the GLOW for propellant. Using equation 4.82, a mission averaged specific impulse of 1080 seconds was calculated for ERIDANUS. With equation 4.73, the specific impulse for ERIDANUS was substituted into this equation, along with the same thrust ratio used in the all-rocket equation. The results are plotted in Figure 6.6 allong with the all-rocket case. In

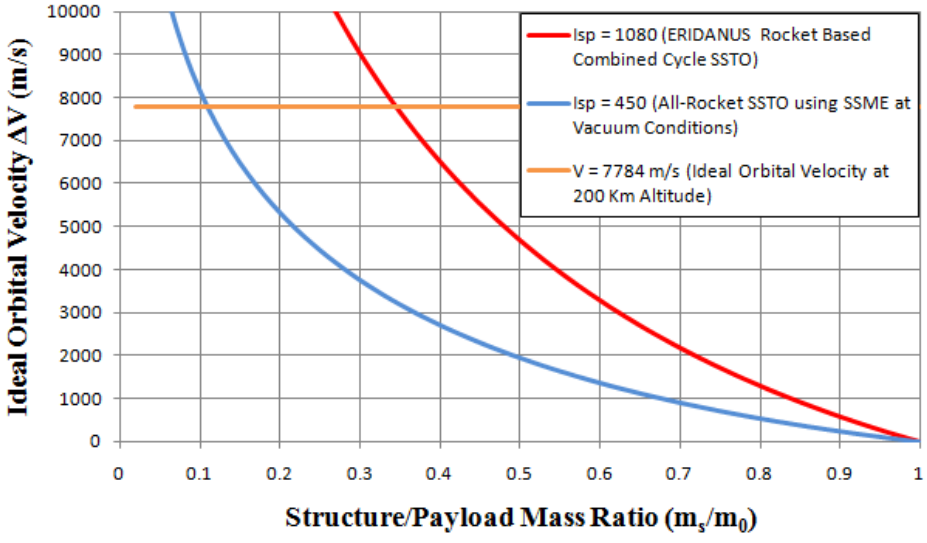


Figure 6.6: Comparisons of RBCC and All-Rocket SSTO Performance

Figure 6.6 it can be seen that increasing the specific impulse of the system by integrating air-breathing and rocket components as is the case with ERIDANUS, has significantly improved the mass available for structure/payload to 35% of the GLOW, while reducing the required propellant to 65%.

## 6.3 Performance Validation Results

In this section validation of the analytical methods used for the ERIDANUS code is demonstrated by comparing the ERIDANUS model to other related RBCC propulsion models. Further validation is accomplished by comparing the performance of ERIDANUS' sub-systems (e.g. ramjet mode/ scramjet mode) with theoretical performance of such engines. Unfortunately, the various codes which are used in validation do not all include the same performance metrics, (e.g. one code plots $F/\dot{m}$ for thrust calculation but another might use thrust coefficient ($C_t$)). Also, many codes do not include details of the analysis methods used; descriptions of what was done are mentioned but no specifics including equations or codes. Most studies include plots of $I_{sp}$ however; $I_{sp}$ will be the primary performance metric used in the validation of ERIDANUS, both in validating the overall system performance across the flight regime of interest, and in validation of specific modes of operation.

### 6.3.1 General System Performance Validation

For the validation of the system performance of ERIDANUS (measuring the specific impulse produced by ERIDANUS across the flight regime of interest), comparisons were made between ERIDANUS and other codes including the NASA GTX Reference Vehicle, the SCCREAM RBCC model used by Olds and Bradford, and the Astronautics Corperation's Ejector Scramjet (ESJ) study for the U.S. Airforce done in 1988 [18, 34, 46]. Of particular interest here is engine performance through the atmosphere in the air-breathing modes (ejector and ramjet/scramjet) from static conditions through Mach 10, and a dynamic pressure trajectory where $q_0 = 47.88$ kPa (1500 psf). Comparison was simply done by comparing plots produced by the ERIDANUS code to plots created based on the data from the other models [18, 34, 46]. In Figure 6.7 it can be seen that the trends between

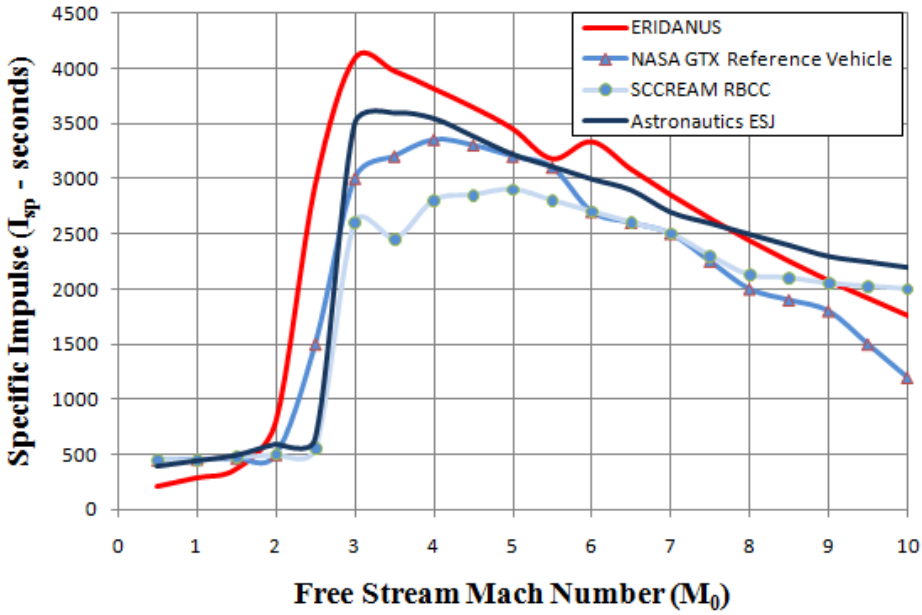


Figure 6.7: Comparison of $I_{sp}$ Data for Various RBCC Concepts [18, 34, 46]

ERIDANUS and the other models seem to corellate.

The specific impulse of each model starts at typical rocket values and rises to values above 3500 seconds near ramjet operation. As the engines produce scramjet-like behavior, the specific impulse slowly drops, approaching rocket like values near and beyond Mach 10. However, the ejector rocket mode of ERIDANUS has lower start off $I_{sp}$ values than the other models. Also ERIDANUS' scramjet mode performance drops off near Mach 10 at a faster rate than the other models at the same Mach number. ERIDANUS' $I_{sp}$ seems to closely follow the pattern of the NASA GTX Reference Vehicle than it does with SCCREAM or the Astronautics ESJ.

Possible explanations for such discrepencies include difference in assumptions of the capture area sizing, and also diffuser performance. The effect of diffuser performance drastically effects the performance of a scramjet. For instance, lower diffuser efficiency (compression efficiency $\eta_c$) limits the amount of stagnation temperature rise by fuel (heat) addition which has a lower limit to avoid the thermal choking of the already supersonic flow entering the burner. This can significantly reduce the resulting $I_{sp}$ during flight.

### 6.3.2 Mode Specific Performance Validation

#### Ejector Rocket Mode Validation

For the ejector rocket mode performance validation, the ERIDANUS' ejector model was compared to both Billig's ejector model [6], and SCCREAM's ejector rocket [46]. Figure 6.8 shows good correllation between the $I_{sp}$ values in ERIDANUS and Billig's model. In fact, both models produce almost identical curves, though ERIDANUS has lower $I_{sp}$ than the Billig model. The differences between the models could be related to selecting different model input/constraints such as selecting a different value for the capture area of the inlet system, and also the lower performance of the ERIDANUS ejector rocket sub-system. Both curves seem to generally agree: in subsonic and trans-sonic flight, the performance is rocket-like, with $I_{sp}$'s below about 600 seconds.

There is obvious thrust augmentation - the $I_{sp}$'s are higher than those of contemporary rockets. As the free stream Mach number approaches 2.5, the bypass ratio, $\beta$ increases from about 2 to 30, and the system behavior becomes more ramjet-like. The ejector rocket assembly and the primary air-flow becomes less important on system performance, and the

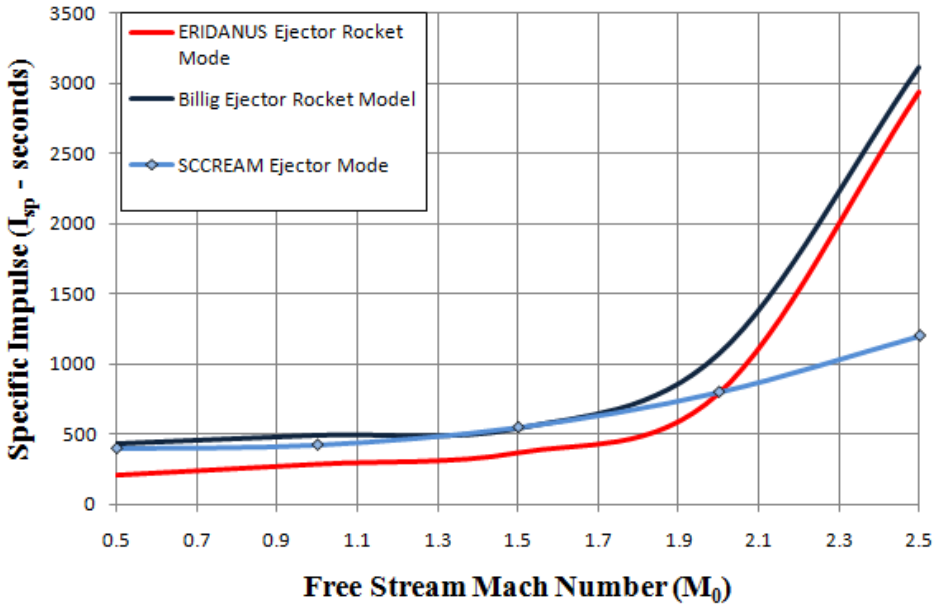


Figure 6.8: Ejector Rocket Performance Comparisons [6, 46]

secondary flow becomes all important. SCCREAM's ejector follows the same behavior, but does not produce the higher $I_{sp}$'s of ERIDANUS or the Billig model. More study is necessary to understand the reason for this discrepancy.

### Ramjet Mode Validation

In Figure 6.9 ERIDANUS' performance in ramjet mode is plotted against a theoretical prediction of ramjet behavior similar to those found in Figure 1.2 [16]. The performance metric chosen in Figure 6.9 is specific impulse. It can be seen that in contrast to the theoretical example which shows a peak performance near Mach 3.5, the ERIDANUS ramjet mode starts with a maximum $I_{sp}$ of about 4000 seconds at Mach 3 and its performance decays as the free stream Mach number approaches Mach 6 and the hypersonic flight regime.

In other words, the ERIDANUS ramjet peaks and drops off at different times and lower values than theory predicts. Though both plots still are within the same $I_{sp}$ range (which of course is a good indication of ERIDANUS' validity) there still is discrepancy. One possible explaination is that the use of a thermal throat in a ramjet is theorized as having lower performance than a ramjet using a physical throat [15, 47]. Since ERIDANUS uses

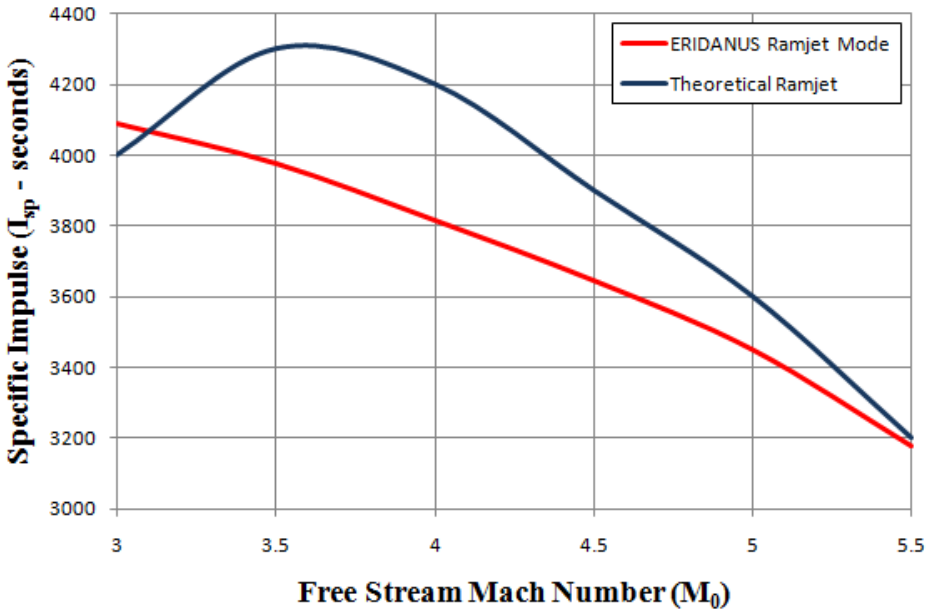


Figure 6.9: Ramjet Mode Performance Comparisons [16]

a thermally choked ramjet mode, as opposed to a conventional throat, it can be inferred that the discrepancy lies in this particular fact.

### Scramjet Mode Validation

A similar theoretically based scramjet performance plot is shown next to the ERIDANUS' scramjet mode plot in Figure 6.10. Here, the $I_{sp}$'s of both scramjet's show simillar trends; the performance of both models indicate higher $I_{sp}$'s (above 3000 seconds) at lower hypersonic speeds (about Mach 6) but decay in engine performance as the flight Mach number approaches 10. ERIDANUS in scramjet mode produces an $I_{sp}$ slope which is less inclined than the predicted expectation. As was mentioned in Section 6.3.1 the behavior of ERIDANUS in scramjet mode might be a result of limitations in allowable stagnation temperature change (during fuel injection/ heat addition). These limitations are imposed by Rayleigh's heating laws as mentioned in Chapter 4. Adding too much heat to a supersonic flow creates a choke condition, which is undesirable in a scramjet burner.

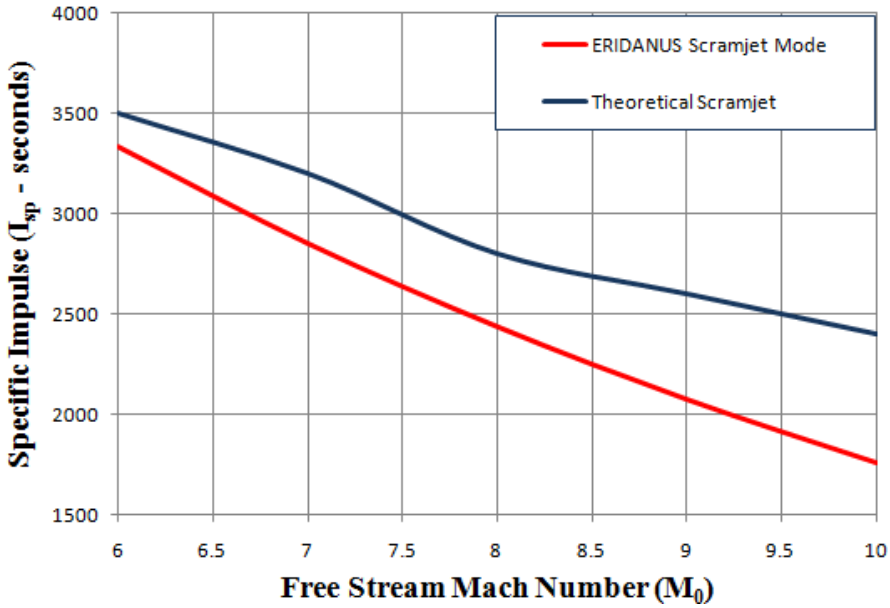


Figure 6.10: Scramjet Performance Comparisons [16]

### 6.3.3 Air-Capture System Validation

The final discussion in this section is focused on the all-important air/ mass flow capture system. The NASA GTX Reference Vehicle model was used as a reference for comparison. Figure 6.11 shows plots of the air capture area $A_0/A_i$ as produced by the GTX Reference Vehicle study and ERIDANUS. Both models seem to show correlation, but the GTX has larger capture ratios earlier on in the flight. The fact that the correlation is so close between the two models adds validity to the ERIDANUS model.

It is interesting to note that in Figure 6.7 the $I_{sp}$'s of ERIDANUS and GTX had the closest correlation, that is their respective plots seemed to show virtually the same trends through out the flight regime of interest. An explanation was related to similarities in the air capture abilities as modeled by both codes. It is evident that through the results as shown by Figure 6.11 there may be validity to this explanation. Interestingly, the GTX model used Computational Fluid Dynamics software for the flow properties throughout the engine. The comparisons between the GTX and RBCC models also demonstrates the power of the one dimensional assumptions. Although two different methods of RBCC engine analysis were used, the results correlate well.

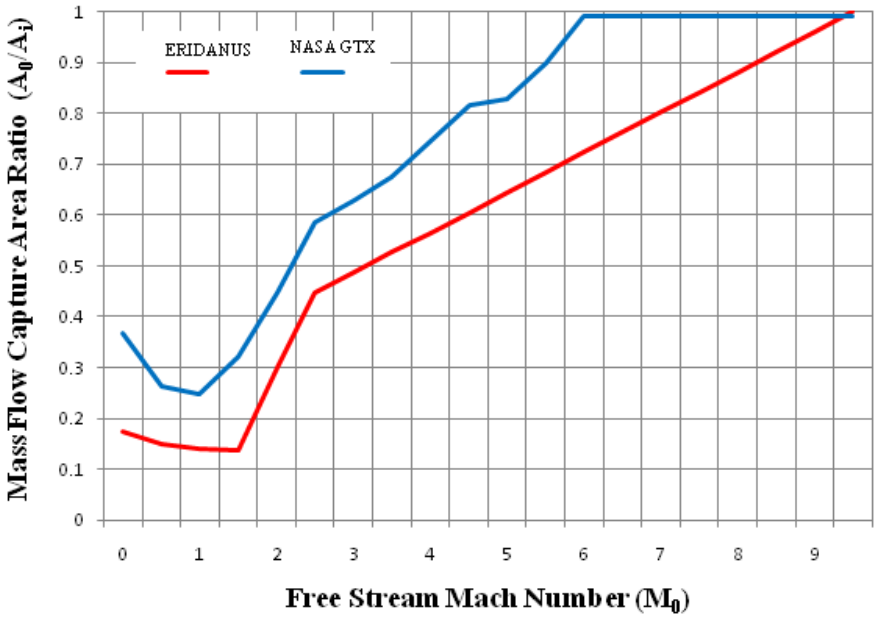


Figure 6.11: Capture Area Ratio Comparisons [34]

# Chapter 7

# Summary and Future Work

*"We shall not cease from exploration and the end of all our exploring will be to arrive where we started and know the place for the first time."*

– T.S. Eliot, as quoted by former Astronaut Michael Collins in "Carrying the Fire: An Astronaut's Journey" [48].

## 7.1 Summary and Review of Thesis

Though the concept of using a Rocket Based Combined Cycle engine for one-stage trans-acceleration to LEO for payload/ propellant performance improvement has been known for over 4 decades, they have been sparsely represented in open literautre. This thesis aimed to address this problem creation of an analytical model of an ejector rocket in a dual combustion propulsion system (ERIDANUS) RBCC engine which does the following:

1. Simulates trans-atmospheric flight in the presence of changing atmospheric conditions from the view point of an RBCC engine

2. Demonstrates the advantages of the integration of the ejector rocket, ramjet, and scramjet on the overall performance of an SSTO against a pure rocket SSTO accelerator

3. Verifies the validity of the model by comparing specific performance metrics includ-

ing net specific impulse, thrust specific fuel consumption, overall efficiency, specific thrust, air mass capture ratio, and total inlet pressure recovery with other theoretical analytical models found in literature.

The ERIDANUS model uses quasi- one dimensional compressible flow equations and the stream thrust control volume method to predict engine performance through changing atmospheric conditions through its climb towards LEO. Performance metrics used to gage the engine's behavior over the wide range of flight conditions include specific impulse, specific thrust, thrust specific fuel consumption, and overal efficiency.

This thesis investigated the effects of integrating of the ejector rocket, and dual mode combustion propulsion system (ramjet/scramjet) on the payload/structure of a hypothetical trans-atmospheric launch system. The ERIDANUS code was used to calculate flow properties at each station during each mode of operation. The results based on the specified performance metrics were plotted to show their variation against the free stream Mach conditions. Of major importance was the effects increasing specific impulse by integrating air-breathing with a rocket sub-system. A method of averaging the varying $I_{sp}$ was created to develop a mission averaged specific impulse ($I_{spAVG}$) which would be useful in analyzing a joint air-breathing/rocket powered propulsion system.

The result showed that ERIDANUS produces an $I_{spAVG}$ of 1080 seconds. This $I_{sp}$ is an improvement over the all-rocket SSTO, increasing the specific impulse for the mission by about 240%. This results in an increase in payload performance, increasing the available mass for payload and structure from the 12% of the GLOW enforced by the all-rocket to 35%. This implies a decrease in the required propellant mass from 88% of the GLOW to 65%. A conclusion which can be drawn from these results is that the integration of the ejector rocket with the dual combustion propulsion system can increase the $I_{spAVG}$ over that of an all-rocket system, and therefore increase the payload/structure and propellant performance of a trans-atmospheric system.

ERIDANUS was validated by comparison of its performance ($I_{sp}$) against those of other models, including the NASA GTX Reference Vehicle, SCCREAM, and the ESJ model produced by the Astronautics Corperation. The validation study indicates that the performance of ERIDANUS is similar to those of the other models. Correlations were

apparent in the review. The conclusion which can be made is that the ERIDANUS RBCC concept as modeled in this thesis is a valid propulsion system for a SSTO vehicle with the assumptions used.

## 7.2 Future Work

Limitations exist in ERIDANUS RBCC model. Vehicle drag and entropy losses were not considered in this study. Vehicle / airframe integration was also not analyzed though an important consideration in engine design. The effect of vehicle size (weight, volume, etc.) and external drag on performance was omitted. The previous omissions though important, were not considered because the rudimentary concept of baseline performance was the goal of this thesis. In a future work, the previous omissions must be included to further strengthen the validity of the model used here. A CFD model simulation of the ERIDANUS RBCC concept would be a useful secondary step in the validaiton of this method in future applicaitons.

A sensitivity study could be included in future work which demonstrates the sensitivity of performance to key input parameters. Also, it would be useful to apply the performance of the ERIDANUS RBCC model to a detailed flight trajectory model to observe the behavior of a conceptual SSTO vehicle powered by an ERIDANUS RBCC engine. These are the tip of the iceberg of the wonderful and fascinating adaptations which can be added to the baseline study in this thesis. The topic of this thesis was chosen because of the author's extreme passion and interest in participating in the construction of a future where common people can dream of flight into space and achieve their dreams without economic constraints due to the expenses of raising payloads to LEO. This thesis was written with the hopes that more focus will be given to 'advanced' and 'Combined Cycle' space worthy propulsion systems both by academia and industry. The tools and resources are available to make the dream of spaceflight for the common person a reality. All that is needed are the right minds and motivations. Truly, the sky is no limit.

# Bibliography

# Bibliography


[1] R. H. Goddard, *The Papers of Robert H. Goddard*, vol. 1. McGraw-Hill, Inc., 1970.

[2] F. S. Billig, "Hypersonic propulsion concpets and challenges," in *Hypersonic Systems and Testing*, 2000.

[3] W. H. Heiser and D. T. Pratt, *Hypersonic Airbreathing Propulsion*. AIAA Education Series, American Institute of Aeronautics and Astronautics, Inc, 1994.

[4] R. Daines and C. Segal, "Combined rocket and airbreathing propulsion systems for space-launch applications," *Journal of Propulsion and Power*, vol. 14, no. 5, 1998.

[5] T. A. Heppenheimer, *Facing the Heat Barrier: A History of Hypersonics*. NASA History Series, National Aeronautics and Space Administration., 2006.

[6] F. S. Billig, *The Low Speed Operation of An Integrated Rocket-Ram-Scramjet For A Transatmospheric Accelerator*, vol. 165 of *Progress in Astronautics and Aeronautics*. American Institute of Aeronautics and Astronautics, Inc, 1996.

[7] A. H. Shapiro, *The Dynamics and Thermodynamics of Compressible Fluid Flow*, vol. 1. The Ronald Press Company, 1953.

[8] "Informational summaries: Astronaut facts book," tech. rep., NASA, 1998.

[9] T. Beardsley, "The way to go in space," *Scienctific American*, pp. 81–97, 1999.

[10] P. Butterworth-Hayes, "European aerospace grows, but problems remain," *Aerospace America*, 2004.

[11] G. N. Henry, "A decision maker's guide to robust, reliable, and inexpensive access to space," 2003.

[12] "Space transportation costs: Trends in price per pound to orbit 1990 - 2000," tech. rep., The Futron Corperation, 2002.

[13] G. A. Hudson, "History of the phoenix VTOL SSTO and recent developements in single-stage launch systems," in *Proceedings of 5th ISCOPS, AAS*, vol. 77, pp. 329 – 351, 1991.

[14] M. J. L. Turner, *Rocket and Spacecraft Propulsion: Principles, Practice and New Developments*. Springer-Praxis Books, 3rd ed., 2009.

[15] C. J. Trefny and T. Benson, "The integration of the turbojet and single-throat ramjet," 1995.

[16] D. Andreadis, "Scramjet engines enabling the seamless integration of air & space operations," 2005.

[17] T. Kanda and K. Tani, "Conceptual study of a rocket-ramjet combined-cycle engine for an aerospace plane," *Journal of Propulsion and Power*, vol. 23, 2007.

[18] R. W. Foster and W. J. Escher, "Studies of an extensively axisymmetric rocket based combined cycle (RBCC) engine powered SSTO vehicle," in *25th AIAA/ASME/SAE/ASEE Joint Propulsion Conference and Exhibit*, 1989.

[19] E. Curran, "The potential and practicality of high speed combined cycle engnies," in *Advisery Group fro Aerospace Research & Developement Conference Proceedings "Hypersonic Combined Cycle Propulsion" Vol. 479*, pp. K1 – K7, 1990.

[20] R. Varvill and A. Bond, "A comparison of propulsion concepts for SSTO reusable launchers," *Journal of British Interplanetary Science*, vol. 56, pp. 108 – 117, 2003.

[21] C. Segal, "Propulsion systems for hypersonic flight," in *RTO AVT Lecutre Series on "Critical Technologies for Hypersonic Vehicle Development"*, 2004.

[22] V. A. Sabel'nikov and V. I. Penzin, *Scramjet Research and Development in Russia*, vol. 189 of *Progress in Astronautics and Aeronautics*. American Institute of Aeronautics and Astronautics, Inc, 2001.

[23] F. Falempin, *Scramjet Developments in France*, vol. 189 of *Progress in Astronautics and Aeronautics*. American Institute of Aeronautics and Astronautics, Inc, 2001.

[24] W. Heiser and D. Pratt, *Aerothermodynamics of the Dual-Mode Combustion System*, vol. 189 of *Progress in Astronautics and Aeronautics*. American Institute of Aeronautics and Astronautics, Inc, 2001.

[25] E. Curran, *Introduction*, vol. 137 of *Progress in Astronautics and Aeronautics*. American Institute of Aeronautics and Astronautics, Inc, 1991.

[26] F. S. Billig, *Propulsion Systems from Take-Off to High Speed Flight*, vol. 137 of *Progress in Astronautics and Aeronautics*. American Institute of Aeronautics and Astronautics, Inc, 1991.

[27] D. L. Kors, "Design considerations for combined air breathing-rocket propulsion systems," in *Advisery Group for Aerospace Research & Developement Conference Proceedings "Hypersonic Combined Cycle Propulsion" Vol. 479*, pp. 12.1 – 12.13, 1990.

[28] P. G. Hill and C. R. Peterson, *Mechanics and Thermodynamics of Propulsion*. Addison-Wesley Publishing Company, 3rd ed., 1970.

[29] N. C. Rauhut, *Ultimate Questions: Thinking About Philosophy*. Penguin Academics, 2004.

[30] W. J. Escher and E. H. Hyde, "A user's primer for comparative assessments of all-rocket and rocket-based combined-cycle propulsion systems for advanced earth-to-orbit space transport applications," in *31st AIAA/ASME/SAE/ASEE Joint Propulsion Conference and Exhibit*, 1995.

[31] J. Olds, "Multidisciplinary design of a rocket-based combined-cycle SSTO launch vehicle using Taguchi Methods," 1993.

[32] J. Olds, "Results of rocket-based combined-cycle SSTO design using parametric MDO Methods," 1994.

[33] J. Olds, "Options for flight testing rocket-based combined-cycle (RBCC) engines.," 1996.

[34] C. J. Trefny and J. M. Roche, "Performance validtation approach for the GTX air-breathing launch vehicle," 2002.

[35] W. E. Burrows, *This New Ocean: The Story of the First Space Age.* Random House, 1998.

[36] J. D. Anderson, *Introduction to Flight.* McGraw Hill Publishing Company, 5th ed., 2005.

[37] G. C. Oates, *Aerothermodynamics of Gas Turbine and Rocket Propulsion.* AIAA Education Series, American Institute of Aeronautics and Astronautics, Inc, 1984.

[38] E. A. Bunt, *Basic Adiabatic Theory.* John Hopkins University Applied Physics Laboratory, 1967.

[39] J. D. Anderson, *Modern Compressible Flow.* McGraw Hill Publishing Company, 3rd ed., 2004.

[40] H. Liepmann and A. Roshko, *Elements of Gasdynamics.* Dover Publishing, Inc, 2001.

[41] G. Sutton, *Rocket Propulsion Elements: An Introduction to the Engineering of Rockets.* John Wiley and Sons, 5th ed., 1986.

[42] W. Thomson, *Introduction to Space Dynamics.* John Wiley and Sons, 1963.

[43] F. J. Hale, ed., *Introduction to Space Flight.* Prentice Hall, 1994.

[44] D. W. Swift, *Voyager Tales: Personal Views of the Grand Tour.* American Institute of Aeronautics and Astronautics, 1997.

[45] R. Pratap, *Getting Started with MATLAB 7: A Quick Introduction for Scientists and Engineers.* Oxford University Press, Inc., 2006.

[46] J. Olds and J. Bradford, "SCCREAM (simulated combined-cycle rocket engine analysis module): A conceptual RBCC engine design tool," 1997.

[47] S. Angelucci, G. Roffe, and P. Baronti, "The single throat ramjet and its application to cruising and accelerating systems," 1979.

[48] M. Collins, *Carrying the Fire: An Astronaut's Journey.* Farrar, Straus, and Giroux, 2009.

# Vita

Nehemiah Joel Williams was born in Philadelphia, Pennsylvania. During much of his childhood and adolescent years, Nehemiah spent countless evenings studying the night skies above Sicklerville, NJ where he was raised. Though he was awarded a Bachelor's of Science degree in Biblical Studies from Philadelphia Biblical University in Langhorne, Pennsylvania, Nehemiah returned to undergraduate academics to study Mechanical Engineering at Temple University in Philadelphia, Pennsylvania. After three years at Temple, Nehemiah was awarded a Bachelor's of Science degree in Mechanical Engineering. Afterwards, Nehemiah applied and was accepted at the University of Tennessee Space Institute's Aerospace Engineering program. Currently, Nehemiah is finishing his Master's of Science degree in Aerospace Engineering at UTSI with a concentration in Space Engineering. After finishing his M.S. degree, Nehemiah plans on pursuing a doctoral degree. Nehemiah wants to research advanced propulsion concepts, including integration of air-breathing, hypersonic and rocket propulsion systems with the hopes of making space flight more robust, accessible, and affordable.